Results

1. El interferón gamma induce la expresión de $p21^{Waf1}$ y bloquea el ciclo celular de los macrófagos evitando así la inducción de apoptosis.

Resumen

Los macrófagos requieren la presencia de M-CSF (*macrophage colony-stimulating factor*) para proliferar y sobrevivir. La activación de los macrófagos con LPS, el principal constituyente de la pared de las bacterias Gram-negativas, o con IFNγ (*interferon gamma*), secretado por los linfocitos T activados, inhibe la proliferación de los macrófagos dependiente de M-CSF. Sin embargo, el mecanismo de inhibición utilizado por cada uno de ellos es distinto y las consecuencias de esta inhibición también.

El tratamiento con LPS o de la eliminación del factor de crecimiento M-CSF inhibe la proliferación celular y bloquea el ciclo celular en la fase G_1 temprana. Este bloqueo esta mediado por una inhibición de la expresión de los complejos ciclina-cdk que regulan la progresión a través del ciclo celular. Además, estos tratamientos inducen la muerte celular de los macrófagos por apoptosis. El IFNγ, sin embargo, inhibe la proliferación de los macrófagos por un bloqueo a nivel de la barrera G_1/S del ciclo celular. Este bloqueo está mediado por la expresión del inhibidor de los complejos ciclina-cdk $p21^{Waf1}$, sin afectar a la expresión de dicho complejos. A diferencia de lo observado con LPS, el bloqueo del ciclo celular inducido por el IFNγ no está asociado con la inducción de apoptosis en los macrófagos.

El diferente comportamiento entre la activación por IFNγ o el LPS y la inducción de apoptosis, nos llevó a estudiar el papel que podían tener estos agentes en la regulación de la apoptosis en macrófagos. Así, observamos que el IFNγ no sólo no induce apoptosis en macrófagos, sino que además protege de la apoptosis inducida por agentes como el LPS, dexametasona y de la eliminación de los factores de crecimiento. Nuestros resultados preliminares sugerían la existencia de una relación entre la progresión del ciclo celular y la protección frente a la apoptosis.

La utilización de oligonucleótidos antisentido de $p21^{Waf1}$ y los experimentos con ratones *knock-out* para que este gen nos han permitido demostrar que la inducción de $p21^{Waf1}$ mediada por el IFNγ es necesaria para proteger a los macrófagos de la apoptosis dependiente del LPS o de la dexametasona. Sin embargo, la inducción de $p21^{Waf1}$ por factores de crecimiento como el IGF-I (*Insulin growth factor-I*) no tiene ningún efecto protector de la apoptosis, sugiriendo que aunque necesaria, la expresión de $p21^{Waf1}$ no es suficiente.

A diferencia de lo que ocurre con el IFNγ, la inducción de $p21^{Waf1}$ inducida por el IGF-I (*insulin-like growth factor-I*) no inhibe la proliferación de los macrófagos. Este resultado sugería que quizás el bloqueo del ciclo celular en un punto concreto era realmente el responsable del efecto protector del IFNγ sobre la apoptosis.

La utilización de inhibidores del ciclo celular como la afidicolina y la OH-Urea, que bloquean el ciclo en la barrera G_1/S, que es la misma fase que el IFNγ, demostró que mientras la OH-Urea tenía un efecto protector frente a la apoptosis, la afidicolina no. El análisis de la expresión de $p21^{Waf1}$ demostró que el efecto de OH-Urea se correlacionaba con la inducción de la expresión de $p21^{Waf1}$. Por lo tanto, aunque el bloqueo del ciclo celular parece ser necesario no es suficiente.

Nuestros resultados sugieren que el tratamiento con IFNγ protege a loa macrófagos de la muerte por apoptosis. Este efecto protector está mediado por la inducción de $p21^{Waf1}$ y por el bloqueo del ciclo celular a nivel de la barrera G_1/S. Ambos procesos son necesarios aunque no suficientes.

Interferon γ Induces the Expression of p21^{waf-1} and Arrests Macrophage Cell Cycle, Preventing Induction of Apoptosis

Summary

Incubation of bone marrow macrophages with lipopolysaccharide (LPS) or interferon γ (IFNγ) blocks macrophage proliferation. LPS treatment or M-CSF withdrawal arrests the cell cycle at early G_1 and induces apoptosis. Treatment of macrophages with IFNγ stops the cell cycle later, at the G_1/S boundary, induces p21^{Waf1}, and does not induce apoptosis. Moreover, pretreatment of macrophages with IFNγ protects from apoptosis induced by several stimuli. Inhibition of p21^{Waf1} with antisense oligonucleotides or using KO mice shows that the induction of p21^{Waf1} by IFNγ mediates this protection. Thus, IFNγ makes macrophages unresponsive to apoptotic stimuli by inducing p21^{Waf1} and arresting the cell cycle at the G_1/S boundary. Therefore, the cells of the innate immune system could only survive while they were functionally active.

Introduction

Under different external stimuli, cells are able to proliferate, to become activated and carry out their function, to remain quiescent, or to die through apoptosis. Although these events were initially considered as independent, recent reports have shown a cross-talk between the proliferative capacity of the cells and their activation or susceptibility to die through apoptosis. Thus, many mechanisms that induce cells to proliferate or become activated also induce them to undergo apoptosis (Evan et al., 1992; Meikrantz and Schlegel, 1995; Zhu and Anasetti, 1995; Levkau et al., 1998).

The commitment of cells to enter the S phase of the cell cycle occurs at a restriction point (R) late in G_1 phase, after which the cells do not need mitogenic growth factors to complete division (Pardee, 1989). The progression from the G_1 to the S phases is controlled by G_1 cyclins that bind to cdks (cyclin-dependent kinases) to form holoenzymes that phosphorylate substrates that facilitate the progression (Sherr, 1994a). When cells enter the cycle from quiescence (G_0), during the G_1 interval, D-type and E-type cyclins are sequentially synthesized (Matsushime et al., 1991); both cyclins are rate limiting for entry in the S phase. D-type cyclins are regulated by extracellular signals, whereas the expression of E, A, and B cyclins during the cell cycle is periodic. Unlike other cdks, cyclin D±dependent kinases have a distinct substrate preference for the retinoblastoma protein (pRb) (Matsushime et al., 1992). pRb binds and negatively regulates transcription factors that are necessary for S phase entry (Sherr, 1994b). However, the phosphorylation of pRb by cyclin D/E-cdk complexes at or near the R point cancels its growth-suppressive function, thus releasing the transcription factors and allowing them to activate genes necessary for S phase entry (Sherr and Roberts, 1995).

Recently, two families of mammalian G_1 cdk inhibitors, the CIP/KIP (p21, p27, and p57) and the INK-4 (p15, p16, p18, and p19), have been described (reviewed in Sherr and Roberts, 1995). These inhibitors help to explain how antiproliferative signals arrest cells in G_1 and also the arrest induced by DNA damage, terminal differentiation, or cell senescence. These cdk inhibitors bind to cyclin-cdk complexes, particularly to G_1-cyclin-cdk complexes, thus inducing cell cycle arrest.

Apoptosis is a genetically controlled process of programmed cell death. Recently, genes important for the regulation of apoptosis have been identified (White, 1996). These include many genes first thought to be involved in cell growth and differentiation (Vaux and Strasser, 1996). Apoptosis sustains tissue homeostasis by balancing the proliferative capabilities of different cells. Thus, cells with a higher proliferation rate are more susceptible to apoptosis. The regulatory coupling of proliferation and apoptosis is suggested by several observations. For example, the expression of the protooncogene c-myc stimulates cell proliferation and can also predispose cells toward apoptosis when growth factors are scarce (Evan et al., 1992). Moreover, the activation of the expression of cyclin D (Freeman et al., 1994) or the activation of various cdks has been linked with the induction of apoptosis (Meikrantz et al., 1994; Shi et al., 1994; Wei et al., 1997; Zhang et al., 1997). More recent work now indicates that the apoptosis regulatory proteins themselves can also directly modulate the cell cycle progression of the cells (Brady et al., 1996; Linette et al,. 1996; Mazel et al., 1996; O'Reilly et al., 1996). Whereas antiapoptotic genes like bcl-2 delay cell cycle progression, bax and other proapoptotic genes increase the number of cycling cells.

To carry out their functional activities, macrophages have to become activated. After interacting with IFNγ,

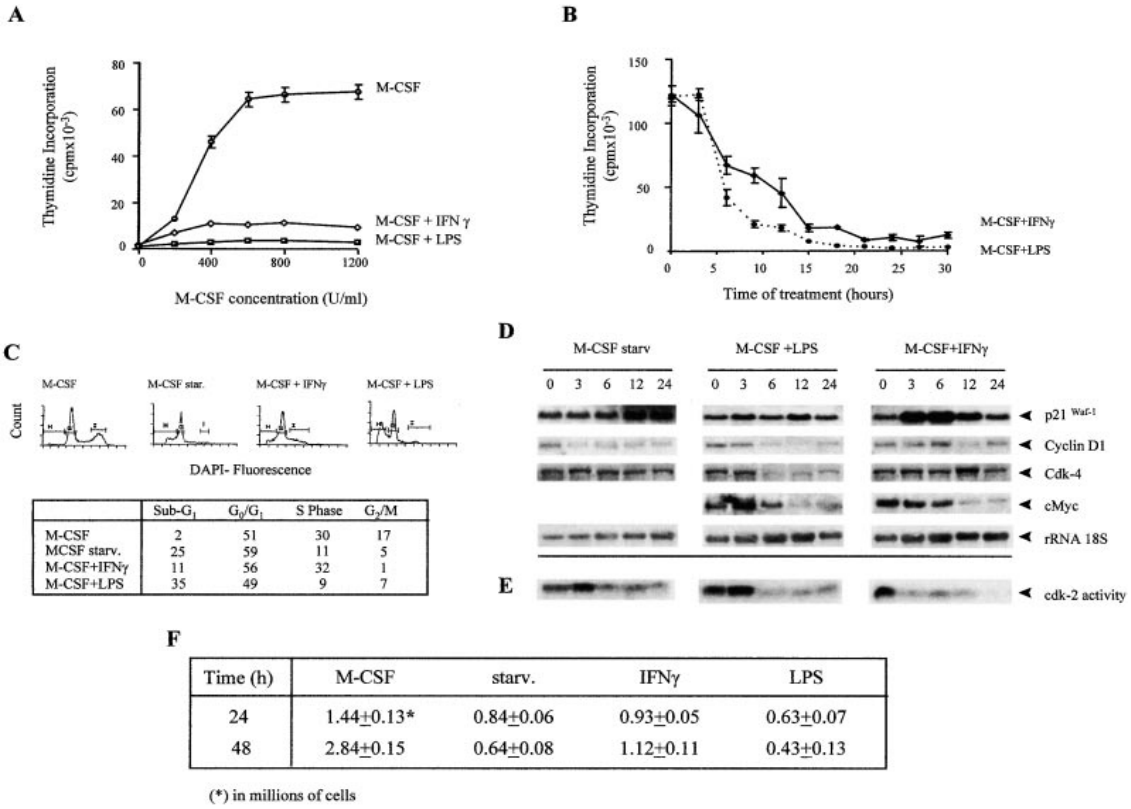

	Sub-G_1	G_0/G_1	S Phase	G_2/M
M-CSF	2	51	30	17
MCSF starv.	25	59	11	5
M-CSF+IFNγ	11	56	32	1
M-CSF+LPS	35	49	9	7

F

Time (h)	M-CSF	starv.	IFNγ	LPS
24	1.44±0.13*	0.84±0.06	0.93±0.05	0.63±0.07
48	2.84±0.15	0.64±0.08	1.12±0.11	0.43±0.13

(*) in millions of cells

Figure 1. LPS and IFN γ Inhibit M-CSF-Dependent Proliferation of Macrophages

(A) M-CSF-dependent ^{3}H-Thymidine incorporation in macrophages. BMDM were grown for 5 days before measuring thymidine incorporation as indicated in the Experimental Procedures. The cells were incubated for 24 hr with different concentrations of M-CSF alone (M-CSF) or supplemented with saturating amounts of IFN γ (250 U/ml) (M-CSF + IFN γ) or LPS (100 ng/ml) (M-CSF + LPS). This figure represents one of four independent experiments with the standard error of triplicates for each point. (B) Time course of IFN g and LPS inhibition of cell proliferation. Macrophages growing in the presence of 1200 U/ml of M-CSF were treated with 250 U/ml IFN γ or 100 ng/ml LPS. ^{3}H-Thymidine was added at 3 hr intervals, and samples were fixed after 2 additional hr of incubation. (C) Cell cycle analysis of BMDM treated with M-CSF, M-CSF starvation, M-CSF + IFN γ, and M-CSF + LPS. Macrophages growing in the presence of 1200 U/ml M-CSF (M-CSF), treated for 24 hr with 250 U/ml of IFN g (M-CSF 1 IFN g), 6 hr with 100 ng/ml LPS (M-CSF + LPS), or starved of M-CSF for 24 hr were washed, stained with DAPI, and fixed. The DNA content was measured using a flow cytometer. Exponentially growing cells appear in the graph with two peaks corresponding to cells in G0/G_1 phase (G) and cells with double DNA content in G_2/M phase (I). Apoptotic cells appear as a peak to the left of the G_0/G_1 peak due to their lower DNA content (H). (D) Northern blot analysis of the effect of M-CSF starvation, IFN γ, or LPS on different components of the cell cycle. (E) Effect of M-CSF starvation, IFN γ, or LPS on cdk2 kinase activity. Kinase activity was assayed by immunoprecipitation of cdk2 and using Histone H1 as a substrate of phosphorylation. (F) Counting of viable cells after M-CSF starvation, IFN γ, or LPS treatment measured by Trypan blue exclusion and using a hemocytometer. Each point was performed in triplicate, and the results were represented as the mean 6±SD.

a cytokine released by activated T lymphocytes, the macrophages undergo biochemical and morphological modifications that allow them to perform their functional activity (Schreiber and Celada, 1985). Although IFN γ is the major macrophage activator, other molecules such as lipopolysaccharid e (LPS) , the main componen t of the wall of gram-negative bacteria, can induce some aspects of macrophage activation.

We studied how and by which mechanism IFN g modulates cell proliferation and apoptosis using bone marrow±derived macrophages (BMDM) as a model. These are nontransformed cells that, when activated with LPS or interferon γ (IFN γ), inhibit macrophage-colony stimulating factor (M-CSF)-dependent proliferation. However, whereas these cells undergo apoptosis with LPS, macrophages treated with IFN γ are not apoptotic. In fact, treatment of these cells with IFN γ protects them from apoptosis induced by LPS, growth factor deprivation, or dexamethasone. IFN g induces p21^{Waf1} expression, the repression of which abrogates the protective effect of IFN γ on apoptosis. Our results demonstrate that the expression of p21^{Waf1} and the blocking of the cell cycle

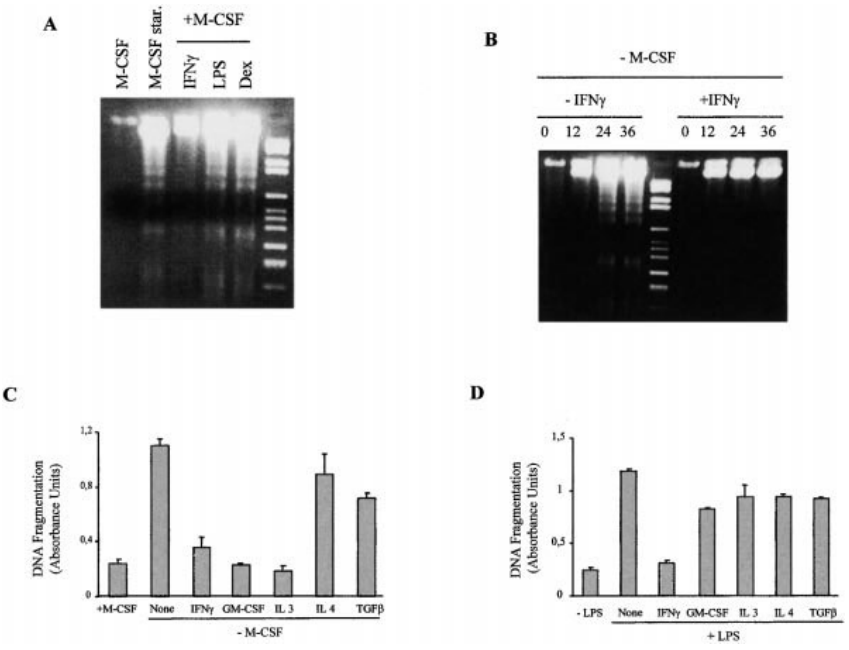

Figure 2. IFNγ Protects Macrophages against Apoptosis

(A) M-CSF starvation or treatment with LPS or dexamethasone induces macrophage apoptosis. Macrophages growing in the presence of 1200 U/ml of M-CSF were treated for 12 hr with 250 U/ml IFNγ, 100 ng/ml LPS, or 10 mg/ml dexamethasone or grown in the absence of M-CSF for 24 hr. Apoptosis was determined visualizing DNA fragmentation.

(B) IFNγ protects macrophages against apoptosis induced by M-CSF starvation. Exponentially growing BMDM in the presence of M-CSF were cultured without M-CSF for 0, 12, 24, and 36 hr. These cells were supplemented with or without 250 U/ml of IFNγ during this period of starvation. Apoptosis was determined by apoptotic DNA laddering using agarose gel electrophoresis. These experiments were performed at least three times with similar results.

(C) IFNγ and the growth factors GM-CSF and IL-3 protect M-CSF starved macrophages from apoptosis. Macrophages were cultured with M-CSF for 24 hr (+ M-CSF) or in the absence of M-CSF but with the media supplemented with 250 U/ml of IFNγ or 10 ng/ml of the following: GM-CSF, IL-3, IL-4, or TGF β. The induction of apoptosis measured as DNA fragmentation was analyzed using an ELISA kit. Each treatment was performed three times, and the results were represented as the mean value plus standard error. (D) IFNg protects macrophages from LPS-induced apoptosis. Macrophages were pretreated with 250 U/ml of IFNγ or 10 ng/ml of GM-CSF, IL-3, IL-4, or TGF β for 12 hr in presence of 1200 U/ml M-CSF and then stimulated with 100 ng/ml of LPS for 6 more hr. Apoptosis was determined as in (C).

at the G_1/S boundary make the cells unresponsive to apoptotic stimuli.

Results

In our studies, we used bone marrow±derived macrophages, which are a homogeneous population of primary and quiescent cells. When treated with M-CSF, macrophages proliferate in a dose-dependent manner (Figure 1A), and withdrawal of M-CSF induces an arrest of macrophage proliferation. Two macrophage activators, IFNγ and LPS, inhibit M-CSF-dependent proliferation (Figures 1A and 1B). After the addition of IFNγ or LPS, the proliferation of macrophages decreases progressively at 12±15 hr. Therefore, macrophages either proliferate with M-CSF or they become activated with IFNγ or LPS and thus stop proliferating.

Macrophages growing in the presence of M-CSF showed a homogeneous distribution throughout the cell cycle (Figure 1C). M-CSF starvation stopped the cell cycle at the beginning of G_1. Although both IFNγ and LPS activate macrophages, they inhibited proliferation and blocked the cell cycle at different points. Inhibition by LPS occurred at the beginning of the G_1 phase (Figure 1C), close to where the cell cycle is inhibited by M-CSF withdrawal. However, IFNγ blocked the cell cycle later, at the G_1/S boundary (Figure 1C). Although some cells were in S phase after IFNγ treatment, they did not incorporate thymidine, and the total number of cells did not increase after 24 hr (Figure 1F). These results are in accordance with the time elapsed until macrophages reentered the S phase, after the end of LPS or IFNγ blockage; i.e., 8 and 1 hr later, respectively (Vadiveloo et al., 1996), thus indicating the relative position of these blocking points within the G_1 phase.

Next, we analyzed the expression of different cell cycle genes that might be modulated by IFNγ, LPS, or M-CSF withdrawal to inhibit proliferation. The cell cycle block induced by M-CSF starvation was caused by an inhibition of cyclin D1 gene expression (64% inhibition) (Figure 1D; Matsushime et al., 1991) similar to that induced by LPS (72% inhibition). LPS also inhibited cdk-4 gene expression (71%). Neither M-CSF withdrawal nor LPS significantly modified $p21^{Waf1}$ gene expression. However, IFNγ induced a transient expression of $p21^{Waf1}$, a dual inhibitor of cyclin-dependent kinases (3.4-fold increase at 6 hr) (Gu et al., 1993; Harper et al., 1993; Xiong et al., 1993). The analysis of the expression of cyclin D_1 and cdk-4 mRNA (Figure 1D) or the formation of these complexes by immunoprecipitation and immunoblotting revealed that neither is significantly modified by IFNγ (data not shown). Moreover, both LPS and IFNγ inhibited the expression of the protooncogene c-myc. We also analyzed the kinase activity of cdk2 using His-

tone H1 as a substrate (Figure 1E). As expected, both IFN g and LPS decreased cdk-2 activity, which is necessary for entry and passage through the S phase of the cell cycle.

All cell types require specific factors to remain viable, and the withdrawal of these factors results in apoptotic cell death (Sachs and Lotem, 1993). Nontransformed macrophages are not an exception to this rule and require the presence of M-CSF for proliferation and survival (Tushinski and Stanley, 1985). After M-CSF withdrawal, the analysis of the cell DNA content showed a subdiploid peak corresponding to apoptotic cells (Figure 1C). After 24 hr of M-CSF withdrawal, this affected around 25% of the total macrophage population. Besides, the treatment for 6 hr with 100 ng/ml LPS clearly induced a subdiploid peak corresponding to apoptotic cells for more than 35% of the total macrophage population. However, the treatment with IFN γ for up to 24 hr had little effect on the induction of apoptosis (Figure 1C). Moreover, the analysis of the number of surviving cells after these treatments confirmed that whereas M-CSF withdrawal or LPS treatment reduced the number of viable cells after 24 and 48 hr, IFN γ did not modify the initial number of cultured cells but inhibited their proliferation in the presence of M-CSF (Figure 1F). DNA laddering analysis confirmed the induction of apoptosis by LPS and M-CSF starvation and the absence of IFN γ effect. The apoptotic gene Bax was particularly induced in cells treated with LPS or M-CSF withdrawal, whereas no induction was observed in IFN γ treated macrophages (data not shown). Besides, we observed that 10 mg/ml dexamethasone also induced apoptosis in BMDM (Figure 2A).

Although both the endogenous (IFN γ) and the exogenous (LPS) macrophage activators blocked cell proliferation, the difference observed in the capacity to induce apoptosis led us to study the effects of IFN γ on agents that induce apoptosis in macrophages. As shown in Figure 2B, M-CSF deprivation induced in BMDM an internucleosomal pattern of DNA fragmentation (DNA laddering) detectable after 24 hr, with a maximum at 36 hr. In a parallel experiment, IFN γ (250 U/ml) was added to macrophages simultaneously to M-CSF removal. Under these conditions, IFN g protected against apoptosis induced by M-CSF starvation (Figure 2B). The incubation of macrophages with 250 U/ml IFN γ suppressed the fragmentation of the DNA during the induction of apoptosis at all the time points tested during 48 hr of M-CSF deprivation. We also studied whether other cytokines besides IFN γ inhibited the induction of apoptosis by M-CSF starvation (Figure 2C). The induction of apoptosis, as described in the Experimental Procedures, was measured as the quantitation of DNA fragmentation using an ELISA technique (Boehringer Mannheim). Only growth factors GM-CSF and IL-3 protected starved

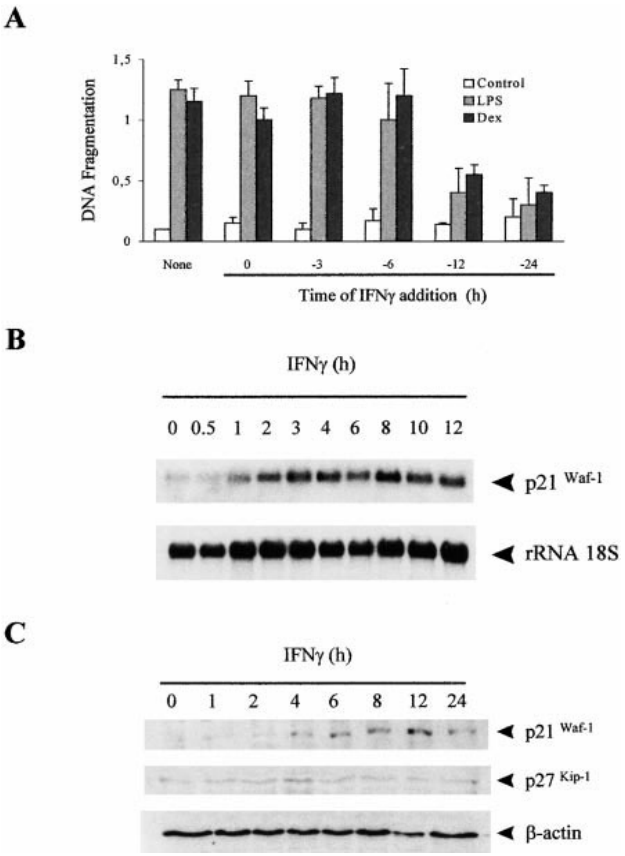

Figure 3. Time Course of IFN γ Protection against Apoptosis Induced by LPS or Dexamethasone

(A) Time of preincubation with IFN γ required to protect against LPS- or dexamethasone-induced apoptosis. BMDM were preincubated with IFN γ (250 U/ml) for the indicated time and then LPS (100 ng/ml) or dexamethasone (10 mg/ml) was added and the cells were incubated for 6 more hr. Apoptosis was determined using an ELISA kit. Each treatment was performed three times, and the results were represented as the mean value plus standard error. (B) Time course of IFN γ-induced expression of $p21^{Waf1}$ mRNA. BMDM were incubated with IFN γ (250 U/ml) for different periods of time and then the expression of $p21^{Waf1}$ was determined by Northern blotting or Western blotting (C). $p27^{kip1}$ expression was also analyzed by Western blotting.

macrophages against apoptosis, whereas IL-4 and TGF β did not. Both GM-CSF and IL-3 induce macrophage proliferation in the absence of M-CSF (Celada and Maki, 1992). To determine if the protective effect of IFN γ on apoptosis in macrophages was related solely to the withdrawal of M-CSF, we tested LPS as an apoptotic stimulus. As shown in Figure 2D, IFN γ also protected LPS-mediated apoptosis. To protect against LPS-induced apoptosis, macrophages must be pretreated for 12 hr with IFN γ. None of the other growth factors or cytokines tested protected against the induction of apoptosis by

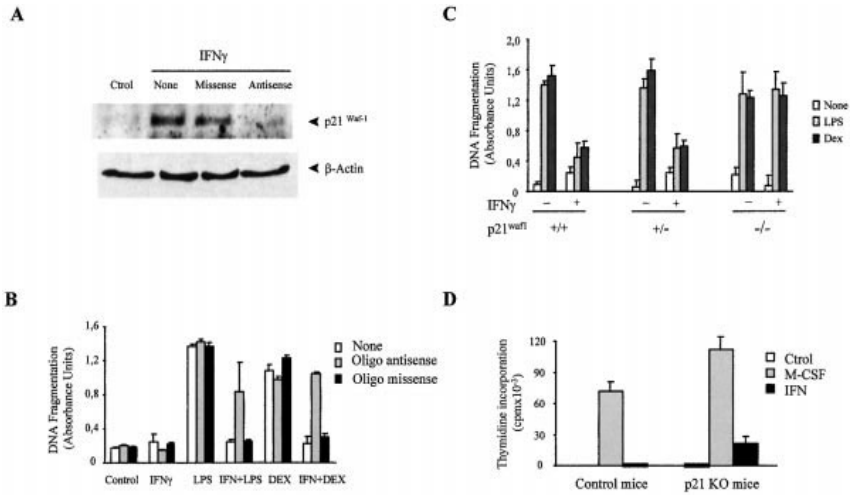

Figure 4. Expression of p21^{Waf1} Is Required for the Antiapoptotic Effect of IFN γ

(A) Antisense oligonucleotides against p21^{Waf1} inhibit the IFN γ induction of p21^{Waf1}. BMDM were incubated for 12 hr with media (control), 10 μM antisense, or missense phosphothioated oligonucleotides. Then, IFN γ (250 U/ml) or media was added and p21^{Waf1} and β-actin expression were determined by Western blotting 24 hr later.

(B) p21^{Waf1} antisense blocks the IFN γ inhibition of LPS- or dexamethasone-induced apoptosis. BMDM were incubated with antisense oligonucleotides as indicated above and pretreated or not with 250 U/ml IFN γ. The induction of apoptosis after 6 hr of treatment with LPS (100 ng/ml) or dexamethasone (10 mg/ml) was analyzed.

(C) IFN γ does not inhibit apoptosis in macrophages from p21^{Waf1} KO mice. IFN γ protective effect was analyzed in BMDM obtained from normal homozygote (+/+), heterozygote (+/-), or knockout (-/-) mice for p21^{Waf1}. Macrophages were pretreated or not with 250 U/ml IFN γ for 24 hr. Then, macrophages were treated for 6 more hr with 100 ng/ml LPS or 10 mg/ml dexamethasone. Induction of apoptosis was measured as indicated above. Each treatment was performed three times, and the results were represented as the mean value plus standard error.

(D) IFN γ inhibits proliferation in macrophages from p21 KO mice. 10^5 macrophages from p21 KO or wild-type mice were incubated in 24-well plates in the presence of 1200 U/ml of M-CSF either alone or with 300 U/ml IFN γ. Proliferation was determined as indicated in the Experimental Procedures. The experiments with the antisense oligonucleotides and p21 KO mice were performed twice, with identical results.

100 ng/ml LPS when they were administered 12 hr before LPS (Figure 2D). Moreover, IFN γ also protected macrophages against apoptosis induced by dexamethasone (Figure 3A). Thus, IFN γ protected specifically against apoptosis induced by different stimuli in macrophages.

The inhibitory effect of IFN γ on the M-CSF-dependent proliferation is not immediate and requires several hours of treatment. At least 12 hr of pretreatment with IFN g was needed to protect against LPS- or dexamethasone-induce d apoptosis ; besid es, the protecti on of IF Nγ ag ain st apoptosis was not effective when both activators were added at the same time (Figure 3A). These results led us to study a possible relationship between cell cycle progression and protection against apoptosis. As treating macrophages with IFN γ induces a stop of the cell cycle at the G_1/S boundary, we analyzed the expression of G_1 cyclin-dependent kinases and cell cycle regulatory proteins involved in the G_1 progression, which could also be regulating apoptosis. IFN γ induced in macrophages the expression of p21^{waf1} without modifying the levels of cyclin D1-cdk-4 mRNA expression (Figure 1D). The IFN γ-induced expression of p21^{waf1} mRNA (Figure 3B) and protein (Figure 3C) was detected after 2 and 4 hr of treatment with IFN γ, respectively, and this expression was maintained during the timing of the experiments. IFN γ induces the expression of p21^{waf1} through a p53-independent pathway that requires Stat-1 activation (Chin et al., 1996). In accordance with this observation, no induction of p53 protein expression by IFN γ was detected (data not shown). Moreover, no induction of p27^{Kip1} was observed after treating the macrophages with IFN γ (Figure 3C).

The data presented thus far indicate that the protection of apoptosis by IFN γ correlated with the inhibition of proliferation and the expression of p21^{waf1}. To determine if the protective effects of IFN γ are only caused by the induction of p21^{waf1} or by the expression/repression of other genes, we designed an experiment to block the induction of p21^{waf1} by IFN γ using antisense constructions. The expression of p21^{waf1} was inhibited with an antisense oligonucleotide complementary to a region that includes the initiation codon of p21^{waf1}. A missense oligonucleotide was used as a control (see the Experimental Procedures). In previous experiments, using fluoresceinated oligonucleotides we determined the time necessary for oligonucleotide uptake by macrophages. Uptake was detected after 8 hr of incubation and reached a plateau after 24 hr of incubation (data not shown). The experiments summarized in Figure 4 were carried out by incubating the macrophages for 12 hr with antisense or missense oligonucleotides, and then IFN g was added for 24 hr in the presence of the same oligonucleotides. Under these conditions, antisense oligonucleotides specifically blocked the expression of p21^{waf1} protein induced by IFN γ (Figure 4A). In parallel experiments, after the oligonucleotide incubation, IFN γ, LPS, or dexamethasone was added for 6 hr more. Apoptosis was then determined. Neither the antisense nor the missense oligonucleotides induced apoptosis or blocked the induction of apoptosis by LPS or dexameth-

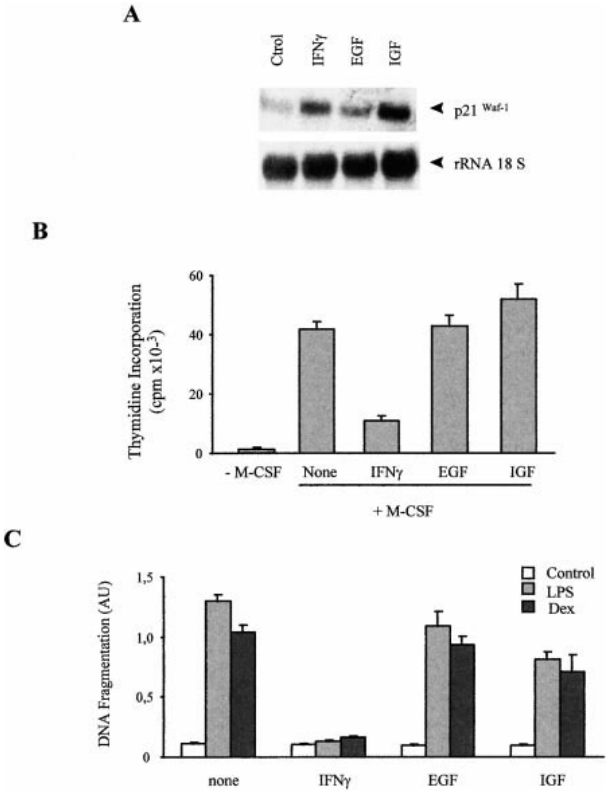

Figure 5. IGF-I Increases p21 ^{Waf1} Expression in Macrophages

(A) BMDM were incubated with media, 250 U/ml IFN γ, 20 nM EGF, or 50 nM IGF-I for 12 hr. p21 ^{Waf1} expression was determined by Northern blotting. (B) IGF-I does not inhibit M-CSF-dependent proliferation. BMDM were incubated in the absence (-M-CSF) or the presence (+ M-CSF) of 1200 U/ml M-CSF and 20 nM EGF, 50 nM IGF-I, or 250 U/ml IFN γ for 24 hr, and then thymidine incorporation was determined. (C) IGF-I does not protect macrophages against apoptosis. BMDM pretreated for 12 hr with media (none), 250 U/ml IFN γ, 20 nM EGF, or 50 nM IGF-I were treated with LPS (8100 ng/ml) or dexamethasone (10 μg/ml). Induction of apoptosis was determined with an ELISA kit directed against histone-associated DNA fragments.

asone. However, the antisense but not the control oligonucleotides inhibited the protective effect of IFN γ on apoptosis induced by LPS or dexamethasone (Figure 4B). These results suggested that the effect of IFN γ protecting macrophages against apoptosis was mediated by p21 ^{waf1} expression.

To confirm whether induction of p21 ^{waf1} is required for the protective effect of IFN γ on apoptosis, we carried out similar experiments with p21 ^{waf1} knockout mice (Deng et al., 1995). LPS and dexamethasone induced the same degree of apoptosis in macrophages from these mice and in those from the controls (Figure 4C). However, whereas IFN γ pretreatment protected macrophages against apoptosis in control mice, no protection was observed in the p21 ^{waf1} KO mice. Thus, p21 ^{waf1} is involved in the protection by IFN γ against apoptosis.

We also analyzed whether p21 ^{Waf1} was involved in the inhibition of proliferation by IFN γ in macrophages from these p21 KO mice (Figure 4D). Macrophages from mice with the p21 gene disrupted proliferated 41% more than cells from the control mice p21 ^{Waf1} . Therefore, p21 ^{Waf1} might be involved in regulating macrophage proliferation. But IFN γ still inhibited macrophage proliferation in these cells, although with a lower rate than in wild-type macrophages. Thus, the induction of p21 ^{Waf1} expression by IFN γ is not necessary, as IFN γ also inhibits proliferation in these cells.

In order to determine if p21 ^{waf1} has a pivotal role as an inhibitor of apoptosis, we treated macrophages with other growth and differentiating factors that have been described to induce the expression of p21 ^{waf1} (Chen et al., 1995; Chin et al., 1996). Macrophages treated with insulin-like growth factor-I (IGF-I) had an increased p21 ^{waf1} mRNA expression (Figure 5A). No such increase was found when the cells were incubated with epidermal growth factor (EGF) in the same conditions. Surprisingly, and in contrast with what was observed with IFN γ, although p21 ^{waf1} was induced in macrophages treated with IGF-1, no inhibition of M-CSF-dependent proliferation was observed (Figure 5B). Besides, apoptosis induced by LPS or dexamethasone was not inhibited by pretreatment with IGF-1 (Figure 5C). These results showed that the protective role of p21 ^{waf1} on the induction of apoptosis is not due to a direct inhibition of apoptosis. Therefore, p21 ^{waf1} was necessary but not sufficient to cause a direct inhibition of apoptosis, and it seemed that, at least, the cell cycle also had to be stopped.

As IFN γ blocked the cell cycle at a different point than LPS (Vadiveloo et al., 1996), we studied whether this effect correlated with apoptosis protection. Using different drugs, we stopped the cell cycle of macrophages at different points, as shown by cytometric analysis (Figure 6A) and for the time necessary to resume cell cycling after removal of the inhibitor (Figure 6B). After 14 hr of treatment, mimosine stopped macrophages at the middle-late G_1, whereas aphidicolin and OH-Urea did so at the G_1/S boundary and nocodazole at the G_2/M phase. Both LPS and dexamethasone induced apoptosis in macrophages pretreated with mimosine, afidicoline, or nocodazole (Figure 6C). However, no apoptosis was induced by LPS or dexamethasone in cells treated with OH-Urea (Figure 6C). As aphidicolin and OH-Urea block the cell cycle at a very similar point (Fox et al., 1987), cell cycle arrest at the G_1/S boundary is not the only mechanism to protect against apoptosis. In agreement with our results that showed that the induction of p21 ^{waf1} was involved in protection against apoptosis, we observed that OH-Urea but not aphidicolin induced the expression of p21 ^{waf1} in macrophages; this induction cor-

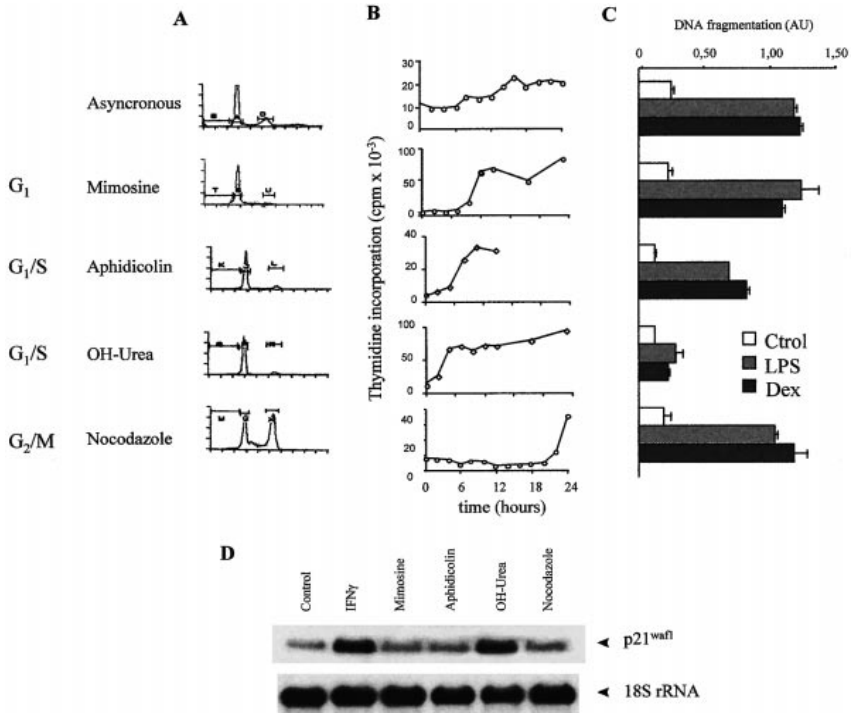

Figure 6. The Macrophages at the G_1/S Boundary that Express $p21^{Waf1}$ Become Resistant to the Apoptotic Stimuli

BMDM were incubated with 400 μM mimosine, 10 μg/ml aphidicolin, OH-Urea, or nocodazole for 14 hr. The position in the cell cycle after the treatment of macrophages with cell cycle inhibitors was determined by cytometric analysis (A) and by the time necessary for [^{3}H]-thymidine incorporation after withdrawal of the inhibitor and M-CSF stimulation (B). After synchronization, the cells were washed and stimulated with 1200 U/ml M-CSF in the presence of 1 μCi/ml of [^{3}H]-thymidine. The samples were obtained every 2 hr. (C) Macrophages treated with OH-Urea are unresponsive to apoptotic stimuli. BMDM were incubated as described in (A), washed, and then LPS (100 ng/ml) or dexamethasone (10 μg/ml) was added for 6 hr, and apoptosis was determined using an ELISA kit. (D) The protective effect of OH-Urea correlates with the expression of $p21^{Waf1}$. The expression of $p21^{Waf1}$ mRNA was analyzed by Northern blotting in macrophages treated for 14 hr with each cell cycle inhibitor or with IFN γ.

related with the protective effect against the induction of apoptosis.

All of these results show that both the expression of $p21^{waf1}$ and the cell cycle arrest at the G_1/S boundary induced by IFN γ are required for the protection against apoptosis mediated by LPS or dexamethasone.

Discussion

One of the features of the immune system is the production of a large amount of any type of cells. Later, most unnecessary cells die through apoptosis. However, the small amount of cells required to develop a functional activity survive. In B lymphocytes, antigen receptor triggering gives these cells a long life (Lam et al., 1997). Similarly, in the absence of appropriate MHC expression in the periphery, the half-life of naive T cells is substantially shortened. Thus, the long persistence of naive T cells in the absence of an intentional antigenic stimulation partially reflects the continued tickling by MHC (Tanchot et al., 1997). Moreover, the viability of the immune cells may be regulated by the presence of growth factors and cytokines. In this regard, the ability of IFN γ to induce programmed cell death has been suggested as a role of this cytokine in the negative selection by apoptosis of the peripheral T and B lymphocyte repertoire (Liu and Janeway, 1990; Grawunder et al., 1993). Nevertheless, IFN γ is also involved in prosurvival signals in normal and leukemic cells (Mangan et al., 1991; Buschle et al., 1993; Bach and Brashler, 1995; Sangfelt et al., 1996). Therefore, depending on the target cells, IFN γ can induce either death or protection against apoptosis.

In this study, we found that IFN γ, the immune mediator that activates macrophages, protects these cells against apoptosis. Therefore, like T and B cells, macrophages survive when they are useful to the immune system and develop a functional activity after activation by IFN γ. The protection by IFN γ against apoptotic stimuli requires the expression of $p21^{Waf1}$ and the arrest of the cell cycle in a very precise position: the G_1/S boundary. This is an example of interaction between proliferation, cell cycling, and apoptosis.

Experiments using antisense and $p21^{Waf1}$ KO mice demonstrated that $p21^{Waf1}$ is the critical molecule induced by IFN γ to block apoptosis. These results are in agreement with previous works that showed the antiapoptotic role of $p21^{Waf1}$. The overexpression of $p21^{Waf1}$ in glioma cells prevents apoptosis (Gomez-Manzano et al., 1997). In differentiating myocytes, the expression of $p21^{Waf1}$ confers resistance against apoptosis (Wang and Walsh, 1996). In differentiating neuroblastoma cells, antisense oligonucleotides to $p21^{Waf1}$ enhance cell death by apoptosis (Poluha et al., 1996). Finally, the expression of p53 in a series of colorectal cancer cell lines resulted in growth arrest in some lines and apoptosis in others. The inactivation of $p21^{Waf1}$ in these cells by homologous recombination changed a cell line with growth arrest to an apoptotic cell, suggesting that, despite inducing growth arrest, $p21^{Waf1}$ could protect against apoptosis

(Polyak et al., 1996). Thus, $p21^{Waf1}$ seems to be a critical molecule for the survival of cells, even with apoptotic stimuli. Although $p21^{Waf1}$ was first described as a p53-induced gene (El-Deiry et al., 1993), in many cases a p53-independent expression of $p21^{Waf1}$ has been found (Parker et al., 1995; Zhang et al., 1995). This seems to be the case of the $p21^{Waf1}$ induction by IFN γ in epidermal cells (Chin et al., 1996) or macrophages (data not shown). The induction of $p21^{Waf1}$ by IFN γ is mediated through the interferon regulatory factor-1 (IRF-1) (Tanaka et al., 1996) and also through STAT1 (Chin et al., 1996). All of these observations indicate that $p21^{Waf1}$, induced or not by p53, could play a role in the control of apoptosis.

Our experiments showed that the protection of IFN γ against apoptosis could be related to the effect of $p21^{Waf1}$. Several reports have shown that the activation of various cdk complexes correlates with apoptosis (Meikrantz et al., 1994; Shi et al., 1994; Wei et al., 1997; Zhang et al., 1997). Therefore, the inhibition of these apoptotic cdk activities by cdk inhibitors like $p21^{Waf1}$ could explain the protection against apoptosis induced by these molecules. However, the fact that $p21^{Waf1}$ induced by IGF-I does not protect macrophages against apoptosis suggests that the expression of $p21^{Waf1}$ is by itself not sufficient and that complementary mechanisms are necessary.

The protective effect of IFN γ may also be caused by the arrest of the cell cycle in a specific point, different from that induced by LPS activation or M-CSF withdrawal. The requirement of preincubation with IFN γ may be related to the time necessary to stop the M-CSF-proliferating macrophages and to enter in the late G_1 phase. Although c-Myc expression has been involved both in IFN γ-mediated inhibition of macrophage proliferation (Vairo et al., 1995) and in regulation of apoptosis (Evan et al., 1992), our results showed that c-myc does not seem to be involved in the protective effect of IFN γ, since its expression is also inhibited by LPS. Also, the role of $p21^{Waf1}$ in IFN γ-mediated growth arrest is unclear (Chin et al., 1996; Sharma and Iozzo, 1998). However, our results with the $p21^{Waf1}$ KO mice demonstrate that although $p21^{Waf1}$ could play a role in the inhibition of macrophage proliferation, its expression is not necessary and thus other mechanisms may be involved. These results are in agreement with those previously published by Sharma and Iozzo (1998).

Blocking the cell cycle progression with inhibitors of cyclin-dependent kinases could make cells resistant to apoptotic stimuli. For example, the apoptotic process termed T cell receptor antigen-induced cell death occurs at late G_1 phase of the cell cycle (Lissy et al., 1998). T cells stimulated to undergo apoptosis can be rescued by effecting an early G_1 block by direct transduction of $p16^{INK4a}$. Similarly, when deprived of nerve growth factor, postmitotic sympathetic neurons and neuroblastoma cells undergo apoptosis and can be rescued by transfection of $p16^{INK4a}$ (Freeman et al., 1994; Kranenburg et al., 1996). Moreover, apoptosis in T cells could be blocked by inhibiting their progression through the S phase treating the cells with OH-Urea (Zhu and Anasetti, 1995; Dao et al., 1997).

The effect of IFN γ on macrophage apoptosis is not only due to an arrest of the cell cycle at the G_1/S boundary, since treatment of macrophages with OH-Urea protects them against apoptosis (as described in T cells); this is not the case with aphidicolin, which blocks the cell cycle at a very similar point. This difference could be due to the fact that OH-Urea but not aphidicolin induces the expression of $p21^{Waf1}$. Therefore, IFN γ protects macrophages against apoptosis by inducing $p21^{Waf1}$ and blocking the cell cycle at the G_1/S boundary. Both events are necessary for protection against apoptosis.

Recently, it has also been reported that $p21^{Waf1}$ protects monocytes against apoptosis during its differentiation (Asada et al., 1999). The authors assign the protective role to the cytoplasmic $p21^{Waf1}$ and suggest that this effect could be independent of that of $p21^{Waf1}$ on the cell cycle, since they use a p21 mutant that can not enter the nucleus and thus cannot affect cell cycle progression. However, in normal conditions the cell cycle blockage induced by IFN γ treatment could be responsible for this cytoplasmic localization of $p21^{Waf1}$.

Our results could have physiological relevance. Neutrophils and macrophages play a critical role during inflammation. Neutrophils take part in the early steps of the inflammatory process, leaving after 24 to 48 hr, whereas macrophages arrive late to the inflammatory foci and remain there until inflammation disappears (Bellingan et al., 1996), that is, while stimulated Th1 cells produce IFN γ. Later, macrophages also disappear. Although both cell types are derived from the same precursor, the GM-CFU, and they share some functional activities, their roles during inflammation are totally different. Neutrophils are primarily involved in phagocytosis and destruction of the agents that cause inflammation. Although macrophages can phagocyte a large number of microorganisms, their primary role is to remove all cellular debris and to induce tissue repair. Shortly after activation, the neutrophils die. The release of nuclear and cytoplasmic components of dying cells is potentially damaging and could be related to the pathogenesis of a wide range of inflammatory diseases (Malech and Gallin, 1987). The cells of the immune system are characterized by their death after activation as a fine mechanism of regulation of their potentially destructive activity. This is the case of activation-induced apoptosis through CD-3 in T cells (Zhu and Anasetti, 1995) or apoptosis

induced by superantigen activation in lymphocytes (Ettinger et al., 1995). During the chronic phases of the immune response, macrophages play a crucial role, not only eliminating non-self structures but also removing all the debris (including apoptotic bodies) and remodeling injured tissues. In some instances, when non-self agents cannot be eliminated, macrophages produce a granuloma to isolate the pathogenic agents. Each granuloma appears as a small spherical organ consisting of some differentiated macrophages, whose function is to limit the expansion of intravascular bacteria and allow their eventual destruction (Adams, 1976; Williams and Williams, 1983). In all cases, in contrast to lymphocytes or neutrophiles, macrophages are long-term living cells within the tissues. Our observations also explain the crucial role of IFN γ on delayed hypersensitivity.

Experimental Procedures

Reagents

LPS, mimosine, aphidicolin, OH-Urea, and nocodazole were all obtained from Sigma Chemical. Recombinant murine IFN γ was kindly donated by Genetech. GM-CSF, IL-3, TGF β, and IL-4 were purchased from R & D Systems. 4, 6-diamidino-2-phenylindole (DAPI) was purchased from Calbiochem. All the other products were of the best grade available and were purchased from Sigma Chemical. Deionized water further purified with a Millipore Milli-Q system was used.

Cell Culture

Bone marrow±derived macrophages were isolated from 6-week-old BALB/c mice (Charles River Laboratories) as previously described (Celada et al., 1984). The cells were cultured in plastic tissue culture dishes (150 mm) in 40 ml DMEM containing 20% FBS and 30% L cell conditioned media as a source of M-CSF. The cells were incubated at 37 C in a humidified 5% CO_2 atmosphere. After 7 days of culture, a homogeneous population of adherent macrophages was obtained. Bone marrow±derived macrophages from $p21^{Waf1}$ knockout mice were isolated in the same conditions. $p21^{Waf1}$ knockout mice (Deng et al., 1995) were kindly donated by Dr. Philip Leder from Harvard Medical School (HHMI).

Antibodies

For the analysis of $p21^{Waf-1}$ and $p27^{Kip-1}$ expression by Western blotting, we used monoclonal anti-mouse $p21^{Waf-1}$ and anti-mouse $p27^{Kip-1}$ antibodies (PharMingen). Primary antibodies against mouse b-actin were purchased from Sigma. A peroxidase-conjugated anti-mouse IgG (Cappel, Turnhout, Belgium) was used as secondary antibody. For the assay of cdk2 kinase activity, we used an anti-cdk2 (M2) antibody from Santa Cruz Biotech.

Plasmids and Constructs

The pMH117 plasmid corresponding to the mouse $p21^{Waf-1}$ full-length cDNA cloned in pEx-lox was kindly provided by Dr. Massague (Sloan Kettering Institute, HHMI, New York, NY). The pET-3d plasmid corresponding to the D_1 cyclin cDNA was cloned in pET-12 (Xiong et al., 1991). The pCMJ3/cdk-4 plasmid contains the full-length mouse cdk-4 cDNA cloned in pBluescript KS (Matsushime et al., 1992). The murine c-myc probe was kindly donated by Dr. Evan (ICRF, London, UK). As a control of RNA loading and transfer, we used a 18S rRNA transcript (Torczynski et al., 1983).

Proliferation Assay

Cell proliferation was measured as previously described (Celada and Maki, 1992) with minor modifications. To analyze the effect of LPS and IFN γ on BMDM proliferation, the cells were deprived of M-CSF for 18 hr and then 10^5 BMDM were incubated for 24 hr in 24-well plates (3424 MARK II; Costar) in 1 ml of complete media in the presence or absence of 100 ng/ml LPS or 250 U/ml IFN γ. Then, the media was removed and replaced by 0.5 ml of media containing [^{3}H]-thymidine (1 μCi/ml). After 2 additional hr of incubation at 37 C, the media was removed and the cells were fixed in ice-cold 70% methanol. To analyze the time course of IFN γ or LPS treatment, after treating the cells with LPS or IFN γ 1 μCi/ml [^{3}H]-thymidine was added at the indicated times, and, after 2 additional hr of incubation the cells were fixed. To analyze the time necessary to enter the S phase of the cell cycle after synchronization, the cells were treated for 14 hr with the indicated cell cycle inhibitors in 24-well plates in 1 ml of complete media. Once the cells were synchronized at each phase of the cell cycle, the media was removed and the cells were washed three times with fresh media to eliminate the inhibitors. The cells were cultured with fresh complete media containing [^{3}H]-thymidine (1 μCi/ml). The samples were obtained in 2 hr intervals; the media was removed and the cells were fixed. In all cases, after fixation the cells were washed in ice-cold 10% trichloroacetic acid (TCA) and solubilized in 1% SDS and 0.3% NaOH. Radioactivity was counted by liquid scintillation using a 1500 Tri-Carb Packard scintillation counter. Each point was performed in triplicate, and the results were expressed as the mean 6±SD.

In parallel experiments, we cultured 10^6 macrophages in tissue-cultured plates with or without 1200 U/ml of M-CSF and treated with 300 U/ml IFN γ or 100 ng/ml LPS for 24 and 48 hr. Then, the number of surviving cells was measured by Trypan blue exclusion with a hemacytometer. Again, each point was performed in triplicate, and the results were expressed as the mean 6±SD.

Analysis of DNA Content with DAPI

Cells (10^6) previously subjected to a specific treatment were resuspended and fixed in ice-cold 70% ethanol. The cells were then washed in PBS, resuspended in 0.2 ml of a solution containing 150 mM NaCl, 80 mM HCl, and 0.1% Triton X-100, and incubated at 0±4 C for 10 min. Afterward, 1 ml of a solution containing 180 mM Na_2HPO_4, 90 mM citric acid, and 2 μg/ml DAPI (pH 7.4) was added to each sample. After incubating the cells at 4 C for 24 hr, their fluorescence was measured with an Epics Elite flow cytometer (Coulter). 12000 cells were counted for each histogram, and the cell cycle distributions were analyzed with the Multicycle program (Phoenix Flow Systems)

Apoptosis Analysis

Fragmentation of DNA due to internucleosomal cleavage was determined as described previously (Hogquist et al., 1991). In brief, 3 x 10^6 cells were harvested and washed in ice-cold PBS. The cells were lysed in 0.5 ml of lysis buffer (50 mM Tris-HCl, 10 mM EDTA, and 1% SDS [pH 8.0]) for 16 hr at 4 C, and the lysates were centrifuged (13000 x g) to separate high molecular weight DNA (pellet) from cleaved low molecular weight DNA (supernatant). The DNA supernatants were phenol extracted twice and precipitated. The pellets were resuspended in Tris-EDTA buffer containing 250 μg/ml RNAse (Boehringer Mannheim, Mannheim, Germany). The samples were heated at 65 C for 10 min and subjected to electrophoresis in a 2% agarose gel containing ethidium bromide.

Low molecular apoptotic DNA, obtained as indicated above, was

also measured using an ELISA technique based on the detection of histone-associated DNA fragments (Cell Death detection ELISA plus, Boehringer Mannheim). Each point was performed in triplicate, and the results were expressed as the mean 6±SD.

Protein Extraction and Western Blot Analysis

Total cell extracts were analyzed by Western blotting as described (Xaus et al., 1999a), using the $p21^{Waf1}$ or $p27^{Kip1}$ antibodies followed by peroxidase-conjugated anti-mouse IgG antibody. The blots were developed with the ECL chemiluminescence system (Amersham) and quantified by densitometric analysis.

Cdk2 Kinase Activity

Kinase activity was assayed by immunoprecipitation of 150 µg of total protein extracts using the anti-cdk2 (M2) antibody (Santa Cruz) followed by incubation with Histone H1 and γ^{32}P-ATP. The immunoprecipitation and Histone H1 kinase assay were performed exactly as described (Kranenburg et al., 1995). The kinase assays were resolved on a 12% SDS polyacrylamide gel, stained with Coomassie Blue to visualize the Histone H1 bands, dried, and exposed for autoradiography. Where required, the bands were quantified using a Molecular Analyst System (Bio-Rad).

Northern Blot Analysis

Total cellular RNA was extracted with the acid guanidinium thiocyanate-phenol-chloroform method (Chomczynski and Sacchi, 1987). The Northern blot was performed as described (Xaus et al., 1999b), using a $p21^{waf-1}$, D_1 cyclin, or a cdk-4 probe. To check for differences in RNA loading, we analyzed the expression of the 18 S rRNA transcript. All probes were labeled with ^{32}P- α-dCTP (ICN Pharmaceuticals) with the oligolabeling kit method (Pharmacia Biotech, Uppsala, Sweden). The bands of interest were quantified with a Molecular Analyst system (Bio-Rad Laboratories).

Antisense Oligonucleotides

Antisense phosphothioated-oligonucleotides specific for mouse $p21^{waf-1}$ were used to block the expression of this cdk inhibitor. Previous to the treatment with IFN γ, the cells were incubated for 12 hr in DMEM with L cell conditioned media, 5% FBS, and 10 mM phosphothioated-oligonucleotides (Biognostik GmbH, Go»ttingen, Germany). Oligonucleotides against mouse $p21^{waf-1}$ were designed as consisting of a fragment of the reverse complement of the mouse $p21^{waf-1}$ cDNA sequence that includes the transcription site. The sequence was 5'-CAGGATTGGACATGGTCGCTGTGGCTGA-3 9 for the antisense oligonucleotide and 59-GCGCCGGTAACCTCAACAGT CATCCACT-3' for the control missense oligonucleotide. The time necessary for the incorporation of the oligonucleotides in the macrophages was determined using the FITC-labeled missense oligonucleotide (Biognostik GmbH).

Acknowledgments

We thank Joan Massague ¬ from the Sloan Kettering Institute, New York; Ramon Merino, University of Cantabria, Santander, Spain; Oriol Bach, University of Barcelona, Spain; and Gerard Evan, ICRF, London, UK, for the gift of several reagents. We are also grateful to Philip Leder, Harvard Medical School (HHMI), Boston, MA, for the generous gift of the $p21^{waf-1}$ KO mice. We specially thank Gabriel Gil, Institut Municipal d'Investigacions Mediques, Barcelona, for his help with the $p21^{waf-1}$ KO mice, cdk2 kinase assays, and for discussions and critical reading of the manuscript. We acknowledge the help received from Jaume Comas and Rosario Gonza¬lez from the flow cytometry facility of the Serveis Cientı¬fico Tecnics de la Universitat de Barcelona. We also acknowledge the editorial assistance of Martin Cullel-Young. This work was supported by grants from the Comision Interministerial de Ciencia y Tecnologia (SAF98/0102 and PM 98/0200) to A. C.

References

Adams, D.O. (1976). The granulomatous inflammatory response. Am. J. Pathol. 84, 164-191.

Asada, M., Yamada, T., Ichijo, H., Delia, D., Miyazono, K., Fukumuro, K., and Mizutani, S. (1999). Apoptosis inhibitory activity of cytoplasmic $p21^{Cip1/Waf1}$ in monocytic differentiation. EMBO J. 18, 1223-1234.

Bach, M.K., and Brashler, J.R. (1995). Evidence that granulocyte/macrophage-colony-stimulating factor and interferon-gamma maintain the viability of human peripheral blood monocytes in part by their suppression of IL-10 production. Int. Arch. Allergy. Immunol. 107, 90-92.

Bellingan, G.J., Caldwell, H., Howie, S.E., Dransfield, I., and Haslett, C. (1996). In vivo fate of the inflamatory macrophage during the resolution of inflammation: inflammatory macrophages do not die locally, but emigrate to the draining lymph nodes. J. Immunol. 157, 2577-2585.

Brady, H.J.M., Gil-Go¬mez, G., Kirberg, J., and Berns, A.J.M. (1996). Bax a perturbs T cell development and affects cell cycle entry of T cells. EMBO J. 15, 6991-7001.

Buschle, M., Campana, D., Carding, S.R., Richard, C., Hoffbrand, A.V., and Brenner, M.K. (1993). Interferon gamma inhibits apoptotic cell death in B cell chronic lymphocytic leukemia. J. Exp. Med. 177, 213-218.

Celada, A., and Maki, R.A. (1992). Transforming growth factor- b enhances the M-CSF and GM-CSF-stimulated proliferation of macrophages. J. Immunol. 148, 1102-1105.

Celada, A., Gray, P.W., Rinderknecht, E., and Schreiber, R.D. (1984). Evidence for a gamma-interferon receptor that regulates macrophage tumoricidal activity. J. Exp. Med. 160, 55-74.

Chen, W.H., Pellegata, N.S., and Wang, P.H. (1995). Coordinated effects of insulin-like growth factor 1 on inhibitory pathways of cell cycle progression in cultured cardiac muscle cells. Endocrinology 136, 5240-5243.

Chin, Y.E., Kitagawa, M., Su, W.C., You, Z.H., Iwamoto, Y., and Fu, X.Y. (1996). Cell growth arrest and induction of cyclin-dependent kinase inhibitor p21 Waf1/Cip1 mediated by STAT 1. Science 272, 719-722.

Chomczynski, P., and Sacchi, N. (1987). Single-step method of RNA isolation by acid guanidinium thiocyanate-phenol-chloroform extraction. Anal. Biochem. 162, 156±159.

Dao, T., Huleatt, J.W., Hingorani, R., and Crispe, I.N. (1997). Specific resistance of T cells to CD95-induced apoptosis during S phase of the cell cycle. J. Immunol. 159, 4261-4267.

Deng, C., Zhang, P., Harper, J.W., Elledge, S.J., and Leder, P. (1995). Mice lacking p21CIP1/WAF1 undergo normal development, but are defective in G_1 checkpoint control. Cell 82, 675-684.

El-Deiry, W.S., Tokino, T., Velculescu, V.E., Levy, D.B., Parson, R., Trent, J.M., Lin, D., Mercer, W.E., Kinzler, K.W., and Vogelstein, B. (1993). WAF1, a potential mediator of p53 tumor supression. Cell 75, 817-825.

Ettinger, R., Panka, D.J., Wang, J.K., Stanger, B.Z., Ju, S.T., and Marshak-Rothstein, A. (1995). Fas ligand-mediated cytotoxicity is directly responsible for apoptosis in normal $CD4^{1}$ T cells responding to a bacterial superantigen. J. Immunol. 154, 4302-4308.

Evan, G.I., Wyllie, H.W., Gilbert, C.S., Littlewood, T.D., Land, H., Brooks, M., Waters, C.M., Penn, L.Z., and Hancock, D.C. (1992). Induction of apoptosis in fibroblasts by c-myc protein. Cell 69, 119-128.

Fox, M.H., Read, R.A., and Bedford, J.S. (1987). Comparison of synchronized chinese hamster ovary cells obtained by mitotic shake-off, hydroxyurea, aphidicolin or methotrexate. Cytometry 8, 315±320.

Freeman, R.S., Estus, S., and Johnson, E.M., Jr. (1994). Analysis of cell cycle-related gene expression in postmitotic neurons: selective induction of cyclin D-1 during programmed cell death. Neuron 12, 343±355.

Gomez-Manzano, C., Fueyo, J., Kyritsis, A.P., McDonnell, T.J., Steck, P.A., Levin, V.A., and Yung, W.K.A. (1997). Characterization of p53 and p21 functional interactions in glioma cells in route to apoptosis. J. Natl. Cancer Inst. 89, 1036±1044.

Grawunder, V., Melchers, F., and Rolin, K.A. (1993). Interferon-gamma arrests proliferation and causes apoptosis in stromal cell/interleukin-7-dependent normal murine pre-B cell lines and clones in vitro, but does not induce diferentiation to surface immunoglobulin-positive B cells. Eur. J. Immunol. 23, 544±551.

Gu, Y., Turck, W., and Morgan, D.O. (1993). Inhibition of CDK2 activity in vivo by an associated 20 K regulatory subunit. Nature 366, 707±710.

Harper, J.W., Adami, G.R., Wei, N., Keyomarsi, K., and Elledge, S.J. (1993). The p21 Cdk-interacting protein Cip is a potent inhibitor of G_1 cyclin-dependent kinases. Cell 75, 805±816.

Hogquist, K.A., Nett, M.A., Unanue, E.R., and Chaplin, D.D. (1991). Interleukin 1 is processed and released during apoptosis. Proc. Natl. Acad. Sci. USA 88, 8485±8489.

Kranenburg, O., de Groot, R.P., van der Eb, A.J., and Zantema, A. (1995). Differentiation of P19EC cells leads to differential modulation of Cyclin-dependent kinase activities and to changes in the cell cycle. Oncogene 10, 87±95.

Kranenburg, O., van der Eb, A.J., and Zantema, A. (1996). Cyclin D_1 is an essential mediator of apoptotic neuronal cell death. EMBO J. 15, 46±54.

Lam, K.P., Kuhn, R., and Rajewsky, K. (1997). In vivo ablation of surface immunoglobulin on mature B cells by inducible gene targeting results in rapid cell death. Cell 90, 1073±1083.

Levkau, B., Koyama, H., Raines, E.W., Clurman, B.E., Herren, B., Orth, K., Roberts, J.M., and Ross, R. (1998). Cleavage of p21Cip1/Waf1 and p27Kip1 mediates apoptosis in endothelial cells through activation of cdk2: role of a caspase cascade. Mol. Cell 1, 553±563.

Linette, G.P., Li, Y., Roth, K., and Korsmeyer, S.J. (1996). Cross-talk between cell death and cell cycle progression: BCL-2 regulates NFAT-mediated activation. Proc. Natl. Acad. Sci. USA 90, 7951±7955.

Lissy, N.A., Van Dyk, L.F., Becker-Hapak, M., Vocero-Akbani, A., Mendler, J.H., and Dowdy, S.F. (1998). TCR antigen-induced cell death occurs from a late G_1 phase cell cycle check point. Immunity 8, 57±65.

Liu, Y., and Janeway, C.A. (1990). Interferon gamma plays a critical role in induced cell death of effector T cell: a posible third mechanism of self-tolerance. J. Exp. Med. 172, 1735±1739.

Malech, H.D., and Gallin, J.I. (1987). Current concepts: immunology. Neutrophils in human diseases. New Engl. J. Med 317, 687±694.

Mangan, D.F., Welch, G.R., and Whal, S.M. (1991). Lipopolysaccharide, tumor necrosis factor- a, and IL-1 b prevent programmed cell death (apoptosis) in human peripheral blood monocytes. J. Immunol. 146, 1541±1546.

Matsushime, H., Roussel, M.F., Ashmun, R.A., and Sherr, C.J. (1991). Colony-stimulating factor 1 regulates novel cyclins during the G_1 phase of the cell cycle. Cell 65, 701±713.

Matsushime, H., Ewen, M.E., Strom, D.K., Kato, J., Hanks, S.K., Roussel, M.F., and Sherr, C.J. (1992). Identification and properties of an atypical catalytic subunit ($p^{34PSKJ3/CDK4}$) for mammalian D-type G_1 cyclins. Cell 71, 323±334.

Mazel, S., Burtrum, D., and Petrie, H.T. (1996). Regulation of cell division cycle progression by bcl-2 expression: a potential mechanism for inhibition of programmed cell death. J. Exp. Med. 183, 2219±2226.

Meikrantz, W., and Schlegel, R. (1995). Apoptosis and the cell cycle. J. Cell. Biochem. 58, 160±174.

Meikrantz, W., Gisselbrecht, S., Tam, S.W., and Schlegel, R. (1994). Activation of cyclin A-dependent protein kinases during apoptosis. Proc. Natl. Acad. Sci. USA 91, 3754±3758.

O'Reilly, L.A., Huang, D.C.S., and Strasser, A. (1996). The cell death inhibitor Bcl-2 and its homologues influence control of cell cycle entry. EMBO J. 15, 6979±6990.

Pardee, A.B. (1989). G_1 events and regulation of cell proliferation. Science 246, 603±608.

Parker, S.B., Eichele, G., Zhang, P., Rawls, A., Sands, A.T., Bradley, A., Olson, E.N., Harper, J.W., and Elledge, S.J. (1995). p53-independent expression of p21Cip1 in muscle and other terminally differentiating cells. Science 267, 1018±1021.

Poluha, W., Poluha, D.K., Chang, B., Crosbie, N.E., Schonhoff, C.M., Kilpatrick, D.L., and Ross, A.H. (1996). The cyclin-dependent kinase inhibitor $p21^{waf1}$ is required for survival of differentiating neuroblastoma cells. Mol. Cell. Biol. 16, 1335±1341.

Polyak, K., Waldman, T., He, T.-C., Kinzler, K.W., and Vogelstein, B. (1996). Genetic determinants of p53-induced apoptosis and growth arrest. Genes Dev. 10, 1945±1952.

Sachs, L., and Lotem, J. (1993). Control of programmed cell death in normal and leukemic cells: new implications for therapy. Blood 82, 15±21.

Sangfelt, O., Einhorn, S., Bjorklund, A.C., Wiman, K.G., Okan, I., and Grander, D. (1996). Wild-type p53-induced apoptosis in a Burkitt lymphoma cell line is inhibited by interferon gamma. Int. J. Cancer. 67, 106±112.

Schreiber, R.D., and Celada, A. (1985). Molecular characterization of interferon g as a macrophage activating factor. Lymphokines 11, 87±118.

Sharma, B., and Iozzo, R.V. (1998). Transcriptional silencing of perlecan gene expression by interferon- g. J. Biol. Chem. 273, 4642±4646.

Sherr, C.J. (1994a). G_1 phase progression: cycling on cue. Cell 79, 551±555.

Sherr, C.J. (1994b). The ins and outs of RB: coupling gene expression on the cell cycle clock. Trends Cell Biol. 4, 15±18.

Sherr, J.C., and Roberts, J.M. (1995). Inhibitors of mammalian G_1 cyclin-dependent kinases. Genes Dev. 9, 1149±1163.

Shi, L., Nishioka, W.K., Th'ng, J., Bradsbury, E.M., Litchfield, D.W., and Greenberg, A.H. (1994). Premature p34Cdc2 activation required for apoptosis. Science 263, 1143±1145.

Tanaka, N., Ishihara, M., Lamphier, J., Nozawa, H., Matsuyama, T., Mak, T.W., Aizawa, S., Tokino, T., Oren, M., and Taniguchi, T. (1996). Cooperation of the tumour suppressors IRF-1 and p53 in response to DNA damage. Nature 382, 816±818.

Tanchot, C., Lemonnier, F.A., Perarnau, B., Freitas, A.A., and Rocha, B. (1997). Differential requirements for survival and proliferation of CD8 naive or memory T cells. Science 276, 2057±2062.

Torczynski, P., Bollon, A.P., and Fuke, M. (1983). The complete nucleotide sequence of the rat 18S ribosomal RNA gene and comparison with the respective yeast and frog genes. Nucleic Acids Res. 11, 4879-4890.

Tushinski, R.J., and Stanley, E.R. (1985). The regulation of mononuclear phagocytes entry into S phase by the colony stimulation factor CSF-1. J. Cell. Physiol. 122, 221-228.

Vadiveloo, P.H., Vairo, G., Novak, U., Royston, A.K., Whitty, G., Filonzi, E.L., Chargoe, E.J., Jr., and Hamilton, J.A. (1996). Differential regulation of cell cycle machinery by various antiproliferative agents is linked to macrophage arrest at distinct G_1 checkpoints. Oncogene 13, 599-608.

Vairo, G., Vadiveloo, P.K., Royston, A.K., Rockman, S.P., Rock, C.O., Jackowski, S., and Hamilton, J.A. (1995). Deregulated c-myc expression overrides IFN g-induced macrophage growth arrest. Oncogene 10, 1969-1976.

Vaux, D.L., and Strasser, A. (1996). The molecular biology of apoptosis. Proc. Natl. Acad. Sci. USA 93, 2239-2244.

Wang, J., and Walsh, K. (1996). Resistance to apoptosis conferred by Cdk inhibitors during myocyte differentiation. Science 273, 359-361.

Wei, T., Williams, R.T., and Lavin, M.F. (1997). Activation of cyclin A-dependent kinases associated with Waf1 degradation during radiation-induced apoptosis. Cell Death Diff. 4, 276-282.

White, E. (1996). Life, death, and the pursuit of apoptosis. Genes Dev. 10, 1-5.

Williams, G.T., and Williams, W.J. (1983). Granulomatous inflammation. A review. J. Clin. Pathol. 36, 723-733.

Xaus, J., Valledor, A.F., Cardo¬ M., Marque¬s, L., Beleta, J., Palacios, J.M., and Celada, A. (1999a). Adenosine inhibits M-CSF-dependent proliferation of macrophages through the induction of $p27^{Kip1}$. J. Immunol, in press.

Xaus, J., Mirabet, M., Lloberas, J., Soler, C., Llurs, C., Franco, C., and Celada, A. (1999b). IFN g up-regulates the A_{2B} adenosine receptor expression in macrophages. A mechanism of macrophage deactivation. J. Immunol. 162, 3607-3614.

Xiong, Y., Connolly, T., Futcher, B., and Beach, D. (1991). Human D-type cyclin. Cell 65, 691-699.

Xiong, Y., Hannon, G.J., Zhang, H., Casso, D., Kobayashi, R., and Beach, D. (1993). p21 is a universal inhibitor of cyclin kinases. Nature 366, 710-714.

Zhang, W., Kornblau, S.M., Kobayashi, T., Gambel, A., Claxton, D., and Deisseroth, A.B. (1995). High levels of constitutive WAF-1/Cip 1 protein are associated with chemoresistance in acute myelogenous leukemia. Clin. Cancer Res. 1, 1051-1057.

Zhang, Q., Singh Ahuja, H., Zakeri, Z.F., and Wolgemuth, D.J. (1997). Cyclin-dependent kinase 5 is associated with apoptotic cell death during development and tissue remodeling. Dev. Biol. 183, 222-133.

Zhu, L., and Anasetti, C. (1995). Cell cycle control of apoptosis in human leukemic T cells. J. Immunol. 154, 192-200.

2. La decorina inhibe la proliferación de los macrófagos estimulada por el M-CSF (*macrophage colony-stimulating factor*) y estimula la supervivencia celular a través de la inducción $p27^{Kip1}$ y de $p21^{Waf1}$.

Resumen

Los macrófagos juegan un papel crítico en la respuesta inflamatoria secretando un gran número de mediadores que modulan las funciones inmunitarias de la célula. Los mediadores más destacados entre otros serian las citocinas, prostaglandinas, metabolitos del oxígeno reactivo, proteoglicanos, etc. Estos últimos forman una parte mayoritaria de la matriz extracelular y están secretados por los monocitos y los macrófagos activados. En el lugar de la inflamación además de observarse el incremento de proteoglicanos debido a la secreción de las células activadas del sistema inmunitario, también se observa la liberación de estos proteoglicanos como resultado de la degradación de la matriz extracelular.

La decorina pertenece a la familia de los pequeños proteoglicanos ricos en leucinas y una de las funciones más importantes es su capacidad para regular la proliferación celular. Esto es debido en parte a la de interacción con los miembros de la familia del receptor del EGF (*epitelial growth factor*) desencadenando así una serie de señales intracelulares dependientes de la cascada de señalización de las MAPKs. También se produce la inducción del $p21^{Waf1}$ y además la decorina ejerce un papel regulador de la actividad del TGF-β. No es infrecuente ver la expresión de decorina en las células epiteliales malignas procedentes de una gran variedad de carcinomas, como próstata, mama, páncreas, colon, etc., sugiriendo un posible papel como molécula antioncogénica. Además de este papel antioncogénico, a la decorina también se le han atribuido propiedades protectoras del desarrollo de determinadas enfermedades como por ejemplo las de origen fibrótico.
Debido a que la mayoría de los efectos de la decorina están relacionados con modelos de células malignas y no hay ningún dato en células normales, nos planteamos estudiar el papel de la decorina en el control de la proliferación macrofágica. Los resultados preliminares obtenidos demostraron que la decorina tenia un efecto inhibidor en los macrófagos que habían sido previamente estimulados con M-CSF (los macrófagos requieren M-CSF para poder proliferar y sobrevivir) o con GM-CSF. Los estudios de distribución del ADN en el contenido de las células reveló que el ciclo celular de los macrófagos tratados con decorina queda bloqueado a nivel de la fase G_1, pero en ningún caso se observó la aparición de apoptosis o la reducción del número de células.

En los macrófagos tratados con decorina se inducía la expresión de las dos proteínas $p21^{Waf1}$ y $p27^{Kip1}$. La utilización de los macrófagos procedentes de los ratones knock-out para los genes $p21^{Waf1}$ y $p27^{Kip1}$ sirvió para demostrar que sólo $p27^{Kip1}$ estaba involucrada directamente con la inhibición de la proliferación. Las células tratadas con decorina, pero no las tratadas con EGF eran capaces de modificar la cinética de la actividad de ERK inducida por el M-CSF. Nuestros resultados sugieren que la inhibición de la proliferación en los macrófagos no es debida a la interacción de la decorina con el receptor del EGF ya que este factor de crecimiento no parece tener ningún tipo de modulación en la proliferación de macrófagos. Debido a que el IFNγ mimetiza muchos de los efectos de la decorina, utilizamos macrófagos de ratones knock-out del receptor del IFNγ, en los que la proliferación no era inhibida por el IFNγ, pero observamos que la decorina seguía teniendo un efecto inhibidor de la proliferación. El conjunto de esta serie de experimentos nos indica que el efecto de inhibición de la proliferación por la decorina es independiente tanto de los receptores del EGF como de los del IFNγ.

Los macrófagos para crecer *in vitro* necesitan adherirse a la superficie de las placas de cultivo y esta adhesión no solo permite la proliferación sino también la viabilidad celular. Los macrófagos se unen con distinta afinidad a las diversas proteínas presentes en la matriz extracelular. Nuestros resultados señalan que tanto la decorina como la fibronectina inducen la adhesión en los macrófagos,

pero inhiben la proliferación cuando estos son estimulados con M-CSF. Mientras que la decorina induce a los dos inhibidores de la cdk: $p21^{Waf1}$ y $p27^{Kip1}$, la fibronectina solamente inducía la expresión de $p27^{Kip1}$. Además, se observó un efecto diferencial entre las dos proteínas de la matriz. La decorina, pero no la fibronectina era capaz de proteger a los macrófagos de la inducción de apoptosis producida por la eliminación del M-CSF.

Los experimentos usando anticuerpos contra las integrinas y el péptido RGD (péptido inhibidor de integrinas de manera inespecífica) que inhibe la adhesión celular al unirse a las integrinas, mostraron que únicamente la inhibición de la proliferación de las células tratadas con fibronectina era dependiente de la vía de señalización a través de las integrinas, pero que los macrófagos activados con decorina inhibian dicha proliferación por un mecanismo independiente de estos receptores.

Decorin inhibits macrophage colony-stimulating factor proliferation of macrophages and enhances cell survival through induction of $p27^{Kip1}$ and $p21^{Waf1}$

Decorin is a small proteoglycan that is ubiquitous in the extracellular matrix of mammalian tissues. It has been extensively demonstrated that decorin inhibits tumor cell growth; however, no data have been reported on the effects of decorin in normal cells. Using nontransformed macrophages from bone marrow, results of this study showed that decorin inhibits macrophage colony-stimulating factor (M-CSF)-dependent proliferation by inducing blockage at the G_1 phase of the cell cycle without affecting cell viability. In addition, decorin rescues macrophages from the induction of apoptosis after growth factor withdrawal. Decorin induces the expression of the cdk inhibitors $p21^{Waf1}$ and $p27^{Kip1}$. Using macrophages from mice where these genes have been disrupted, inhibition of proliferation mediated by decorin is related to $p27^{Kip1}$ expression, whereas $p21^{Waf1}$ expression is necessary to protect macrophages from apoptosis. Decorin also inhibits M-CSF-dependent expression of MKP-1 and extends the kinetics of ERK activity, which is characteristic when macrophages become activated instead of proliferating. The effect of decorin on macrophages is not due to its interaction with epidermal growth factor or interferon-γ receptors. Furthermore, decorin increases macrophage adhesion to the extracellular matrix, and this may be partially responsible for the expression of $p27^{Kip1}$ and the modification of ERK activity, but not for the increased cell survival.

Introduction

Stimulated monocytes and macrophages secrete a diverse set of mediators that influence cellularimmune functions and inflammation. These mediators include proinflammatory and anti-inflammatory cytokines, prostaglandins, leukotrienes, and reactive oxygen metabolites.[1] At the inflammatory sites, proteoglycans are both secreted by activated mononuclear leukocytes and released as a result of extracellular matrix (ECM) degradation. Thus, proteoglycans, which are major constituents of the ECM, are another class of molecules produced by monocytes and macrophages[2,3] that are potential modulators of the immune response.

Decorin belongs to a family of small leucine-rich proteoglycans[4,5] and is found in the ECM of several of tissues such as skin,[6,7] cartilage,[8,9] and bone.[10] The biologic importance of these molecules is unclear. In vitro binding studies have shown that some of them interact with several types of collagen[11,12] and act as important regulators of collagen fibrillogenesis. In support of this hypothesis, a decorin-deficient mouse was found to have fragile skin with an abnormal organization of collagen fibers.[13] Decorin may also affect the production of other ECM components by regulating the activity of transforming growth factor-b (TGF-b).[14,15] Additionally, decorin can modulate the interactions of matrix molecules (eg, fibronectin) with cells.[16-18] These observations suggest that decorin and perhaps other proteoglycans regulate the production and assembly of the ECM at several levels and hence the remodeling of connective tissue.

Different observations have revealed that decorin is involved in the control of cell proliferation. The forced expression of decorin in Chinese hamster ovary (CHO) cells leads to a decreased growth rate, lower saturation density, and altered morphology.[19] It has been suggested that decorin causes these effects by sequestering TGF-b, an autocrine growth stimulator for these cells.[15] In addition, decorin is markedly up-regulated during quiescence in human diploid fibroblasts[20,21] and its expression is strongly suppressed on viral transformation with SV40.[20] Recently, an antioncogenic role for decorin has been reported.[22] Decorin is rarely expressed by malignant epithelial cells from a wide variety of human tumors, including colon, pancreas, prostate, and breast carcinomas.[23] In human colon carcinoma cells, the de novo expression of decorin reverted the cells to a normal phenotype; the cells lost anchorage-independent growth, failed to generate tumors in severe combined immunodficient mice, and became arrested in the G_1 phase of the cell cycle.[24] When decorin expression was abrogated by treatment with decorin-specfic antisense oligodeoxynucleotides, the cell re-entered the cell cycle.[24] This growth arrest induced by decorin was associated with a marked expression of $p21^{Waf1}$. Moreover, decorin inhibits proliferation in tumor cells with different histogenetic backgrounds through the induction of $p21^{Waf1}$, and it has been reported that decorin interacts with components of the epidermal growth factor (EGF) receptor family expressed by these cells.[22,25]

Besides the antioncogenic role of decorin, a protective role of decorin in fibrotic diseases has been observed.[26,27] However, there are no data regarding the effects of decorin on normal cells. We have analyzed the role of decorin in the control of macrophage proliferation. We have used primary bone marrow-derived macrophage (BMDM) cultures, which provide a homogeneous population that responds to physiologic proliferative or activating stimuli.[28] Decorin inhibits macrophage colony-stimulating factor (M-CSF)± dependent proliferation of macrophages and induces the expression of $p21^{Waf1}$ and, in contrast with other cellular models, also $p27^{Kip1}$. Moreover, decorin increases both the adhesion of these cells and their resistance to die after withdrawal of growth factor. The effects of decorin in macrophages are not mediated through interaction with EGF or interferon-g (IFN-γ) receptors.

Materials and methods

Reagents

Recombinant purified decorin was a generous gift from E. Ruoslahti (The Burnham Institute, La Jolla, CA). Histone H1 was obtained from Roche Molecular Biochemicals (Indianapolis, IN). Fibronectin, vitronectin, poly-2-hydroxyethyl methacrylate (PHM), collagen, and laminin were obtained from Sigma Chemical (St Louis, MO). [^{3}H]-Thymidine was obtained from Amersham Pharmacia Biotech (Uppsala, Sweden). 4, 6-Diamidino-2-phenylindole (DAPI) and the RGD peptide were purchased from Calbiochem (La Jolla, CA). All the other products were of the best grade available and were purchased from Sigma. Deionized water further purified with a Millipore Milli-Q system (Bedford, MA) was used.

Cell culture

The BMDMs were isolated from 6-week-old balb/c mice (Charles River Laboratories, Wilmington, MA) as described.[29] The cells were cultured in plastic tissue culture dishes (150 mm) in 40 mL Dulbecco modified Eagle medium (DMEM) containing 20% fetal bovine serum (FBS) and 30% L cell-conditioned media as a source of M-CSF. The cells were incubated at 37 C in a humidified 5% CO_2 environment. After 7 days of culture a homogeneous population of adherent macrophages was obtained (> 99% Mac-1^1). The purity of the culture was checked regularly by flow cytometry using anti-Mac-1 antibodies (BD Pharmingen, Heidelberg, Germany). To render the cells quiescent, when the macrophages were 80% confluent they were deprived of L cell-conditioned medium for 18 hours before carrying out the experiment. BMDMs from knock-out mice were isolated in the same conditions. The $p21^{Waf1}$ and $p27^{Kip1}$ knock-out mice were obtained from Dr J. Roberts (Howard Hughes Medical Institute (HHMI), Seattle, WA) and IFN-γ receptor knock-out mice were a kind gift by Dr M. Modolell (Max Plank Institute, Freiburg, Germany).

Antibodies and constructs

The analysis of $p21^{Waf1}$ and $p27^{Kip1}$ expression by Western blotting was performed with monoclonal antimouse $p21^{Waf1}$ and $p27^{Kip1}$ antibodies (BD Pharmingen). Antibodies to cdk-4 and cyclin D_1 were obtained from Santa Cruz Biotechnology (Santa Cruz, CA). Peroxidase-conjugated antimouse IgG (Cappel, Turnhout, Belgium) was used as secondary antibody. A primary antibody against mouse β-actin was used as loading control and purchased from Sigma. The antibody against cdk-2 (M-2) used for the analysis of cdk-2 activity and the polyclonal antimouse β_1-integrin antibody were obtained from Santa Cruz Biotechnology.

The pMH117 plasmid corresponds to the mouse $p21^{Waf1}$ full-length complementary DNA (cDNA) cloned in pEx-lox and was kindly provided by Dr J. Massague (Sloan Kettering Institute, HHMI, New York, NY). The MKP-1 probe was obtained from Dr R. Bravo (Bristol-Myers Squibb, Princeton, NJ). The probe for the 18S ribosomal RNA (rRNA) was obtained as described.[30]

Proliferation assay

Cell proliferation was measured as previously described[31] with minor modifications. The cells were deprived of M-CSF for 18 hours and then 10^5 macrophages were incubated for 24 hours in 24-well plates (3424 MARK II; Costar, Cambridge, MA) in 1 mL complete medium in the presence or absence of the indicated reagents. In some cases, the plates were precoated with the indicated ECM proteins. After this period, the media was removed and replaced with 0.5 mL media containing [^{3}H]-thymidine (0.037 MBq). After 6 additional hours of incubation at 37 C, the media was removed and the cells were fixed in ice-cold 70% methanol. After 3 washes in ice-cold 10% trichloroacetic acid, the cells were solubilized in 1% sodium dodecyl sulfate (SDS), 0.3 N NaOH. Radioactivity was counted by liquid scintillation using a 1500 Tri-Carb Packard scintillation counter. Each point was performed in triplicate and the results were expressed as the mean 6±SD.

In parallel experiments, 1 x 10^6 cells were plated in 35-mm cell culture dishes and after 24 to 48 hours of culture in the indicated conditions, the viable cells were collected and counted by trypan blue exclusion using a hemocytometer. Again, each experiment was performed 3 times and the results were expressed as the mean 6±SD.

Apoptosis assay

Low molecular apoptotic DNA created by internucleosomal cleavage was measured as described,[32] using an enzyme-linked immunosorbent assay (ELISA) technique based on the detection of histone-associated DNA fragments (Cell Death Detection ELISA Plus, Roche Diagnostics, Mannheim, Germany). Each point was performed in triplicate, and the result was expressed as the mean 6±SD.

Analysis of DNA content with DAPI

Cells (10^6) were previously subjected to a speciÆctreatment and then the DNA content was analyzed as described previously.[33] Twelve thousand cells were counted for each histogram, and cell cycle distributions were analyzed with the Multicycle program (Phoenix Flow Systems, San Diego, CA)

Adhesion analysis

Cell adhesion to the substrate was analyzed by crystal violet staining. Flat-bottomed ELISA plates were precoated in 50 µL/well phosphate-buffered saline (PBS) containing the indicated amount of each matrix protein, or bovine serum albumin (BSA) as a control, overnight at 4 C or for 2 hours at 37 C. After coating, the wells were blocked with PBS and 1.5% BSA for 1 hour at 37 C. Then, 10 000 cells/well were cultured for only 30 to 60 minutes due to the high capacity of macrophages to attach themselves at any surface. The cells were washed twice in PBS and fixed with 4% paraformaldehyde for 30 minutes at room temperature. After 3 washes by immersion with twice-distilled water, the cells were stained in a solution of 0.1% crystal violet in twice-distilled water for 20 minutes. After 3 new washes, the plates were dried at 37 C, developed by adding 0.1 M HCl for 5 minutes, and quantified using an ELISA reader at 630 nm. Each sample was analyzed in triplicate and the results were represented as the mean 6±SD.

Protein extraction and Western blot analysis

Western blot analysis was performed as previously described.[32] Cell lysates (100 µg/lane) were loaded. The analysis of $p21^{Waf1}$ and $p27^{Kip1}$ expression was performed with monoclonal antimouse $p21^{Waf1}$ and $p27^{Kip1}$ antibodies (BD Pharmingen). Antibodies to cdk-4 and cyclin D_1 were obtained from Santa Cruz Biotechnology. A primary antibody against mouse β-actin was used as loading control and purchased from Sigma. Peroxidase-conjugated antimouse IgG was used as secondary antibody. All antibody incubations were performed for 1 hour at room temperature.

Determination of ERK activity by in-gel kinase assay

Total protein (50 µg) was separated by 12.5% SDS-polyacrylamide gel electrophoresis (SDS-PAGE) in the presence of 0.1 mg/mL myelin basic protein (MBP) (Sigma) copolymerized in the gel. After electrophoresis, SDS was removed by washing the gel with 2 changes of 20% 2-propanol in 50 mM Tris-HCl (pH 8.0) for 1 hour at room temperature. The gel was then incubated with 50 mM Tris-HCl (pH 8.0) containing 5 mM b-mercaptoethanol (buffer A) for 1 hour at room temperature. The proteins were denatured

by incubating the gel with 2 changes of 6 M guanidine-HCl for 1 hour at room temperature and then renatured by incubating with 5 changes of buffer A containing 0.04% Tween-20 for 16 hours at 4 C. To perform the phosphorylation assay, the gel was first equilibrated in 40 mM Hepes-NaOH (pH 7.4) containing 2 µM DTT, 0.1 mM EGTA, 15 mM $MgCl_2$, 300 mM sodium orthovanadate for 30 minutes at 25 C and then incubated for 1 hour in the same solution containing 50 µM adenosine triphosphate (ATP) and 3.7 MBq ^{32}P-g-ATP (ICN Pharmaceuticals, Costa Mesa, CA). The reaction was stopped by washing the gel with 5% trichloroacetic acid containing 10 mM sodium pyrophosphate to inhibit phosphatase activity. The gel was dried, exposed to x-ray films (Kodak) and quantified using a Bio-Rad Molecular Analyst System (Bio-Rad Labs, Richmond, CA).

Northern blot analysis

Total cellular RNA (20 µg), extracted with the acid guanidinium thiocyanate-phenol-chloroform method was separated in 1% agarose with 5 mM MOPS (3-[N-morpholino]propanesulfonic acid), pH 7.0/1 M formaldehyde buffer, transferred overnight to a GeneScreen membrane (Life Science Products, Boston, MA) and fixed by UV irradiation (150 millijoule). All the probes were labeled with ^{32}P-a-dCTP (ICN Pharmaceuticals) using the oligolabeling kit method (Amersham Pharmacia). After incubating the membranes for 18 hours at 65 C in hybridization solution (20% formamide, 5 x Denhart, 5 3 standard sodium citrate [SSC], 10 mM EDTA, 1% SDS, 25 mM Na_2HPO_4, 25 mM NaH_2PO_4, 0.2 mg/mL salmon sperm DNA, and 10^6 cpm/mL ^{32}P-labeled probe), they were exposed to Kodak films.

Cdk-2 activity

Quiescent macrophages were cultured in 60-mm plates precoated with 10 µg/mL BSA or decorin and stimulated with 1000 U/mL M-CSF for the indicated times. The analysis of cdk-2 activity was performed as described elsewhere, without modifications.[33]

Results

In the present work, we used macrophages obtained from bone marrow cultures, because they represent a homogeneous population of macrophages that require M-CSF to proliferate and survive. Under the effect of M-CSF, macrophages proliferate in a dose-dependent manner. When decorin (10 µg/mL) was precoated to the plates, macrophage proliferation was inhibited (Figure 1A). This effect was dose-dependent, and macrophage proliferation was completely inhibited at a concentration of 100 µg/mL decorin (Figure 1B). It is important to note that the indicated concentrations of decorin correspond to the concentration of the precoating solution and that we are not able to quantify the amount of decorin adsorbed to the plate after precoating, but other proteins under the same conditions bound less than 10% to 20%. Decorin also inhibits macrophage proliferation in the presence of either recombinant M-CSF or granulocyte-macrophage colony-stimulating factor (GM-CSF) proteins (Figure 1C).

The inhibitory effect of decorin was confirmed by flow cytometry (Figure 1D) and by cell counting (Figure 1E). The distribution of the DNA content of cells stained with DAPI showed that macrophages treated with decorin were blocked mainly at the G_1 phase of the cell cycle (73%), whereas macrophages growing in normal conditions showed a distribution corresponding to an active proliferating population (51% cells at G_1 phase; Figure 1C). Moreover, the inhibition of proliferation was not due to a lower cell viability because we did not detect any subdiploid peak corresponding to apoptotic cells (Figure 1C) or a decrease in the cell number

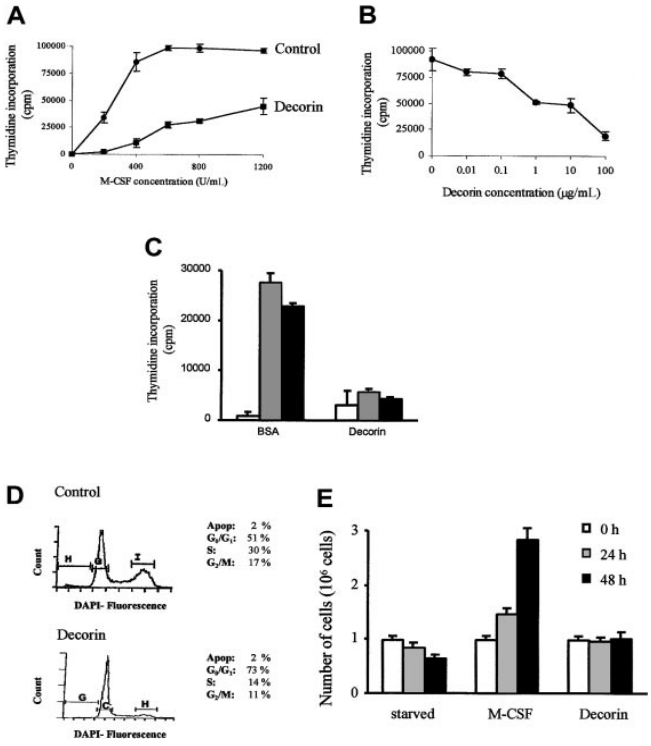

Figure 1. Decorin inhibits the M-CSF±dependent proliferation of BM-DMs. (A) BMDMs were obtained after 7 days of culture in the presence of M-CSF. Then, 10^5 macrophages were incubated in the presence of the indicated amounts of M-CSF in 24-well plates precoated with BSA (10 mg/mL; control) or with decorin (10 mg/mL). Proliferation was determined as described in "Materials and methods." (B) Decorin inhibits macrophage proliferation in a dose-dependent manner. The 10^5 macrophages were incubated in 24-well plates precoated with the indicated amounts of decorin in the presence of 1000 U/mL M-CSF. For both panels A and B, each determination was made in triplicate and the values represented correspond to the mean 6 SD of one representative of 3 independent experiments. (C) Decorin also blocks proliferation of macrophages induced by recombinant M-CSF (□, 2 ng/mL), GM-CSF (■, 10 ng/mL), or control (□). (D) Decorin blocks the cell cycle at G_1 phase. The 10^6 macrophages were cultured in the presence of 1000 U/mL M-CSF in 35-mm Petri dishes precoated with BSA or with 100 mg/mL decorin for 24 hours. DNA content was measured by DAPI staining and flow cytometry. Cell cycle distribution was analyzed using the Multicycle program (Phoenix Flow Systems). (E) Counting of viable cells cultured in 100 µg/mL decorin-precoated plates for 24 to 48 hours. The cells were counted by trypan blue exclusion using a hemocytometer. Each point was performed in triplicate, and the results were represented as the mean 6±SD.

after 48 hours of culture in the presence of 100 µg/mL decorin (Figure 1E).

It has been reported that decorin inhibits proliferation through the expression of $p21^{Waf1}$ in certain tumor cellular models.[25,34] Therefore, we analyzed the expression of this cdk inhibitor in macrophages treated with decorin. Western blot analysis showed that decorin induced the expression of $p21^{Waf1}$ in a time- and dose-dependent manner (Figure 2A). However, and in contrast with other cellular models, decorin also induced in macrophages the expression of another cdk inhibitor, $p27^{kip1}$ (Figure 2A). No differences were observed in the expression of cyclin D_1, E, cdk-2, and cdk-4 protein analyzed by Western blot (data not shown). Moreover, the analysis of cdk-2 activity measured as in vitro phosphorylation of histone H1 showed that treatment of macrophages with decorin inhibits cdk-2 activity (Figure 2B). To characterize the involvement of each of these 2 molecules in the inhibitory effect of decorin, we used macrophages obtained from mice where these genes have been disrupted by homologous recombination. Decorin inhibited proliferation in macrophages from $p21^{Waf1}$ knock-out mice but no effect was observed in macrophages from $p27^{Kip1}$ knock-out mice (Figure 2C). Thus, although decorin in macrophages induced the expression of both $p21^{Waf1}$ and $p27^{Kip1}$, only $p27^{Kip1}$ was involved in the inhibition of proliferation by decorin, in contrast with what has been reported in tumor cells.[34]

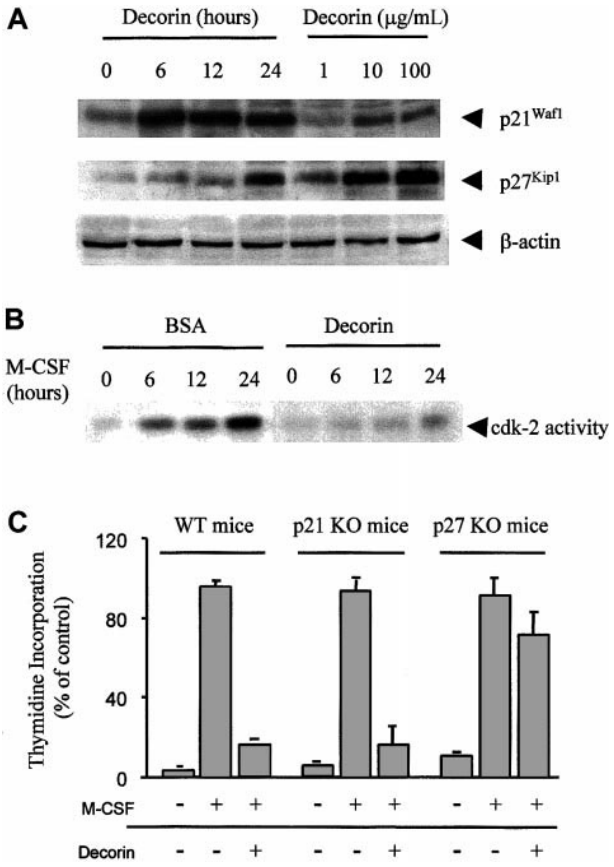

Figure 2. Decorin inhibits macrophage proliferation through $p27^{Kip1}$ expression. (A) Decorin induces the expression of both $p21^{Waf1}$ and $p27^{Kip1}$. The expression of $p21^{Waf1}$ and $p27^{Kip1}$ after treatment with decorin was analyzed by Western blotting. Macrophages were cultured in 100 mg/mL decorin precoated surface for the indicated times or for 24 hours at the indicated concentrations of decorin. Then 100 mg total protein was loaded per lane. Expression of $p21^{Waf1}$ and $p27^{Kip1}$ was analyzed using monoclonal antibodies as described in "Materials and methods." The expression of b-actin was used as a control of sample loading and transfer efficiency. This is representative of 4 independent experiments. (B) Decorin inhibits cdk-2 activity. The cdk-2 activity induced by M-CSF in macrophages cultured on plates precoated with BSA or decorin was measured as histone H1 phosphorylation in vitro at the indicated times after M-CSF stimulation. (C) Decorin did not inhibit M-CSF±dependent proliferation of BMDMs from $p27^{Kip1}$ knock-out mice. After 7 days of culture, a total of 10^5 macrophages from wild-type, $p27^{Kip1}$, or $p21^{Waf1}$ knock-out mice were cultured for 24 hours in BSA or 10 mg/mL precoated plates in the presence of 1000 U/mL of M-CSF. Proliferation was determined by [^{3}H]-thymidine incorporation. Each determination was made in triplicate, and the values represented correspond to the mean 6± SD of 2 independent experiments.

Due to these differences between primary macrophages and tumor cells, and because it has been described that decorin inhibits tumor cell growth through its interaction with the EGF receptor,[22,25] the activation of the ERK pathway and the expression of $p21^{Waf1}$, we analyzed the involvement of this pathway in our model. Both IFN-γ and decorin inhibit M-CSF±dependent macrophage proliferation (Figure 3A) and induce $p21^{Waf1}$ messenger RNA (mRNA) expression (Figure 3B). However, no induction of $p21^{Waf1}$ or inhibition of macrophage proliferation was observed after treatment with 20 mM EGF, thus suggesting that this growth factor and its receptor do not modulate macrophage proliferation. We also analyzed the effect of decorin and EGF on the activation of the ERK pathway. In-gel kinase assays showed that the treatment of macrophages with M-CSF induced the activation of ERK-1 and ERK-2 with a maximal activation after 5 minutes, but this activation decreased quickly and basal levels were reached after 15 to 30 minutes. In contrast, the treatment with decorin or EGF alone did not induce ERK activation. However, decorin, but not EGF, modified and extended the kinetics of ERK activity induced by M-CSF (Figure 3C). The extension of the ERK activity in response to decorin correlated with the inhibition of the MKP-1 expression (Figure 3D), a phosphatase responsible for ERK dephosphorylation and inactivation.[35]

The differences observed between the treatment with decorin and EGF suggest that the inhibition of macrophage proliferation induced by decorin could not be mediated through its interaction with the EGF receptor, because this growth factor does not seem to modulate macrophage proliferation in BMDMs. However, IFN-g mimics most of the effects of decorin; that is, it inhibits macrophage proliferation, induces the expression of $p21^{Waf1}$, and also inhibits MKP-1 and extends ERK activity (manuscript in preparation). Therefore, we tested whether the action of decorin through the activation of the IFN-γ receptor could explain the inhibition of proliferation. As expected, IFN-γ does not inhibit the proliferation of macrophages obtained from IFN-γ receptor knock-out mice. However, decorin still inhibited the proliferation of macrophages

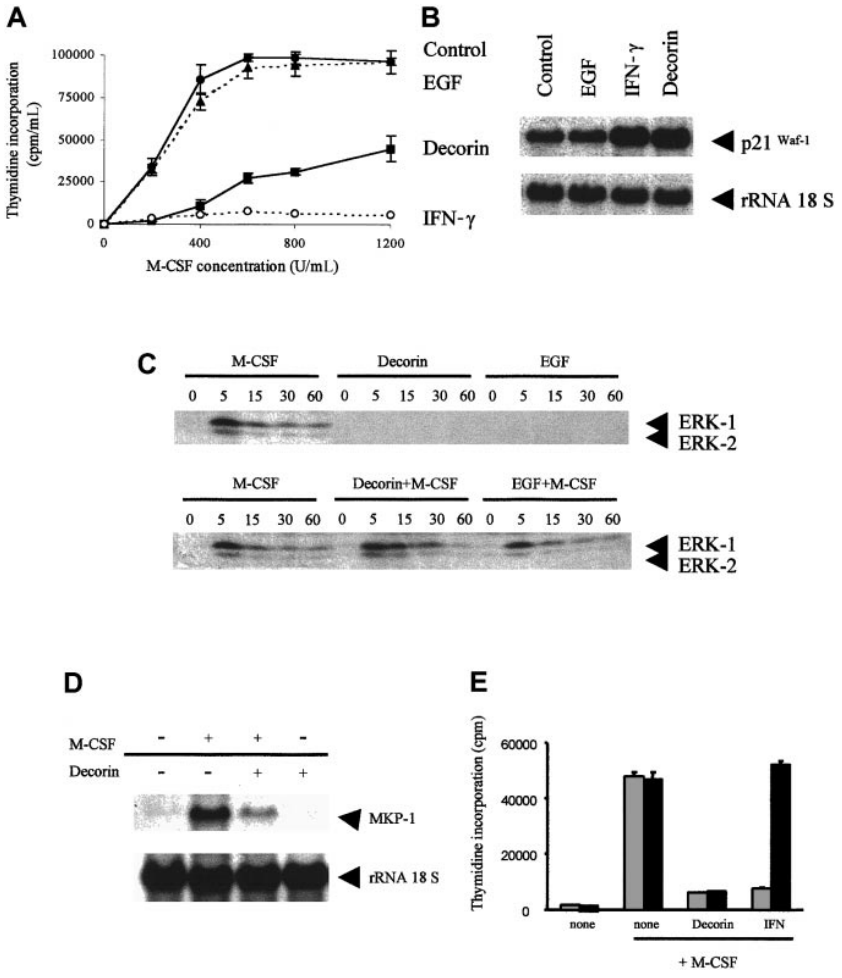

Figure 3. The inhibitory effect of decorin is independent of the EGF or IFN-γ receptors. (A) Decorin and IFN-γ, but not EGF, inhibit macrophage proliferation. Macrophages were either treated with 20 nM EGF, 300 U/mL IFN-γ, or 10 mg/mL decorin or remained untreated for 24 hours in the presence of 1000 U/mL M-CSF, and proliferation was determined as indicated in "Materials and methods." Each determination was made in triplicate, and the values represented correspond to the mean 6 SD of one representative of 3 independent experiments. (B) Decorin and IFN-γ, but not EGF, induce the expression of $p21^{Waf1}$ mRNA in BMDMs. Macrophages were treated for 3 hours with either 20 nM EGF, 300 U/mL IFN-γ, or 10 μg/mL decorin or remained untreated. Expression of $p21^{Waf1}$ was determined by Northern blotting. (C) Decorin, but not EGF, elongates the M-CSF±induced activation of ERK. Quiescent macrophages were stimulated with one or a combination of the following: 1000 U/mL M-CSF, 20 nM EGF, or 10 μg/mL decorin for the indicated times. ERK activity was determined by in-gel kinase assay. (D) Decorin inhibits MKP-1 expression induced by M-CSF. Quiescent macrophages cultured on plates precoated with BSA or 10 μg/mL decorin were stimulated with M-CSF for 30 minutes. The expression of MKP-1 was analyzed by Northern blotting. The levels of the 18S rRNA transcript were used as a loading and transfer control. (E) Decorin inhibits the proliferation of macrophages from IFN-γ receptor knockout mice. The 10^5 macrophages from control (□) and IFN-g receptor knock-out (■) mice were cultured in the presence of 1000 U/mL M-CSF and treated with 300 U/mL IFN-γ or 100 μg/mL decorin. Proliferation was determined after 24 hours by [^{3}H]-thymidine uptake. Each determination was made in triplicate, and the values represented correspond to the mean 6±SD of 2 independent experiments.

from these mice (Figure 3E), thus showing that the effects of decorin are independent of the IFN-γ receptor.

Macrophages growing in vitro adhere to the surface of the plates, and it has been described in several cellular models that this adhesion is important for the proliferation and viability of the cells.[36,37] Because decorin is a component of the ECM, we decided to test how this proteoglycan affects macrophage adhesion and if this was important in modulating proliferation and viability.

We observed that decorin enhanced the adhesion of macrophages to the surface of plastic dishes (Figure 4A). Moreover, macrophages growing in dishes precoated with decorin showed a higher degree of spreading than nontreated macrophages, and their ameboid morphology changed to a more complex morphology with pseudopoda ramification (Figure 4B).

Macrophages bind with different affinities to several proteins present in the ECM. We found that BMDMs showed a higher level of binding to plates precoated with fibronectin and vitronectin, whereas laminin reduced their adhesion (Figure 5A). We then tested how macrophage adhesion affected their proliferation. Using an inhibitor of cellular adhesion, P-OH-M, that blocked macrophage adherence to the dishes (Figure 5A), we showed that these cells must adhere to proliferate (Figure 5B). Surprisingly, a strong adhesion could also decrease macrophage proliferation. Macrophages growing on a fibronectin surface, to which they attach strongly, proliferate less than macrophages growing on a control BSA-precoated surface (Figure 5B). Macrophages cultured on a surface to which they attach slightly (ie, laminin-coated surface) showed a higher level of proliferation than control cells. Similar results were obtained using vitronectin or collagen I (data not shown). We could not dismiss the fact that the different effects on proliferation were due to signaling through different integrin receptors. However, our results suggest that, although macrophage anchorage is necessary to proliferate, the proliferation of macrophages could be modulated by their degree of adhesion.

So far, our results showed that both decorin and fibronectin enhance macrophage adhesion and inhibit M-CSF±dependent proliferation. To determine if the effect of decorin on macrophage proliferation is mediated by its effect on adhesion, we checked the mechanism by which adhesion to fibronectin modulates macrophage proliferation.

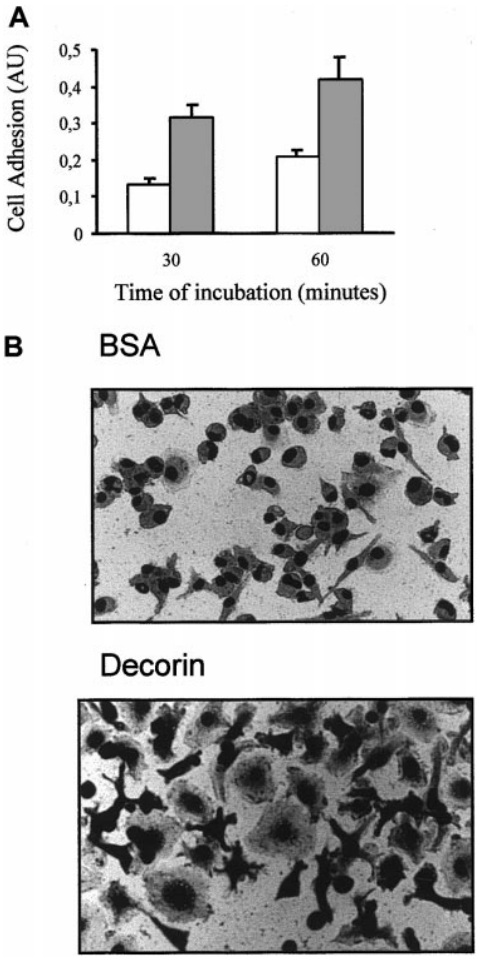

Figure 4. Decorin increases macrophage adhesion. (A) Cells (10 000) were cultured on plates precoated with BSA (□) or 10 mg/mL decorin (▨) for only 30 and 60 minutes. After several washes, adhesion of macrophages was analyzed by crystal violet staining as indicated in "Materials and methods." Each determination was made in triplicate, and the values represented correspond to the mean 6±SD of 5 independent experiments. (B) Photographs of BMDMs attached to BSA-coated (control) or decorin-coated surfaces using a phase contrast microscope with an objective of x 40.

When the expression of several components of the machinery that regulate progression through the G_1 phase of the cell cycle was analyzed, we found that both decorin and fibronectin did not modify the expression of either cyclin D_1, cdk4 (Figure 6A), cdk-2, or cyclin E protein expression (data not shown). However, whereas decorin induced the expression of both cdk inhibitors $p21^{Waf1}$ and $p27^{Kip1}$, fibronectin only induced $p27^{Kip1}$ expression (Figure 6A). Similar to decorin, fibronectin also inhibited cdk-2 activity (data not shown). The adhesion of macrophages to a fibronectin-coated surface also extended ERK activity in response to M-CSF (Figure 6B) by inhibiting MKP-1 expression (Figure 6C). Also, the inhibitory effect of fibronectin on macrophage proliferation was abolished in macrophages from $p27^{Kip1}$ knock-out mice but not in those from $p21^{Waf1}$ knock-out mice (Figure 6D). This suggested that an increased macrophage adhesion probably inhibited macrophage proliferation, and this correlated with an extended ERK activity and the induction of $p27^{Kip1}$.

Because fibronectin inhibited proliferation in a way similar to decorin, and macrophages could produce fibronectin, we checked whether the effects of decorin on macrophage adhesion and proliferation were only mediated by the release of fibronectin induced by decorin.

Decorin modulates the interactions of matrix molecules, such as fibronectin, with the cells.[16,17] Therefore, we analyzed the effect of decorin on macrophage adhesion to fibronectin. The treatment of macrophages with decorin enhanced their adhesion to a fibronectin-coated surface but did not modify their adhesion to laminin-coated surfaces (Figure 7). Because adhesion analysis is performed for only 30 to 60 minutes, it is unlikely that the effect of decorin will be mediated through an increase of fibronectin secretion induced by decorin. Moreover, Northern blot analysis of fibronectin expression in macrophages demonstrated that decorin did not induce or increase fibronectin expression induced by M-CSF in macrophages (data not shown). This suggests that decorin binds to fibronectin through a different domain than the one recognized by macrophages and also that decorin and fibronectin are probably recognized by different receptors on macrophages.

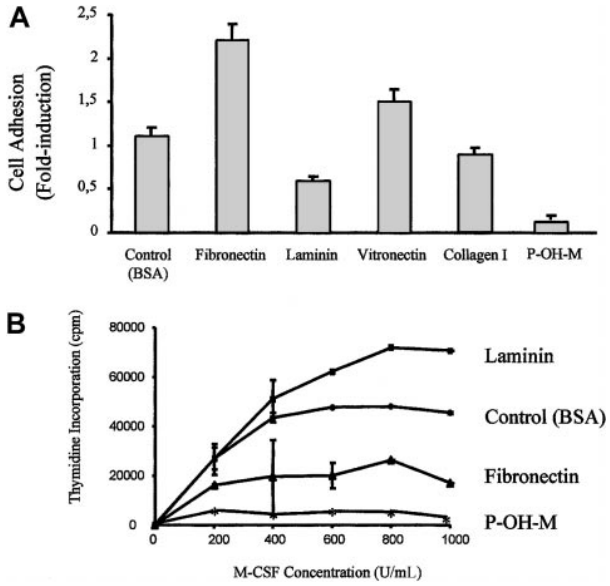

Figure 5. The adhesion of macrophages modulate their proliferation. (A) Macrophages adhere preferably to fibronectin- or vitronectin-precoated surfaces. Cells (10 000) were cultured for 60 minutes on plates precoated with 10 µg/mL BSA (control), 10 µg/mL of the indicated components of the ECM, or 25 µg/mL P-OH-M, an inhibitor of cell adhesion. Macrophage adhesion was analyzed by crystal violet staining. Each determination was made in triplicate, and the values represented correspond to the mean 6±SD of 3 independent experiments. (B) Adhesion modulates macrophage proliferation. Macrophages adhered to plates precoated with 10 µg/mL BSA, laminin or fibronectin, or 25 µg/mL P-OH-M were stimulated with the indicated concentrations of M-CSF and their proliferation was analyzed by [^{3}H]-thymidine incorporation after 24 hours. Each point was made in triplicate, and the values represented correspond to the mean 6±SD of 2 independent experiments.

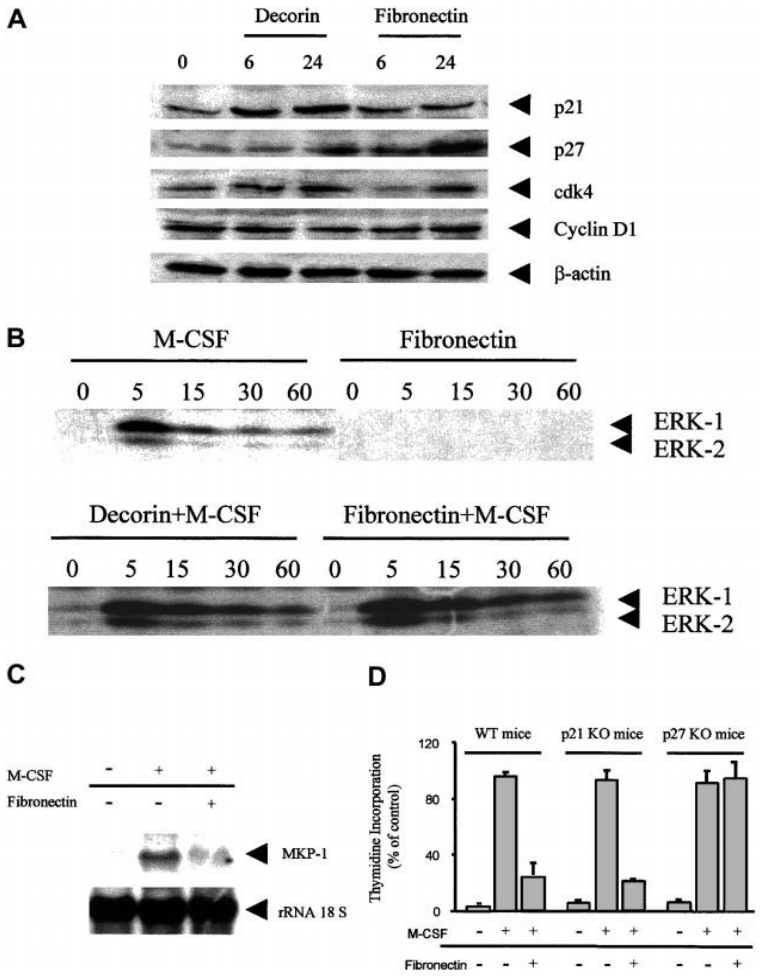

Figure 6. Fibronectin also inhibits macrophage proliferation through $p27^{Kip1}$ expression. (A) Fibronectin induces $p27^{Kip1}$ but not $p21^{Waf1}$ expression. The expression of these components of the cell cycle machinery was analyzed by Western blotting. Macrophages were cultured on plates precoated with 10 μg/mL decorin or fibronectin for 6 or 24 hours. Then, 100 μg total protein was loaded per lane. The expression of b-actin was used as a sample loading and transfer efficiency control. This is the result of 3 independent experiments. (B) Decorin and fibronectin elongate the activation of ERK induced by M-CSF. Quiescent macrophages were grown on plates precoated with 10 μg/mL fibronectin or 10 μg/mL decorin and were then treated with or without 1000 U/mL M-CSF for the indicated times. ERK activity was determined by in-gel kinase assay. (C) Fibronectin also inhibits MKP-1 expression induced by M-CSF. Quiescent macrophages cultured on plates precoated with BSA or 10 μg/mL fibronectin were stimulated with M-CSF for 30 minutes. The expression of MKP-1 was analyzed by Northern blotting. The levels of the 18S rRNA transcript were used as a loading and transfer control. (D) Fibronectin did not inhibit M-CSF±dependent proliferation of BMDMs from $p27^{Kip1}$ knock-out mice. After 7 days of culture, a total of 10^5 macrophages from wild-type, $p27^{Kip1}$, or $p21^{Waf1}$ knock-out mice were cultured for 24 hours on plates precoated with BSA or 10 μg/mL fibronectin in the presence of 1000 U/mL M-CSF. Proliferation was determined by [^{3}H]-thymidine incorporation. Each determination was made in triplicate, and the values represented correspond to the mean 6±SD of 2 independent experiments.

To definitively discard that the effects of decorin could be mediated by the secretion of fibronectin or through fibronectin receptors, we blocked the fibronectin signal pathway using anti-β_1± polyclonal antibodies. We observed that anti-β_1 antibodies reduced

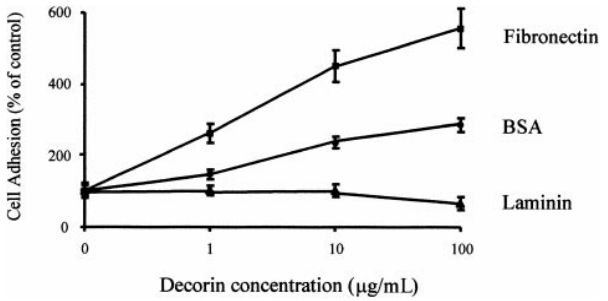

Figure 7. Decorin enhances macrophage adhesion to fibronectin but not to laminin. 10^4 macrophages were cultured on plates precoated with 10 μg/mL fibronectin or laminin together with the indicated amounts of decorin. After 60 minutes, adhesion of BMDMs was determined by crystal violet staining as described in "Materials and methods." Each determination was made in triplicate, and the values shown correspond to the mean 6±SD of 5 independent experiments.

fibronectin-induced adhesion, whereas no effect was observed on decorin adhesion (Figure 8A). Adhesion of macrophages was almost completely blocked using an RGD peptide, which is a nonspecific integrin inhibitor. Interestingly, the effect of anti-b_1 antibodies on adhesion again correlated inversely with macrophage proliferation. Anti-β_1 antibodies blocked the inhibitory effect of fibronectin on macrophage proliferation but had no effect on decorin inhibition (Figure 8B). In the presence of RGD peptides, macrophages do not proliferate.

Also, attachment to the ECM may modulate cell viability.[35] Previously, we had reported that the expression of $p21^{Waf1}$ together with a blockage of the cell cycle protected macrophages from apoptosis.[33] Because decorin increased macrophage adhesion to the ECM, induced $p21^{Waf1}$ expression, and inhibited proliferation, we decided to further explore the role of decorin in the control of macrophage survival. From the experiments described in Figure 1, we concluded that decorin did not induce apoptosis in BMDMs. Instead, decorin protected macrophages from apoptosis induced by growth factor withdrawal (Figure 9). In contrast with its effect on macrophage proliferation, the increase in adhesion induced by

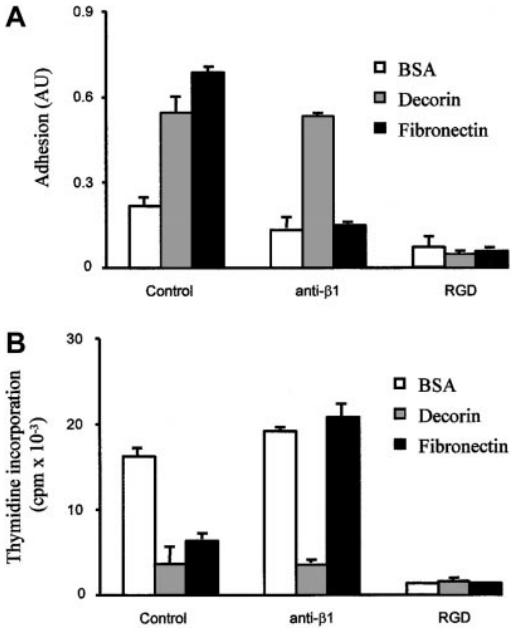

Figure 8. Fibronectin, but not decorin, mediates its effects through β_1-integrin receptors. (A) Adhesion of macrophages to fibronectin is mediated by a β_1-integrin. The 10 000 cells, previously stimulated with 1 mM RGD peptides or 5 μg/mL anti-b_1 antibodies for 1 hour, were cultured for 60 minutes on plates precoated with 10 μg/mL BSA (control) or 10 μg/mL decorin or fibronectin. Macrophage adhesion was analyzed by crystal violet staining. Each determination was made in triplicate, and the values represented correspond to the mean 6±SD of 2 independent experiments. (B) The effect of fibronectin, but not that of decorin, on macrophage proliferation was inhibited by anti-β_1 antibodies. Macrophages cultured as in panel A were stimulated with 1000 U/mL M-CSF and their proliferation was analyzed by [^{3}H]-thymidine incorporation after 24 hours. Each point was made in triplicate, and the values represented correspond to the mean 6±SD of 3 independent experiments.

decorin was not the mediator of this event, because the culture of macrophages on a fibronectin-coated surface did not protect macrophages from apoptosis induced by M-CSF starvation (Figure 9). Similar to our previous observations with IFN-γ, this effect was caused by the expression of $p21^{Waf1}$. Decorin did not inhibit apoptosis in macrophages from $p21^{Waf1}$ knock-out mice, whereas no differences were found in macrophages from $p27^{Kip1}$ knock-out mice (Figure 9).

Discussion

Macrophages are derived from undifferentiated stem cells in the bone marrow and through the blood they reach the different tissues where, in most cases, they undergo apoptosis. In the presence of specific growth factors or cytokines, macrophages proliferate, become activated, or differentiate. To carry out their functional activities, macrophages must become activated. After interacting with IFN-γ, a cytokine released by activated T lymphocytes, macrophages undergo biochemical, morphologic, and functional modications that allow them to perform their functional activity.[38] IFN-γ also blocks their proliferation and protects them from apoptosis.[33]

At the inflammatory sites, different proteoglycans (such as decorin) are secreted by macrophages.[39] Therefore, we wanted to know its effect on BMDMs, a homogeneous population of nontransformed cells.[28] Decorin inhibits M-CSF±dependent proliferation of macrophages and inhibits apoptosis induced by growth factor withdrawal. After the treatment with decorin, we detected the induction of both cdk inhibitors ($p21^{Waf1}$ and $p27^{Kip1}$). Using mice with these genes disrupted by homologous recombination, we have found that $p27^{Kip1}$ is responsible for the antiproliferative effect of decorin, whereas $p21^{Waf1}$ is required to induce protection against apoptosis.

The inhibition of M-CSF±dependent proliferation in macrophages by decorin confirms previous observations in several tumor cells.[34] However, the mechanism of inhibition is different from what has been described because in tumor cells the growth-suppressive properties of decorin require a functional cdk inhibitor $p21^{Waf1}$.[34] Our observation is in accordance with the fact that fibrillar collagen, a molecule that interacts closely with decorin both in vitro[40] and in vivo,[13] inhibits smooth muscle cell proliferation by inducing the expression of $p27^{Kip1}$.[41] In addition, we have observed that binding of macrophages to fibronectin, another protein of the ECM that binds to decorin, also inhibits macrophage proliferation through the induction of $p27^{Kip1}$.

We have found other differences compared to tumor cells. It has also been reported that decorin causes a rapid phosphorylation of the EGF receptor and a concurrent activation of the ERK signal pathway, which leads to a protracted induction of endogenous $p21^{Waf1}$ and, ultimately, cell cycle arrest.[22,25] Although we did not detect a direct activation of the ERK pathway by decorin, the latter extended the ERK activity induced by M-CSF. In previous works we have described that this elongation is important for the

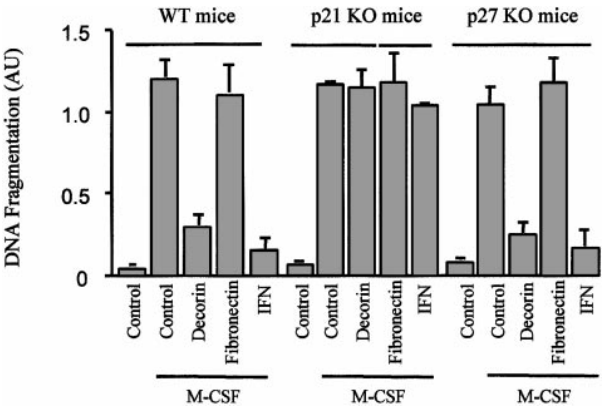

Figure 9. Decorin, but not fibronectin, protects macrophages from apoptosis induced by M-CSF starvation. Macrophages from wild-type, $p21^{Waf1}$ knock-out, and $p27^{Kip1}$ knock-out mice cultured on plates precoated with BSA, decorin, or fibronectin were treated with 300 U/mL IFN-γ. The cells were then cultured in the absence of M-CSF for 24 hours. Apoptosis induced by M-CSF starvation was measured by ELISA, a method that detects fragmented histone-associated low-molecular-weight DNA. That is characteristic of the apoptotic process. Each point was made in triplicate, and the values are represented as the mean 6±SD of 2 independent experiments.

regulation of macrophage proliferation and activation.[42,43] Besides, we have observed that decorin does not interact with EGF or IFN-γ receptors to inhibit macrophage proliferation.

An increasing number of observations indicate that proteoglycans can regulate cell proliferation through interaction with various growth factors.[44] The expression of decorin in CHO cells has a dramatic effect on their morphology and growth properties.[19] This effect is partly caused by the ability of decorin to bind to TGF-β, which stimulates the growth of those cells.[15] Current studies indicate that the nature of the local ECM can modulate cell responses to a given signal in several ways, such as by modifying the affinity of the ligand for its cognate receptor or by influencing on proteolytic processing and internalization.[4] We believe these could not be the mechanisms that explain the antiproliferative effect of decorin. Decorin binds to TGF-β, and in previous studies we have shown that TGF-β increases the proliferation of macrophages.[31] However, the blockage of TGF-β signaling using antibodies specific for this cytokine abolishes the enhancement of proliferation induced by TGF-β without modifying the normal proliferative capacity of macrophages.[31] Moreover, decorin does not seem to act by sequestering growth factors required by macrophages, such as M-CSF, because decorin also inhibits the proliferation of RAW 264.7, a macrophagic cell line that is growth independent of M-CSF (data not shown). Moreover, the fact that decorin also inhibits the proliferation of macrophages using recombinant M-CSF suggests that no other growth factors or mitogenic derivatives (ie, proteoglycan±M-CSF) present in the L cell-conditioned media should mediate the effects of decorin. Also, the inhibition of GM-CSF±induced proliferation by decorin suggests that the effect of decorin is a general mechanism of proliferation.

The growth of adherent cells such as fibroblasts or macrophages requires signals not only from growth factor receptors but also from integrins.[36,45,46] That is also true for macrophages, because the total inhibition of their adhesion blocks macrophage proliferation. However, we thereby show for the first time that the level of this adhesion has a strong effect on the modulation of the level of macrophage proliferation. A strong attachment induced by decorin or fibronectin is enough to reduce macrophage proliferation, whereas a slight adhesion such as that induced by laminin increases proliferation. The use of anti-β_1 antibodies and RGD peptides confirm this hypothesis. Macrophages adhere to plastic dishes mainly through integrin receptors, because RGD peptides almost totally block this adhesion. Moreover, macrophages need to adhere to proliferate; in this regard, RGD and P-OH-M inhibit both macrophage adhesion and proliferation. Besides, the studies using anti-β_1 antibodies and RGD suggest that the effect of decorin is mediated through a non±β_1-integrin receptor, whereas fibronectin uses a β_1-integrin receptor. The fact that decorin has a synergic effect on macrophage adhesion to fibronectin also suggests that decorin uses a different receptor than fibronectin. However, more studies are necessary to determine which receptor is used by decorin in macrophages.

A few examples have been described for the G_1 phase blockage mediated by cellular adhesion. This effect is caused by the increase of the expression of $p27^{Kip1}$, which inhibits cyclin E-cdk2 kinase activity.[41,47,48] Cell-to-cell contact induces the cells to stop proliferating during normal organ development. More recently it has become clear that such contact-mediated growth arrest is caused by the up-regulation of $p27^{Kip1}$. This is shown in the $p27^{Kip1}$ knock-out mice, which are generally bigger and have a significantly expanded hematopoietic progenitor pool.[49,50] We have observed that the inhibitory effect on macrophage proliferation induced by adhesion to some ECM components (ie, decorin or fibronectin) is also mediated through the expression of $p27^{Kip1}$.

In addition, the signals mediated by the ECM are important for cell survival. A laminin-rich ECM is a potential survival factor for differentiated mammary alveolar epithelial cells both in vivo and in vitro.[51] It has been suggested that the laminin-rich ECM acts through $a_6\beta_1$-integrin receptors to affect cell survival, partly by stabilizing phosphoinositol-3 kinase-dependent survival responses to insulin (or insulinlike growth factor 1).[52,53] Our results with decorin are very interesting and confirm previous results from our group.[33] Decorin protects macrophages from apoptosis induced by M-CSF starvation. In this case, the effect of decorin is not mediated by the increase in adhesion. As we have described elsewhere,[33] the induction of $p21^{Waf1}$ and the blockage of the cell cycle induced by decorin (or IFN-γ) are responsible for the protective effect against apoptosis. The results obtained using $p21^{Waf1}$ knock-out mice confirm this conclusion.

Our results could have physiologic relevance. Although the concentration of decorin precoating solution used in our studies (10-100 μg/mL) could seem slightly higher than that estimated to occur in collagenous matrices (5-12.5 μg/mL) found in vivo,[22] the amount of decorin adsorbed to the plate should be significantly lower. Macrophages play a critical role during inflammation. From blood, macrophages reach the inflammatory foci and remain there until inflammation disappears.[54] In the tissues, macrophages need to survive in the absence of growth factors. Whereas stimulated Th1 cells remain at the inflammatory loci and produce IFN-γ, macrophages are protected against apoptosis.[33] In addition to IFN-γ, the elements that form the ECM, such as decorin, could also protect against apoptosis. An example of this situation may be found in the formation of granulomas that can appear in the course of certain infiammatory responses. The macrophages in these granulomas secrete decorin.[55,56] Each granuloma can be viewed as a small spherical organ made of a variety of differentiated macrophages whose function is to limit the expansion of, and allow the eventual destruction of, extravascular bacteria.[57,58] Decorin may favor macrophage survival and accumulation in granulomas, thus leading to bacterial elimination. Our observations on IFN-γ and decorin could provide an explanation for long-term living macrophages within the tissues.

Acknowledgments

We specially thank Dr E. Ruoslahti and Dr Richard Maki from The Burnham Institute, La Jolla, CA, for the kind gift of all the purified decorin used in this work as well as for all their support. We also thank Dr J. Roberts from HHMI, Seattle, WA, and Dr Modolell from the Max Plank Institute, Freiburg, Germany, for the $p21^{Waf1}$/

$p27^{Kip1}$ and IFN-γR knock-out mice, respectively. We specially thank Dr Gabriel Gil, Institut Municipal d'Investigacions Biomèdiques, Barcelona, Spain, for his help with the $p21^{Waf1}$ and $p27^{Kip1}$ knock-out mice.

References

1. Nathan CF. Secretory products of macrophages. J Clin Invest. 1987;79:319-326.
2. Laskin JD, Dokidis A, Sirak AA, Laskin DL. Distinct patterns of sulfated proteoglycan biosynthesis in human monocytes, granulocytes and myeloid leukemic cells. Leuk Res. 1991;15:515-523.
3. Uhlin-Hansen L, Langvoll D, Wik T, Kolset SO. Blood platelets stimulate the expression of chondroitin sulfate proteoglycan in human monocytes. Blood. 1992;80:1058-1065.
4. Iozzo RV, Murdoch AD. Proteoglycans of the extracellular environment: clues from the gene and protein side offer novel perspectives in molecular diversity and function. FASEB J. 1996;10:598-614.
5. Iozzo RV. The family of the small leucine-rich proteoglycans: key regulators of matrix assembly and cellular growth. Crit Rev Biochem Mol Biol. 1997;52:141-174.
6. Choi HU, Neame PJ, Johnson TL, et al. Characterization of the dermatan sulfate proteoglycan, DS-PGII, from bovine articular cartilage and skin isolated by octyl-sepharose chromatography. J Biol Chem. 1989;264:2876-2884.
7. Nakamura T, Matsunaga E, Shinkai H. Isolation and some structural analyses of a proteodermatan sulphate from calf skin. Biochem J. 1983;213:289-296.
8. Poole AR, Webber C, Pidoux I, Choi HU, Rosenberg LC. Localization of a dermatan sulfate proteoglycan (DS-PGII) in cartilage and the presence of an immunologically related species in other tissues. J Histochem Cytochem. 1986;34:619-625.
9. Rosenberg LC, Choi HU, Tang L-H, et al. Isolation of dermatan sulfate proteoglycans from mature bovine articular cartilages. J Biol Chem. 1985;260:6304-6313.
10. Fisher LW, Termine JD, Dejter SW, et al. Proteoglycans of developing bone. J Biol Chem. 1983;258:6588-6594.
11. Bidanset DJ, Guidry C, Rosenberg LC, Choi HU, Timpl R, Hook M. Binding of the proteoglycan decorin to collagen type VI. J Biol Chem. 1992;267:5250-5256.
12. Schonherr E, Witch-Prehm P, Harrach B, Robeneck H, Rauterberg J, Kresse H. Interaction of biglycan with type I collagen. J Biol Chem. 1995;270:2776-2783.
13. Danielson KG, Baribault H, Holmes DF, Graham H, Kadler KE, Iozzo RV. Targeted disruption of decorin leads to abnormal collagen fibril morphology and skin fragility. J Cell Biol. 1997;136:729-743.
14. Hildebrand A, Romaris M, Rasmussen LM, et al. Interaction of the small interstitial proteoglycan biglycan, decorin and fibromodulin with transforming growth factor beta. Biochem J. 1994;302:527-534.
15. Yamaguchi Y, Mann DM, Ruoslahti E. Negative regulation of transforming growth factor-β by the proteoglycan decorin. Nature. 1990;346:281-284.
16. Lewandowska K, Choi HU, Rosenberg L, Zardi L, Culp LA. Fibronectin-mediated adhesion of fibroblasts: inhibition by dermatan sulfate proteoglycan and evidence for a cryptic glycosaminoglycan-binding domain. J Cell Biol. 1987;105:1443-1454.
17. Schmidt G, Robenek H, Harrach B, et al. Interaction of small dermatan sulfate proteoglycan from fibroblasts with fibronectin. J Cell Biol. 1987;104:1683-1691.
18. Winnemoller M, Schmidt G, Kresse H. Influence of decorin on fibroblast adhesion to fibronectin. Eur J Cell Biol. 1991;54:10-17.
19. Yamaguchi Y, Ruoslahti E. Expression of human proteoglycan in Chinese hamster ovary cells inhibits cell proliferation. Nature. 1988;336:244-246.
20. Coppock DL, Kopman C, Scandalis S, Gilleran S. Preferential gene expression in quiescent human lung fibroblasts. Cell Growth Differ. 1993;4:483-493.
21. Mauviel A, Santra M, Chen YQ, Uitto J, Iozzo RV. Transcriptional regulation of decorin gene expression. Induction by quiescence and repression by tumor necrosis factor-α. J Biol Chem. 1995;270:11692-11700.
22. Santra M, Eichstetter I, Iozzo RV. An anti-oncogenic role for decorin. J Biol Chem. 2000;275:35153-35161.
23. Iozzo RV, Cohen I. Altered proteoglycan gene expression and the tumor stroma. Experientia. 1993;49:447-455.
24. Santra M, Skorski T, Calabreta B, Lattime EC, Iozzo RV. De novo decorin gene expression suppresses the malignant phenotype in human colon carcinoma cells. Proc Natl Acad Sci U S A. 1995;92:7016-7020.
25. Moscatello DK, Santra M, Mann DM, McQuillan DJ, Wong AJ, Iozzo RV. Decorin suppresses tumor cell growth by activating the epidermal growth factor receptor. J Clin Invest. 1998;101:406-412.
26. Isaka Y, Brees DK, Ikegaya K, et al. Gene therapy by skeletal muscle expression of decorin prevents fibrotic disease in rat kidney. Nat Med. 1996;4:418-423.
27. Giri SN, Hyde DM, Braun RK, Gaarde W, Harper JR, Pierschbacher MD. Antifibrotic effect of decorin in a bleomycin hamster model of lung fibrosis. Biochem Pharmacol. 1997;54:1205-1216.
28. Celada A, Borras FE, Soler C, et al. The transcription factor PU.1 is involved in macrophage proliferation. J Exp Med. 1996;184:61-69.
29. Celada A, Gray PW, Rinderknecht E, Schreiber RO. Evidences for a γ-interferon receptor that regulates macrophage tumoricidal activity. J Exp Med. 1984;160:55-74.
30. Torczynski P, Bollon AP, Fuke M. The complete nucleotide sequence of the rat 18S ribosomal RNA gene and comparison with the respective yeast and frog genes. Nucleic Acid Res. 1983;11:4879-4890.
31. Celada A., Maki RA. Transforming growth factor-a enhances the M-CSF and GM-CSF-stimulated proliferation of macrophages. J Immunol. 1992;148:1102-1105.
32. Xaus J, Comalada M, Valledor AF, et al. LPS induces apoptosis in macrophages mostly through the autocrine production of TNF-α. Blood. 2000;95:3823-3831.
33. Xaus J, Cardo M, Valledor AF, Soler C, Lloberas J, Celada A. Interferon γ induces the expression of $p21^{waf1}$ and arrests macrophage cell cycle, preventing induction of apoptosis. Immunity. 1999;11:103-113.
34. Santra M, Mann DM, Mercer EW, Skorski T, Calabretta B, Iozzo RV. Ectopic expression of decorin protein core causes a generalized growth suppression in neoplastic cells of various histogenic origin and requires endogenous p21, an inhibitor of cyclin-dependent kinases. J Clin Invest. 1997;100:149-157.
35. Sun H, Charles CH, Lau LF, Tonks NK. MKP-1 (3CH134), an immediate early gene product, is a dual specificity phosphatase that dephosphorylates MAP kinase in vivo. Cell. 1993;75:487-493.
36. Ruoslahti E, Reed JC. Anchorage dependence, integrins, and apoptosis. Cell. 1994;77:477-478.
37. Giancotti FG. Integrin signalling: specificity and control of cell survival and cell cycle progression. Curr Opin Cell Biol. 1997;9:691-700.
38. Celada A, Nathan CF. Macrophage activation revisited. Immunol Today. 1994;15:100-102.
39. Uhlin-Hansen T, Wik L, Kjellen L, Berg E, Forsdahl F, Kolset SO. Proteoglycan metabolism in normal and inflammatory human macrophages. Blood. 1993;82:2880-2889.
40. Vogel KG, Trotter JA. The effects of proteoglycans on the morphology of collagen fibrils formed in vitro. Collagen Relat Res. 1987;7:105-114.
41. Koyama H, Raines EW, Bornfeldt KE, Roberts JM, Ross R. Fibrillar collagen inhibits arterial smooth muscle proliferation through regulation of cdk2 inhibitors. Cell. 1996;87:1069-1078.
42. Valledor AF, Xaus J, Marques L, Celada A. Macrophage colony-stimulating factor induces the expression of mitogen-activated protein kinase phosphatase-1 through a protein kinase C-dependent pathway. J Immunol. 1999;163:2452-2462.
43. Valledor AF, Comalada M, Xaus J, Celada A. The differential time-course of extracellular-regulated kinase activity correlates with the macrophage response toward proliferation or activation. J Biol Chem. 2000;275:7403-7409.
44. Ruoslahti E. Proteoglycans in cell regulation. J Biol Chem. 1989;264:13369-13372.
45. Howe A, Aplin AE, Alahari SK, Juliano RL. Integrin signalling and cell growth control. Curr Opin Cell Biol. 1998;10:220-231.
46. Zhu X, Ohtsubo M, Bohmer RM, Roberts JM, Assoian RK. Adhesion-dependent cell cycle progression linked to the expression of cyclin D1, activation of cyclin E-cdk2, and phosphorylation of the retinoblastoma protein. J Cell Biol. 1996;133:391-403.
47. Chen CS, Mrksich M, Huang S, Whitesides GM, Ingber DE. Geometric control of cell life and death. Science. 1997;276:1425-1428.
48. Jiang Y, Prosper F, Verfaillie CM. Opposing effects of engagement of integrins and stimulation of cytokine receptors on cell cycle progression of normal human hematopoietic progenitors. Blood. 2000;95:846-854.

49. Johnson D, Frame MC, Wake JA. Expression of the v-Src oncoprotein in fibroblasts disrupts normal regulation of the cdk inhibitor p27 and inhibits quiescence. Oncogene. 1998;16:2017-2028.
50. Nakayama K, Ishida N, Shirane M, et al. Mice lacking p27(Kip1) display increased body size, multiple organ hyperplasia, retinal dysplasia, and pituitary tumors. Cell. 1996;85:707-720.
51. Finlay D, Healy V, Furlong F, O' Connell FC, Keon NK, Martin F. MAP kinase pathway signalling is essential for extracellular matrix determined mammary epithelial cell survival. Cell Death Differ. 2000;7:302-313.
52. Boudreau N, Sympson CJ, Werb Z, Bissell MJ. Suppression of ICE and apoptosis in mammary epithelial cells by extracellular matrix. Science. 1995;267:891-893.
53. Farrelly N, Lee YJ, Oliver J, Dive C, Streuli CH. Extracellular matrix regulates apoptosis in mammary epithelium through a control on insulin signalling. J Cell Biol. 1999;144:1337-1348.
54. Bellingan GJ, Caldwell H, Howie SE, DransÆeld, Haslett C. In vivo fate of the inflammatory macrophage during the resolution of inflammation: inflammatory macrophages do not die locally, but emigrate to the draining lymph nodes. J Immunol. 1996;157:2577-2585.
55. Asakura S, Colby TV, Limper AH. Tissue localization of transforming growth factor-beta 1 in pulmonary eosinophilic granuloma. Am J Respir Care Med. 1996;154:1525-1530.
56. Limper AH, Colby TV, Sanders MS, Asakura S, Roche PC, DeRemee RA. Immunohistochemical localization of transforming growth factor-beta 1 in the nonnecrotizing granulomas of pulmonary sarcoidosis. Am J Respir Crit Care Med. 1994; 149:197-204.
57. Adams DO. The granulomatous inflammatory response. Am J Pathol. 1976;84:164-191.
58. Williams GT, Williams WJ. Granulomatous inflammation. A review. J Clin Pathol. 1983;36:723-733.

3. La decorina revierte el efecto represivo del TGF-β producido de manera endocrina en los macrófagos activados.

Resumen

Algunas de las citocinas o de los factores de crecimiento hacen que los macrófagos proliferen, se activem, se diferencien o mueran mediante apoptosis. El IFNγ es el activador más potente de los macrófagos y bloquea su proliferación a la vez que los protege de los procesos apoptoticos. Esta protección permite a los macrófagos sobrevivir en los lugares de inflamación. Al igual que el IFNγ, la decorina (un proteoglicano de la matriz extracelular), inhibe la proliferación y protege a los macrófagos de la inducción de apoptosis a través de la expresión de $p27^{Kip1}$ y de $p21^{Waf1}$ respectivamente. La decorina es secretada por los monocitos y los macrófagos en los puntos de inflamación y modula la respuesta inmunitaria. Este proteoglicano también modula la síntesis e interacción de otras proteínas de la matriz extracelular.

Debido a las propiedades que tienen en común el IFNγ y la decorina, se pensó en la posibilidad de que la decorina ejerza un papel de activación en los macrófagos. Para este estudio se han utilizado cultivos primarios de macrófagos de la médula ósea de ratón, que es una población homogénea que prolifera activamente y responde a estímulos de activación. Los resultados muestran que la decorina aumenta la activación inducida tanto por el LPS como por el IFNγ. El tratamiento con decorina de los macrófagos activados con IFNγ induce un incremento de la expresión del complejo principal de histocompatibilidad (MHC) de tipo II. También se ve incrementada la expresión de sintasa inducible del oxído nítrico (iNOS) y la del mRNA de las citocinas inducidas por el IFNγ.

La activación de los macrófagos se encuentra modulada tanto por la adhesión celular como por la señalización a través de la vía de las integrinas. Si se cultivan los macrófagos en placas tratadas con distintas proteínas de la matriz extracelular las células muestran distintos grados de adhesión para cada una de las proteínas. Mientras que la decorina, la vitronectina y la fibronectina incrementan la adhesión de los macrófagos, las proteínas como la laminina y el colágeno la disminuyen. También se observó que aquellas proteínas que ejercían un mayor poder de adhesión a su vez inhibían más drásticamente la proliferación de los macrófagos. Los experimentos con fibronectina muestraron que esta no es capaz de modular la activación de los macrófagos inducida por el LPS o el IFNγ. Nuestros resultados indican que tanto el efecto de adhesión, como el efecto antiproliferativo de la decorina no son suficientes para explicar el papel que ejerce aumentando la activación en los macrófagos.

Los estudios realizados con TGF-β marcado con ^{125}I muestran que esta citocina se une a la superficie de los macrófagos y que la decorina es capaz de inhibir la unión del TGF-β a su receptor. Además, la decorina es capaz de revertir los efectos inhibitorios que tiene esta citocina en la activación de los macrófagos. Nuestros experimentos demuestran que los efectos de la decorina en la activación de los macrófagos son debidos al secuestro del TGF-β producido de forma endógena.

En conclusión, en nuestro trabajo hemos demostrado que la decorina aumenta tanto la activación de los macrófagos inducida por el LPS como por el IFNγ, como se demuestra por el incremento en la expresión del MHC de clase II, iNOS y de la expresión de citocinas. El efecto de este proteoglicano en la activación de los macrófagos es debido a su capacidad de bloquear la unión del TGF-β producido de forma autocrina a los receptores de la superficie de los macrófagos.

Decorin Reverses the Repressive Effect of Autocrine-Produced TGF-β on Mouse Macrophage Activation

Several cytokines or growth factors induce macrophages to proliferate, become activated, differentiate, or die through apoptosis. Like the major macrophage activator IFN-γ, the extracellular matrix protein decorin inhibits proliferation and protects macrophages from the induction of apoptosis. Decorin enhances the IFN-γ-induced expression of the IAα and IAβ MHC class II genes. Moreover, it increases the IFN-γ- or LPS-induced expression of inducible NO synthase, TNF-α, IL-1β, and IL-6 genes and the secretion of these cytokines. Using a number of extracellular matrix proteins, we found a negative correlation between adhesion and proliferation. However, the effects of decorin on macrophage activation do not seem to be mediated through its effect on adhesion or proliferation. Instead, this proteoglycan abolishes the binding of TGF-β to macrophages, as shown by Scatchard analysis of ^{125}I-labeled TGF-β, which, in the absence of decorin, showed a K_d of 0.11 ± 0.03 nM and ~ 5000 receptors/cell. This was con rmedwhen we treated macrophages with Abs to block the endogenously produced TGF-β, which enhanced macrophage activation in a way similar to decorin. The increase in activation mediated by decorin demonstrates that macrophages are under negative regulation that can be reversed by proteins of the extracellular matrix.

Macrophages play a key role in the immune response. These phagocytic cells are produced in the bone marrow and transported in blood to distinct tissues. Most macrophages die through apoptosis; however, in the presence of certain cytokines or growth factors, they proliferate, differentiate into several cell types (Kupffer cells, Langerhans, microglia, etc.), or become activated to develop their functions. At the inflammatory loci, macrophage phagocyte bacteria, remove cell debris, release several mediators, present Ags to T lymphocytes, and contribute to the resolution of inflammation (1).

IFN-γ, which is released by activated T lymphocytes or NK cells, is the most potent activator of macrophages and induces the expression of > 300 genes (2). We found that this cytokine also blocks macrophage proliferation and protects against apoptosis (3). This protection allows macrophages to survive at the inflammatory loci when IFN-γ is present and explains the key role that T lymphocytes play in delayed hypersensitivity (4, 5).

At the inflammatory loci, proteoglycans are secreted by monocytes and macrophages (6, 7) and modulate the immune response. Decorin and other related molecules form a family called small leucine-rich proteoglycans, which are found in the extracellular matrix (ECM)[5] of a variety of tissues (8). Although the biological role of these molecules is unclear, several observations indicate that decorin and perhaps other proteoglycans regulate the remodeling of connective tissue. In particular, binding studies in vitro have shown that decorin interacts with several types of collagen, and it is believed to be a key regulator of collagen fibrillogenesis (9). This proteoglycan may also affect the production of other ECM components (10, 11). Additionally, decorin modulates the interactions of matrix molecules such as fibronectin with cells (12, 13).

Decorin, like IFN-γ, inhibits the proliferation of macrophages and enhances cell survival through the expression of $p27^{Kip1}$ and $p21^{waf-1}$, respectively (14). Since we previously found that activation by IFN-γ or LPS inhibits the proliferation of these phagocytic cells (15), here we studied the effect of decorin on macrophage activation. We used primary cultures of bone marrow-derived macrophages, a homogeneous cell population that responds to physiological proliferative or activating stimuli (16). Decorin enhances both LPS- and IFN-γ-induced activation, as shown by the capacity to increase MHC class II, inducible NO synthase (iNOS), and cytokine expression. The effect of this proteoglycan is explained by its ability to block the binding of autocrine-produced TGF-β on the surface of macrophages.

Materials and Methods

Reagents

Recombinant purified decorin was a gift from Dr. E. Ruoslahti (The Burnham Institute, La Jolla, CA). LPS, BSA, collagen I, vitronectin, laminin, and fibronectin were obtained from Sigma-Aldrich (St. Louis, MO). [^{3}H]thymidine, TGF-β, and ^{125}I-labeled TGF-β were purchased from Amersham Pharmacia Biotech (Uppsala, Sweden). IFN-γ was a gift from Genentech (South San Francisco, CA). All other products were of the highest analytical grade available and were purchased from Sigma-Aldrich. Deionized water that had been further purified with a Millipore Milli-Q system (Bedford, MA) was used.

Cell culture

Bone marrow-derived macrophages were isolated from 6-wk-old BALB/c mice (Charles River Laboratories, Wilmington, MA) as previously described (16). Cells were cultured in plastic tissue culture dishes (150 mm) in 40 ml of DMEM containing 20% FBS and 30% L cell-conditioned medium as a source of M-CSF. They were then incubated at 37°C in a humidified 5% CO_2 atmosphere. After 7 days of culture, a homogeneous population of adherent macrophages was obtained (>99% Mac-1^+).

In some circumstances cells were cultured on a precoated plate using distinct components of the ECM or BSA as a control. For precoating, the plates were incubated overnight at 4°C with a PBS solution of the indicated concentration of each ECM component. After coating, the plates were blocked with PBS/10 μg/ml BSA for 1 h at 37°C, the blocking solution was then removed, and the cells were cultured with normal complete

[5] Abbreviations used in this paper: ECM, extracellular matrix; iNOS, inducible NO synthase.

medium.

Abs and constructs

For analysis of IA surface expression by flow cytometry, we used purified anti-mouse $IA^{d,b}$ mAbs (BD PharMingen, San Diego, CA). FITC-conjugated anti-mouse IgG (Cappel, Turnhout, Belgium) was used as secondary Ab. An unrelated primary Ab purchased from Sigma-Aldrich was used as the control. For Western blot analysis we used a rabbit Ab against mouse iNOS (M-19; Santa Cruz Biotechnology, Santa Cruz, CA) and a mouse anti-β-actin Ab (Sigma-Aldrich) as a control. Peroxidase-conjugated anti-rabbit or anti-mouse IgG (Cappel) were used as secondary Abs. Blocking polyclonal Abs against TGF-β were obtained from Promega (Madison, WI). For analysis of TGF-β expression by Western blot, the same Abs were used.

The cDNA probes for IA-α and IA-β used for Northern blot analysis were gifts from P. Cosson (Basel Institute for Immunobiology, Basel, Switzerland). A rat iNOS cDNA fragment (17) was used to detect IFN-γ- and LPS-induced iNOS expression. For TNF-β mRNA detection we used a cDNA probe obtained from Dr. M. Nabholz (Institut Suisse de Recherches Experimentales sur le Cancer, Epalinges, Switzerland). To study the expression of IL-1β, we obtained a probe by digesting the construct pGEM1/IL-1β (provided by Dr. R. Wilson, Glaxo Research and Development Limited, Greenford, U.K.) with *Eco*RI/*Pst*I. The IL-6 cDNA probe was a gift from Dr. S. Rohatgi (Center for Blood Research, Boston, MA). The probe for 18S rRNA was obtained as described previously (18).

Cell surface staining

Cell surface staining was performed using specific Abs and was assessed using cytofluorometric analysis (19) with mouse mAb anti-mouse IA^{db} (1 μg/10^6 cells). Adhered macrophages were collected by cell scrapping. An unrelated Ab was used as a control for nonspecificity. Cells were then washed by centrifugation through an FBS cushion. Stained cell suspensions were analyzed using an EPICS XL flow cytometer (Coulter, Hialeah, FL). Only viable cells were analyzed for surface staining, gating them based on the forward and side light scatter signals.

ELISAs

The secretion of inflammatory cytokines (TNF-α, IL-1β, and IL-6) was analyzed by ELISA using commercial murine kits following the manufacturer's recommendations (Cytoset system; BioSource, Nivelles, Belgium). In brief, 5 x 10^5 macrophages were cultured in 24-well precoated plates in 0.5 ml of complete medium for 2 h. Once they attach to the plates, cells were stimulated with subsaturating amounts of IFN-γ or LPS as described, and the supernatants were recollected 24 h later and immediately used for ELISA analysis. Each sample was analyzed in triplicate, and the results are presented as the mean ± SD.

Proliferation and adhesion analysis

Cell proliferation was analyzed by [^{3}H]thymidine incorporation, and cell adhesion to the substrate was determined by crystal violet staining as previously described (14). Each sample was analyzed in triplicate, and the results are presented as the mean ± SD.

Scatchard and TGF-β binding analysis

To analyze the binding of TGF-β to macrophages and the capacity of decorin to modulate this process we cultured 10^6 cells/well in 12-well plates precoated with 10 g/ml BSA or decorin. We then washed them with Krebs-Ringer-HEPES (128 mM NaCl, 5 mM KCl, 5 mM Mg SO_4, 1.3 mM $CaCl_2$, and 50 mM HEPES; pH 7.4). For the binding analysis we incubated cells with the indicated amounts of iodinated TGF-β. For the Scatchard analysis, ^{125}I-labeled TGF-β (100 pM) binding was competed with increasing amounts of cold TGF-β. Cells were incubated on a rotating platform for 3 h at 4°C. They were then washed and cross-linked for 15 min at 4°C with 0.5 ml of dioctyl sodium sulfosuccinate solution (6 µ g/ml in Krebs-Ringer-HEPES). After two washes with 0.25 M sucrose, 10 mM Tris-HCl, and 1 mM EDTA, proteins were solubilized with 200 l of 0.5% Triton-Tris-HCl-EDTA and protease inhibitors for 40 min at 4°C. The supernatants were then transferred to test tubes, boiled for 1 min, and counted using a Packard gamma counter (Downers Grove, IL). Each point was determined in triplicate, and the results are expressed as the mean ± SD.

Northern blot analysis

Northern blot analysis was performed as previously described (14) using 20 μg of total cellular RNA/lane. To check for differences in RNA loading, we analyzed the expression of the 18S rRNA transcripts. All probes were labeled with [α-^{32}P]dCTP (ICN Pharmaceuticals, Costa Mesa, CA) with the oligolabeling kit method (Amersham Pharmacia Biotech). The bands of interest were quantified with a Molecular Analyst system (Bio-Rad, Richmond, CA).

Protein extraction and Western blot analysis

Western blot analysis was performed as previously described (19). One hundred micrograms of protein from cell lysates was loaded per lane and separated on a 7.5% SDS-PAGE. For iNOS immunoblotting, we used a rabbit Ab against mouse iNOS (M-19; Santa Cruz Biotechnology) and a mouse anti-β-actin Ab (Sigma-Aldrich) as a control. For the analysis of TGF-α expression a polyclonal Ab directed to biologically active human TGF-α (Promega) was used. Peroxidase-conjugated anti-rabbit and anti-mouse IgG (Cappel) were used as secondary Abs. Incubations were performed for 1 h at room temperature. ECL detection was performed (Amersham Pharmacia Biotech), and the membranes were exposed to x-ray films (Amersham Pharmacia Biotech).

Statistical analysis

To calculate the statistical differences between the control and treated samples (decorin or fibronectin), we used Student's paired *t* test. Values of p 0.05 or less were interpreted as significant.

Results

Decorin enhances IFN-γ- and LPS-dependent macrophage activation

Having shown that decorin inhibits the M-CSF-dependent proliferation of macrophages (14) and that the proliferative state of these cells modulates their activity (15), here we studied the effects of this proteoglycan on macrophage activation. For this purpose we used macrophages obtained from bone marrow cultures, since they represent a homogeneous, nontransformed population that can be activated in vitro to induce proliferation, differentiation, or apoptosis.

First, we analyzed the effect of decorin on MHC class II expression induced by IFN-γ, the main macrophage activator (2). Macrophages were cultured on plates precoated with 10 μg/ml decorin or with 10 μg/ml BSA as a control. It is important to note that the indicated concentrations of decorin correspond to the concentration of the precoating solution and that we were not able to quantify the amount of decorin adsorbed on the plate after precoating, but other proteins under the same conditions bound <10–20%. Once attached to the plates, when cells were stimulated with subsaturating amounts of IFN-γ (10 U/ml), flow cytometry after 48 h showed that decorin induced a statistically significant increase in MHC II protein surface expression compared with those treated only with IFN-γ (Fig. 1, *a* and *b*). The increase in IA protein surface expression correlated, as measured by Northern blotting, with a rise in the expression of IA-α and IA-β mRNA (Fig. 1*c*).

The effect of decorin on IFN-γ-induced activation was not spe-

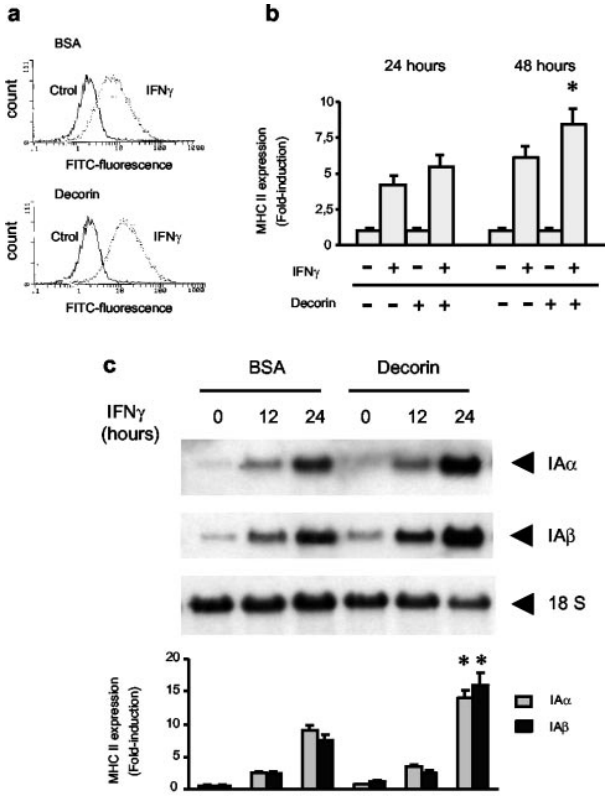

FIGURE 1. Decorin increases IFN-γ-induced MHC class II expression. *a*, Decorin increases IFN-γ-induced MHC class II surface expression The expression of IA molecules on the cell surface was analyzed by flow cytometry. Macrophages were cultured on a 10 μg/ml precoated BSA or decorin surface for 24 h in the presence (dotted histogram) or absence (solid line histogram) of subsaturating amounts of IFN-γ (10 U/ml). *b*, Quantitation of IA surface expression using Immuno-4 software. The values shown correspond to the mean $\pm$ SD of three independent experiments. *, $p < 0.01$ between BSA- and decorin-treated samples. *c*, Decorin increases IFN-γ-induced MHC class II mRNA expression. The expression of IA-α and IA-β mRNA was analyzed by Northern blotting. Macrophages were cultured on a 10μ g/ml precoated BSA or decorin surface and stimulated with subsaturating amounts of IFN-γ (10 U/ml) for the indicated times. Quantification of the bands of interest was performed by densitometry, and the figure shows the mean $\pm$ SD of four representative experiments. *, $p < 0.01$ between BSA- and decorin-treated samples.

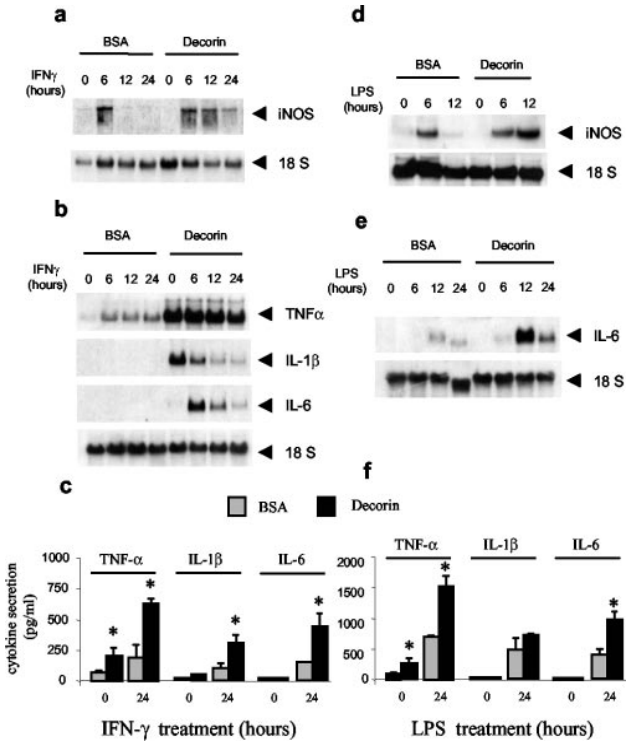

FIGURE 2. Decorin enhances IFN-γ- and LPS-dependent macrophage activation. Cells were cultured in plates precoated with BSA (10 μg/ml) or decorin (10 μg/ml) and treated with subsaturating amounts of IFN-γ (10 U/ml) or LPS (1 ng/ml) for the indicated times. The iNOS (*a* and *d*) and cytokine (*b* and *e*; TNF-β, IL-1 , or IL-6) mRNA expression was analyzed by Northern blotting. ELISA analysis of TNF-β, IL-1 , and IL-6 of the IFN-γ-treated (*c*) or LPS-treated (*f*) macrophages in the presence or the absence of decorin were performed as indicated in *Materials and Methods*. *, $p < 0.01$ between BSA- and decorin-treated samples. Results are representative of at least three independent experiments.

cific for MHC II genes, since it also increased the expression of iNOS and cytokine mRNA induced by IFN-γ. Decorin slightly increased the levels of iNOS mRNA induced by 10 U/ml IFN-γ at 6 h and elongated the expression kinetics of this enzyme (Fig. 2*a*). Subsaturating amounts of IFN-γ induced low levels of TNF-α, IL-1β, or IL-6 mRNA expression, which were only visible after overexposing the film. Culture of macrophages on plates precoated with 10 μg/ml decorin was enough to induce maximal expression of TNF-α and IL-1β mRNA (Fig. 2*b*). The addition of 10 U/ml IFN-γ did not increase this expression. While decorin alone did not induce the expression of IL-6, subsaturating amounts of IFN-γ did (Fig. 2*b*). ELISA analysis of the supernatants allows extends our findings, since they showed that decorin increases the secretion of these inflammatory cytokines. Although decorin alone induces maximal mRNA expression of TNF-α and IL-1β, it induced only small amounts of secreted TNF-α and no IL-1β (Fig. 2*c*). However, decorin increased the secreted amounts of these cytokines in response to subsaturating amounts of IFN-γ (Fig. 2*c*).

Because decorin enhances several aspects of macrophage activation induced by the endogenous activator IFN-γ, we studied the effects of some components of the bacterial wall such as LPS, which could modulate diverse functions of these macrophages. We observed that with subsaturating amounts of LPS (1 ng/ml), decorin elongated the expression of iNOS (Fig. 2*d*) and enhanced that of IL-6 (Fig. 2*e*). Similar to what we observed in macrophages treated with IFN-γ, ELISA analysis showed that decorin also increases the secretion of inflammatory cytokines such as TNF-α or IL-6 (Fig. 2*f*). Thus, this proteoglycan enhanced the macrophage activation induced by both endogenous and exogenous activators.

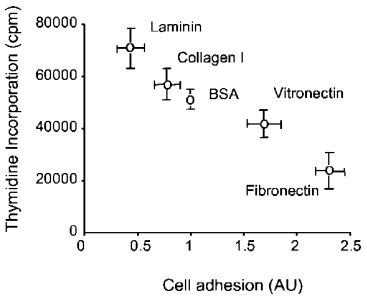

FIGURE 3. Negative correlation between adhesion and proliferation. Proliferation was determined by [^{3}H]thymidine incorporation, and adhesion was determined by by crystal violet staining in cells cultured in 10 μg/ml of the indicated ECM proteins or BSA-precoated plates for 24 h. Each point was performed in triplicate, and results are represented as the mean ± SD of five independent experiments. The adhesive and proliferative capacities of macrophages in untreated plates were not modified by the precoating of the plate with 10 μg/ml BSA.

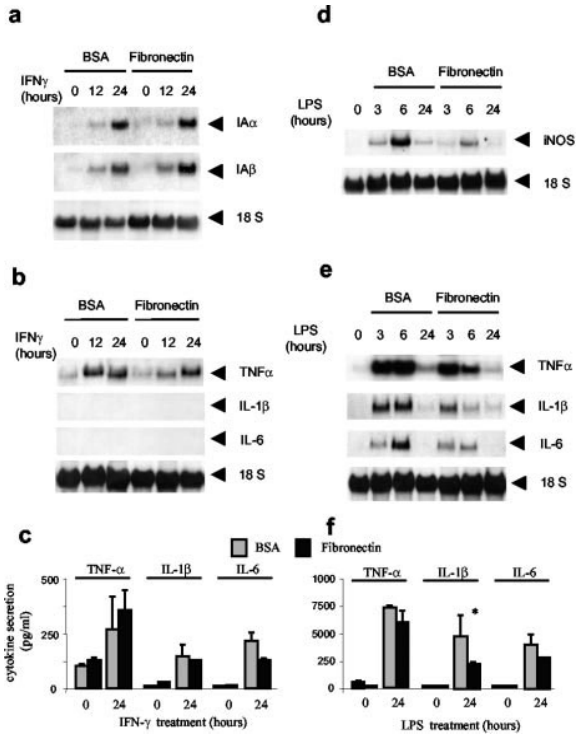

FIGURE 4. Fibronectin does not modulate IFN-γ- or LPS-induced macrophage activation. Bone marrow-derived macrophages were cultured in plates precoated with BSA (10 μg/ml) or fibronectin (10 μg/ml) and treated with subsaturating amounts of IFN-γ (10 U/ml) or LPS (1 ng/ml) for the indicated times. MHC class II (IA-α and IA-β; *a*), cytokine (TNF-β, IL-1β, or IL-6; *b* and *e*), or iNOS (*d*) mRNA expression were analyzed by Northern blotting. Results are representative of four independent experiments. ELISA analysis of TNF-β, IL-1β, and IL-6 of the IFN-γ-treated (*c*) or LPS-treated (*f*) macrophages in the presence or the absence of decorin was performed as indicated in *Materials and Methods*. *, $p < 0.01$ between BSA- and fibronectin-treated samples.

Decorin-induced adhesion does not mediate the decorin enhancement of macrophage activation

Since LPS and IFN-γ activate macrophages via distinct pathways, we attempted to identify a possible common mechanism used by decorin to enhance these pathways. Consistent with previous observations, decorin inhibited macrophage proliferation and enhanced their adhesion (14). We also demonstrated that the proliferative state of macrophages could modulate the activation capabilities of these cells (15). Moreover, cellular adhesion and integrin signaling are potent modulators of macrophage activity (20, 21). To explore the possible consequences of increased adhesion and the anti-proliferative effect on the enhanced activation induced by decorin, we used other components of the ECM that modify macrophage adhesion.

Macrophages cultured in plates treated with diverse ECM proteins showed varying degrees of adhesion. While decorin, vitronectin, and fibronectin increased macrophage adhesion on plates treated with BSA, laminin and collagen I decreased this process (Fig. 3). We found a negative correlation between the degree of adhesion and proliferation (Fig. 3). Specifically, cells grown on fibronectin or decorin surfaces, to which they attached strongly,

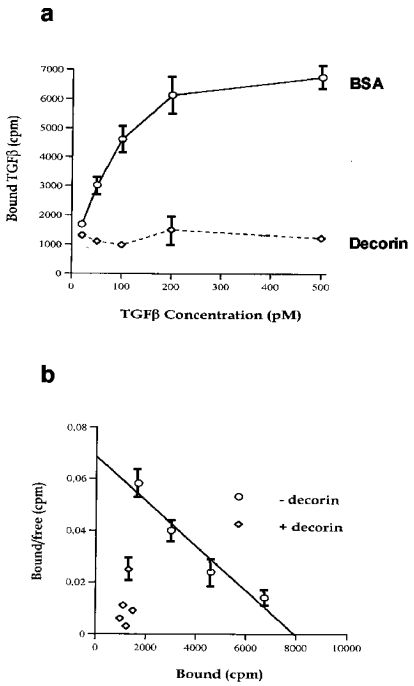

FIGURE 5. Decorin binds TGF-β and inhibits TGF-β binding to its receptor. *a*, Saturating curves of ^{125}I-labeled TGF binding to macrophages cultured on a surface precoated with 10 μg/ml BSA or decorin. Binding experiments were performed as described in *Materials and Methods*. Each point was determined in triplicate and is presented as the mean ± SD. *b*, Scatchard analysis of ^{125}I-labeled TGF-β in the presence of increasing concentrations of unlabeled TGF-β in macrophages cultured on a surface precoated with 10 μg/ml BSA or decorin. Each measurement was made in triplicate and is presented as the mean ± SD. The Scatchard analysis shows one representative of three independent experiments.

proliferated less than those cultured on a BSA-precoated surface (Fig. 3). By contrast, those cultured on a surface to which they attached slightly, such as laminin, showed more proliferation than control cells.

In contrast to decorin, fibronectin did not increase the MHC class II mRNA expression induced by IFN-γ (Fig. 4*a*) or enhance the expression or secretion of inflammatory cytokines in response to subsaturating amounts of IFN-γ (Fig. 4, *b* and *c*). More differences between decorin and fibronectin were observed when we analyzed the effect of fibronectin on LPS activation of macrophages. In particular, fibronectin in response to subsaturating amounts of LPS did not induce an increase in the expression of iNOS and cytokines, but instead reduced some of them (Fig. 4, *d-f*).

The effects of decorin on macrophage activation are due to the sequestration of endogenous TGF-β

Our results indicate that the antiproliferative or adhesion-inducing effects of decorin on macrophages are not sufficient to explain its ability to enhance the activation of these cells. We therefore studied other possible mechanisms. For example, it has been reported

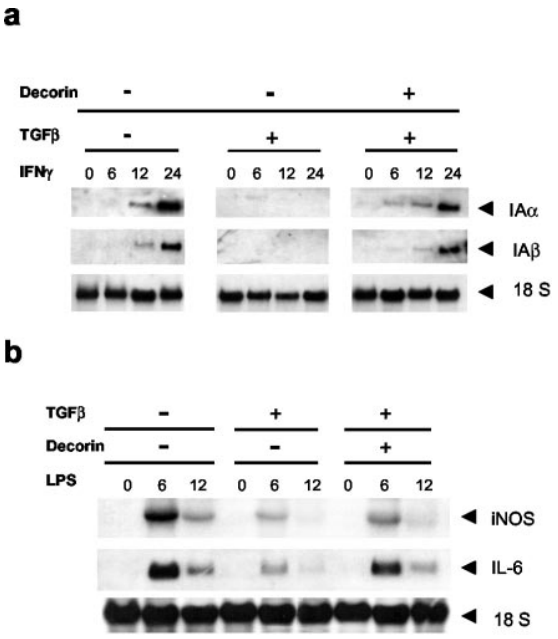

FIGURE 6. Decorin blocks the immunosuppressive effect of TGF-β on macrophage activation. *a*, TGF-β suppresses IFN-γ-induced MHC II expression, and this effect is reversed by decorin. Macrophages were cultured on plates precoated with BSA or decorin. Once attached, cells were stimulated with 1 ng/ml TGF-β for 30 min and then activated with subsaturating amounts of IFN-γ for 6, 12, and 24 h. The expression of IA mRNAs was analyzed by Northern blot. *b*, TGF-β blocks LPS-induced iNOS and IL-6 expression, and this effect is inhibited by decorin. Macrophages were cultured in plates precoated with 10 g/ml BSA or decorin. They were then stimulated with 1 ng/ml TGF-β for 30 min and activated with subsaturating amounts of LPS for the indicated times. The expression of iNOS and IL-6 mRNAs was analyzed by Northern blot. The results in *a* and *b* are representative of at least three independent experiments.

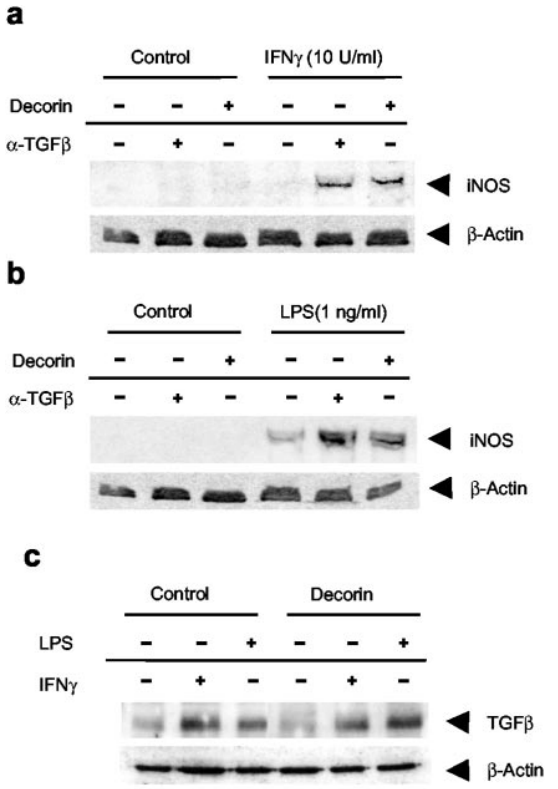

FIGURE 7. The effects of decorin on macrophage activation are due to sequestration of endogenous TGF-β. Cells were cultured in plates precoated with 10 g/ml BSA or decorin. After attachment to the plate, BSA-adhered cells were treated with 1 g/ml anti-TGF-β polyclonal Abs for 30 min or were left untreated. Then BSA- and decorin-precoated plates were stimulated with subsaturating amounts of IFN-γ (*a*) or LPS (*b*) for 6 h or were left unstimulated, and the expression of iNOS was analyzed by Western blot analysis. Each experiment was performed twice. *c*, Expression of TGF-β after treatment with subsaturating amounts of IFN-γ (10 U/ml) or LPS (1 ng/ml) for 6 h was analyzed by Western blotting as indicated in *Materials and Methods*. Results are representative of three independent experiments.

that decorin binds TGF-β (22, 23). However, results do not agree about whether the decorin-TGF-β complex has a positive or negative effect on the interaction of TGF-β with its receptor on the cell surface (22, 23). Due to the repressive effect of TGF-β on both LPS- and IFN-γ-dependent activation (24), we decided to explore the interaction of decorin with TGF-β.

^{125}I-labeled rTGF-β bound to macrophages in a specific and saturable manner at 4°C (Fig. 5). In these experiments 96–98% of the total binding was specific, since it was blocked in the presence of a 100-fold excess of unlabeled TGF-β. Binding was also homogeneous, noncooperative, and of moderately high affinity (Fig. 5*a*). Furthermore, TGF-β binding was dose-dependent and saturable at 250 pM (Fig. 5*a*). Scatchard analysis showed that macrophages bound TGF-β with a K_d of 0.116 $\pm$ 0.03 nM, and the number of receptors on the macrophage surface was 4793 $\pm$ 813 receptors/cell, similar to that reported for other cell types (re-

viewed in Ref. 25) (Fig. 5*b*). However, culture of cells on a plate precoated with 10 μg/ml decorin abolished the binding of TGF-β to macrophages even at the highest ^{125}I-labeled TGF-β level tested (500 pM; Fig. 5). Collectively, these binding experiments showed that TGF-β binds to the macrophage surface and that decorin inhibits binding of the cytokine, preventing it from interacting with its receptor in macrophages.

Next, we explored whether decorin could suppress the inhibitory capability of exogenous TGF-β to block macrophage activation. Treatment of macrophages with 10 ng/ml TGF-β was sufficient to completely block the expression of IFN-γ-induced MHC class II mRNA. However, when macrophages were cultured in the presence of decorin, TGF-β did not block MHC II expression (Fig. 6*a*). Similar results were observed when we analyzed the effects of TGF-β and decorin on the expression of iNOS or IL-6 mRNA induced by LPS (Fig. 6*b*).

Our results show that decorin blocked the binding of TGF-β to the corresponding receptor, thereby reversing its inhibitory effects on macrophage activation. However, these results do not explain the increase in macrophage activation produced by decorin in the absence of exogenous TGF-β. However, an explanation was provided when IFN-γ- or LPS-activated macrophages were treated with blocking Abs against TGF-β. Like decorin, under these conditions anti-TGF-β Abs increased iNOS expression induced by subsaturating amounts of IFN-γ (Fig. 7*a*) or LPS (Fig. 7*b*). Anti-TGF-β and decorin had no effect on iNOS expression in the absence of macrophage activators.

Moreover, Western blot analyses showed that at subsaturating amounts, both IFN-γ and LPS induced the expression of TGF-β in macrophages (Fig. 7*c*). Since decorin did not modify this expression, the blocking effect of this proteoglycan was due to TGF-β sequestration and inhibition of TGF-β binding to its receptor.

Discussion

Under a range of external stimuli, macrophages proliferate, become activated and carry out their function, remain quiescent, or die through apoptosis. Like other immune cells, macrophages are produced in large excess, and only the few cells required to develop a functional activity survive. We found that IFN-γ not only activated macrophages, but also prevented the induction of apoptosis through the expression of the cdk inhibitor p21^{waf-1} and the arrest of cell cycling at the G_1/S boundary (3).

In a previous study we observed that decorin, like IFN-γ, blocks macrophage proliferation and protects against apoptosis through the induction of p21^{waf1} (14). In the present study we found that decorin enhanced both IFN-γ- and LPS-mediated activation. This enhancing effect was originally linked to the capacity of decorin to increase cell adhesion on the basis that fibronectin, another ECM protein that induces cell adhesion, also inhibits macrophage proliferation. However, we observed that decorin increased the activation mediated by both LPS and IFN-γ, whereas fibronectin did not.

Because decorin-induced adhesion did not seem to be a sufficient mechanism to increase macrophage activation, we analyzed the repressive effect of this proteoglycan on TGF-β. This cytokine is produced by macrophages in an autocrine manner, and it down-regulates activation (26). TGF-β antagonizes IFN-γ-driven processes of macrophage activation, such as the production of H_2O_2, NO, the up-regulation of iNOS, the release of TNF-β, or the IFN-γ-induced death of intracellular microorganisms (27–30). TGF- also shows an inhibitory effect on IFN-γ-induced MHC class II genes and is mediated by a conserved proximal promoter element (31). The repressive effect of TGF-β on IFN-γ is based on cross-talk between the molecules involved in signal transduction pathways. The TGF-β/SMAD signaling cascades are inhibited by IFN-γ/STAT pathways and vice versa (32, 33). In addition, TGF-β inhibits LPS-induced activation of macrophages. This cytokine inhibits LPS-induced iNOS expression (34) or reduces the expression of proinflammatory cytokines during septic shock (35).

Our results also show that treatment of macrophages with decorin alone is sufficient to induce the mRNA expression of some cytokines, such as TNF-β and IL-1α, but it is not able to induce their secretion. This indicates that although treatment with decorin alone could modulate gene transcription, it does not regulate the post-transcriptional mechanisms involved in cytokine secretion. Increased expression and secretion of these inflammatory cytokines induced by decorin were only observed in the presence of macrophage activators such as LPS or IFN-γ.

Here we found that macrophages bound TGF-β with an affinity and number of binding sites per cell similar to those observed in other cell types (25). Decorin also blocked the binding of TGF-β to macrophages, which could be due to binding of decorin to TGF-β and inhibition of the interaction with the cell surface receptor. In vitro, decorin binds a variety of adhesive and nonadhesive proteins, including fibronectin, thrombospondin, various types of collagens, C1q, as well as TGF-β (8). Therefore, our results indicate that this proteoglycan inhibits the effects of TGF-β in macrophages. In response to subsaturating amounts of IFN-γ or LPS, decorin may compete with macrophages for the autocrine TGF-β produced. This could explain the beneficial effect of decorin on IFN-γ- or LPS-mediated activation.

Our findings further show that macrophages are subjected to negative regulation through the autocrine production of TGF-β. In fact, studies involving mouse models in which TGF-β was inactivated through disruption of the gene show an excessive inflammatory response (36), an increased expression of MHC II genes (37), and an increased production of NO (38). In addition, the inflammatory process in TGF-β1 knockout mice seems to be closely associated with the development of autoimmunity, as shown by the development of a massive mononuclear cell infiltration in multiple tissues, including lungs, heart, and salivary glands (36–38). All these data indicate that autocrine production of TGF-β plays a key role in the active suppression of inflammation in the absence of adequate proinflammatory stimuli. Therefore, macrophages in the absence of stimuli are in a preactivated state, which is maintained by inhibitory cytokines such as TGF-β.

Our results may have clinical and physiological relevance. Here we present a mechanism that blocks the endogenous inhibitor TGF-β. The presence of decorin in tissues could account for increased macrophage activation. These phagocytic cells play a critical role during inflammation. In the early stages, neutrophils are

present at the inflammatory loci, but leave after 24–48 h. Later, macrophages reach these loci, where they remain until inflammation disappears (39), i.e., for as long as stimulated Th1 cells produce IFN-γ. In the late phases of inflammation, macrophages eliminate nonself structures, remove all debris (including apoptotic bodies), and remodel impaired tissues. However, during chronic inflammation, such as rheumatoid arthritis, macrophages play a key role in the pathogenesis (40). In these situations the persistence of these phagocytic cells may be related to the presence of molecules that block their deactivation. Several soluble mediators, such as TGF-β (28–30), IL-10 (30, 41), adenosine (19), etc., block macrophage activation. Macrophages are restrained from tissue-damaging activation by CD200R (a myeloid-specific receptor on the phagocytes) when it engages on other cells the glycoprotein CD200 (42, 43). Depending on the balance between activators and inhibitors, macrophages remain at the inflammatory loci and release enzymes or cytokines that could be deleterious for the articulation (44). In this context, decorin or other molecules of the ECM may contribute to the pathogenesis of chronic inflammation by blocking inhibitors. In this regard, in an animal model of experimental autoimmune encephalomyelitis, systemic administration of Abs specific for TGF-β identified a role for endogenous TGF-β in suppression of the disease (45).

Acknowledgments

We give special thanks to Dr. E. Ruoslahti (The Burnham Institute, La Jolla, CA) for the gift of the purified decorin used in this study. We also thank Dr. J. Gascon (Hospital Clinic, Barcelona, Spain) and Puleva Biotech (Granada, Spain) for their help with some reagents. We thank Tanya Yates for editorial help.

References

1. Celada, A., and C. F. Nathan. 1994. Macrophage activation revisited. *Immunol. Today 15:100.*
2. Boehm, U., T. Klamp, and M. Groot. 1997. Cellular responses to interferon . *Annu. Rev. Immunol. 15:749.*
3. Xaus, J., M. Cardo, A. F. Valledor, C. Soler, J. Lloberas, and A. Celada. 1999. Interferon induces the expression of $p21^{waf1}$ and arrests macrophage cell cycle, preventing induction of apoptosis. *Immunity 11:103.*
4. Gudmundsson, G., and G. W. Hunninghake. 1997. Interferon- is necessary for the expression of hypersensitivity pneumonitis. *J. Clin. Invest. 99:2386.*
5. Kaufman, S. H. E. 1995. Immunity to intracellular microbial pathogens. *Immunol. Today 16:338.*
6. Uhlin-Hansen, L., D. Langvoll, T. Wik, and S. O. Kolset. 1992. Blood platelets stimulate the expression of chondroitin sulfate proteoglycan in human monocytes. *Blood 80:1058.*
7. Uhlin-Hansen, T., L. Wik, L. Kjellen, E. Berg, F. Forsdahl, and S. O. Kolset. 1993. Proteoglycan metabolism in normal and inflammatory human macrophages. *Blood 82:2880.*
8. Iozzo, R. V. 1997. The family of the small leucine-rich proteoglycans: key regulators of matrix assembly and cellular growth. *Crit. Rev. Biochem. Mol. Biol. 52:141.*
9. Danielson, K. G., H. Baribault, D. F. Holmes, H. Graham, K. E. Kadler, and R. V. Iozzo. 1997. Targeted disruption of decorin leads to abnormal collagen fibril morphology and skin fragility. *J. Cell Biol. 136:729.*
10. Hildebrand, A., M. Romaris, L. M. Rasmussen, D. Heinegard, D. R. Twardzik, W. A. Border, and E. Ruoslahti. 1994. Interaction of the small interstitial proteoglycan biglycan, decorin and fibromodulin with transforming growth factor . *Biochem. J. 302:527.*
11. Yamaguchi, Y., D. M. Mann, and E. Ruoslahti. 1990. Negative regulation of transforming growth factor- by the proteoglycan decorin. *Nature 346:281.*
12. Lewandowska, K., H. U. Choi, L. Rosenberg, L. Zardi, and L. A. Culp. 1987. Fibronectin-mediated adhesion of fibroblasts: inhibition by dermatan sulfate proteoglycan and evidence for a cryptic glycosaminoglycan-binding domain. *J. Cell Biol. 105:1443.*
13. Schmidt, G., H. Robenek, B. Harrach, J. Glossl, V. Nolte, H. Hormann, H. Richter, and H. Kresse. 1987. Interaction of small dermatan sulfate proteoglycan from fibroblasts with fibronectin. *J. Cell Biol. 104:1683.*
14. Xaus, J., M. Comalada, M. Cardó, A. F. Valledor, and A. Celada. 2001. Decorin inhibits M-CSF-proliferation of macrophages and enhances cell survival trough induction of $p27^{kip1}$ and $p21^{waf1}$. *Blood 98:2124.*
15. Xaus, J., M. Comalada, M. Barrachina, C. Herrero, E. Goñalons, C. Soler, J. Lloberas, and A. Celada. 2000. The expression of MHC class II genes in macrophages is cell cycle dependent. *J. Immunol. 165:6364.*
16. Celada, A., F. E. Borras, C. Soler, J. Lloberas, M. Klemsz, C. Van Beveren, S. McKerscher, and R. A. Maki. 1996. The transcription factor PU.1 is involved in macrophage proliferation. *J. Exp. Med. 184:61.*
17. Cuevas, P., M. Garcia Calvo, F. Carceller, D. Reimers, M. Zazo, B. Cuevas, I. Muñoz-Willery, V. Martinez-Coso, S. Lamas, and G. Jiménez-Gallego. 1996. Correction of hypertension by normalization of endothelial levels of fibroblast growth factor and nitric oxide synthase in spontaneously hypertensive rats. *Proc. Natl. Acad. Sci. USA 93:11996.*
18. Torczynski, P., A. P. Bollon, and M. Fuke. 1983. The complete nucleotide sequence of the rat 18S ribosomal RNA gene and comparison with the respective yeast and frog genes. *Nucleic Acids Res. 11:4879.*
19. Xaus, J., M. Mirabet, J. Lloberas, C. Soler, C. Lluis, R. Franco, and A. Celada. 1999. IFN-γ up-regulates the A_{2B} adenosine receptor expression in macrophages: a mechanism of macrophage deactivation. *J. Immunol. 162:3607.*
20. Berton, G., and C. A. Lowell. 1999. Integrin signallin in neutrophils and macrophages. *Cell. Signalling 11:621.*
21. Jun, C. D., H. J. Yoon, H. M. Kim, and H. T. Chung. 1995. Fibronectin activates murine peritoneal macrophages for tumor cell destruction in the presence of IFN-γ. *Biochem. Biophys. Res. Commun. 206:969.*
22. Takeuchi, Y., Y. Kodama, and T. Matsumoto. 1994. Bone matrix decorin binds transforming growth factor-β and enhances its bioactivity. *J. Biol. Chem. 269: 32634.*
23. Yamaguchi, Y., and E. Ruoslahti. 1988. Expression of human proteoglycan in Chinese hamster ovary cells inhibits cell proliferation. *Nature 336:244.*
24. Letterio J. J., and A. B. Roberts. 1998. Regulation of immune responses by TGF-β. *Annu. Rev. Immunol. 16:137.*
25. Massague, J., S. Cheifetz, F. T. Boyd, and J. L. Andres. 1990. TGF receptors and TGFβ binding proteoglycans: recent progress in identifying their functional properties. *Ann. NY Acad. Sci. 593:59.*
26. Assoian, R. K., B. E. Fleurdelys, H. C. Stevenson, P. J. Miller, D. K. Madtes, E. W. Raines, R. Ross, and M. B. Sporn. 1987. Expression and secretion of type-β transforming growth by activated human macrophages. *Proc. Natl. Acad. Sci. USA 84:6020.*
27. Ding, A., C. F. Nathan, J. Graycar, R. Derynck, D. J. Stuehr, and S. Srimal. 1990. Macrophage deactivating factor and transforming growth factors β1, -β2, and -β3 inhibit induction of macrophage nitrogen oxide synthesis by IFN . *J. Immunol. 145:940.*
28. Tsunawaki, S., M. Sporn, A. Ding, and C. Nathan. 1988. Deactivation of macrophages by transforming growth factor- . *Eur. J. Immunol. 334:260.*
29. Vodovotz, Y., C. Bogdan, J. Paik, Q.-W. Xie, and C. F. Nathan. 1993. Mechanism of supression of macrophage nitric oxide release by transforming growth factor-β. *J. Exp. Med. 178:605.*
30. Bogdan, C., J. Paik, Y. Vodovotz, and C. F. Nathan. 1992. Contrasting mechanism for supression of macrophage cytokine release by transforming growth factor- and interleukin 10. *J. Biol. Chem. 267:23301.*
31. Reimold, A. M., C. J. Kara, J. W. Rooney, and L. H. Glimcher. 1993. Transforming growth factor β1 repression of the HLA-DR gene is mediated by conserved proximal promoter elements. *J. Immunol. 151:4173.*
32. Pitts, R. L., S. Wang, E. A. Jones, and A. J. Symes. 2001. Transforming growth factor- and ciliary neurotrophic factor synergistically induce vasoactive intestinal peptide gene expression through the cooperation of Smad, STAT and AP-1 sites. *J. Biol. Cell. 276:19966.*
33. Ulloa, L., J. Doody, and J. Massague. 1999. Inhibition of transforming growth factor- /SMAD signaling by the interferon- /STAT pathway. *Nature 397:710.*
34. Werner, F., M. K. Jain, M. W. Feinberg, N. E. Sibinga, A. Pellacani, P. Wiesel, M. T. Chin, J. N. Topper, M. A. Perrella, and M. E. Lee. 2000. Transforming growth factor (TGF)-β1 inhibition of macrophage activation is mediated via Smad3. *J. Biol. Chem. 275:36653.*
35. Imai, K., A. Takeshita, and S. Hanazawa. 2000. Transforming growth factor- inhibits lipopolysaccharide-stimulated expression of inflammatory cytokines in mouse macrophages through downregulation of activation protein 1 and CD14 receptor expression. *Infect. Immun. 68:2418.*
36. Kulkarni, A. B., C. G. Huh, D. Becker, A. Geiser, M. Lyght, K. C. Flanders, A. B. Roberts, M. B. Sporn, J. M. Ward, and S. Karlsson. 1993. Transforming growth factor 1 null mutation in mice causes excessive inflammatory response and early death. *Proc. Natl. Acad. Sci. USA 90:770.*

37. Geiser, A. G., J. J. Letterio, A. B. Kulkarni, S. Karlsson, A. B. Roberts, and M. B. Sporn. 1993. Transforming growth factor β1 (TGFβ1) controls expression of major histocompatibility genes in the postnatal mouse: aberrant histocompatibility antigen expression in the pathogenesis of the TGF-β1 null mouse phenotype. *Proc. Natl. Acad. Sci. USA 90:9944.*
38. Vodovotz, Y., A. G. Geiser, L. Chesler, J. J. Letterio, A. Campbell, M. S. Lucia, M. B. Sporn, and A. B. Roberts. 1996. Spontaneously increased production of nitric oxide and aberrant expression of the inducible nitric oxide synthase in vivo in the transforming growth factor β1 null mouse. *J. Exp. Med. 183:2337.*
39. Belligan, G. J., H. Caldwell, S. E. Howie, I. Dransfield, and C. Haslett. 1996. In vivo fate of the inflammatory macrophage during the resolution of inflammation: inflammatory macrophages do not die locally, but emigrate to the draining lymph nodes. *J. Immunol. 157:2577.*
40. Janossy, G., G. Panayi, O. Duke, M. Bofill, L. W. Poulter, and G. Goldstein. 1981. Rheumatoid arthritis: a disease of T-lymphocyte/macrophage immunoregulation. *Lancet 2:839.*
41. O'Farrell, A. M., Y. Liu, K. W. Moore, and A. L. Mui. 1998. IL-10 inhibits macrophage activation and proliferation by distinct signaling mechanism: evidence for Stat-3-dependent and-independent pathways. *EMBO J. 17:1006.*
42. Wright, G. J., M. J. Puklavec, A. C. Willis, R. M. Hoek, J. D. Sedgwick, M. H. Brown, and A. N. Barclay. 2000. Lymphoid/neurol cell surface OX2 glycoprotein recognizes a novel receptor on macrophages implicated in the control of their function. *Immunity 13:233.*
43. Hoek, R. M., S. R. Rumls, C. A. Murphy, G. J. Wrigh, R. Goddard, S. M. Zurawski, B. Blom, M. E. Homola, W. J. Streit, M. H. Brown, et al. 2000. Down-regulation of the macrophage lineage through interaction with OX2 (CD200). *Science 290:1768.*
44. Nathan, C. F., and W. A. Muller. 2001. Putting the brakes on innate immunity: a regulatory role for CD 200? *Nat. Immunol. 2:17.*
45. Miller, A., O. Lider, A. B. Roberts, M. B. Sporn, and H. L. Weiner. 1992. Suppressor T cells generated by oral tolerization to myelin basic protein suppress both in vitro and in vivo immune responses by the release of transforming growth factor after antigen-specific triggering. *Proc. Natl. Acad. Sci. USA 89:421.*

4. Muerte celular programada desencadenada por un péptido que mimetiza la anexina V y es dependiente de la integrina αvβ5.

Resumen

Las integrinas son receptores heterodiméricos de la superficie celular que juegan un papel importante en la respuesta de la célula a su entorno. Estas proteínas participan en la adhesión celular (incluyendo adhesión célula-célula y adhesión a la matriz extracelular), proliferación, migración y supervivencia. Los dominios citoplasmáticos de las integrinas son cruciales para mediar la señalización hacia el interior de la célula. Además, una vez que las integrinas son activadas son capaces de transmitir la señalización al exterior celular. El dominio citoplasmático de la integrina β5 ha sido descrito como regulador de la emigración y de la proliferación de las células. Hasta el momento, solamente se conoce una molécula que interacciona con el dominio citoplasmático de la β5 que se denomina TAP20.

Debido a que la adhesión celular mediada por las integrinas afecta a la supervivencia, estabamos interesados en poder determinar el papel específico que jugaba el dominio citoplasmático de la integrina β5 en este proceso. Por ello pensamos que los péptidos que se unieran al dominio citoplasmático de la β5 podrían mimetizar la unión de las proteínas asociadas a αvβ5. Para abordar la búsqueda de estos péptidos utilizamos el metodo del *phage display*, técnica que permite la identificación de motivos peptídicos que reconocen de una manera específica los dominios de interacción de las proteínas.

Con este fin se incubó la forma recombinante del dominio citoplasmático de la β5 con una genoteca de bacteriófagos que tenían péptidos de 9 amino ácidos. Después de tres rondas de selección, el bacteriófago que se recuperó con mayor frecuencia expresaba la secuencia VVISYSMPD. Se confirmó que dicho bacteriófago se unía de forma específica a la propia subunidad β5 y no a otras subunidades como la β1 y β3 con las que comparte más del 40% de homología. Posteriormente, los estudios de inhibición que se realizaron con el péptido sintético confirmaron que VVISYSMPD se une al dominio citoplasmático de la β5 de forma específica y dependiente de la dosis.

Con el propósito de realizar los estudios funcionales se sintetizó una forma internalizable del péptido que nos permitió estudiar su distribución en el interior de la célula y los efectos biológicos. Cuando de incubó el péptido con células endoteliales estimuladas con VEGF se observó que inducía una muerte celular masiva. En los estudios de tinción celular con ioduro de propidio, mostraron que la muerte celular inducida por el péptido presentaba características típicas de apoptosis. Además se observó que los inhibidores de las caspasas prevenían de la muerte inducida por el péptido, confirmando así que el péptido inducía apoptosis en las células endoteliales. Los experimentos con las células aisladas del ratón *knock-out* para la β5 integrina y las células transfectadas con la integrina demostraron que la acción del péptido es dependiente de la expresión de αvβ5 ya que no se observó apoptosis cuando la subunidad β5 no está en cada tipo celular.

La unión del péptido VVISYSMPD al dominio citoplasmático de la β5 sugería la existencia de una proteína citoplasmática que se asociara con esta integrina. Para poder identificarla se siguió un proceso de purificación mediante extractos celulares a través de distintas columnas de afinidad. Además, mediante inmunización de conejos se generaron anticuerpos específicos para el péptido VVISYSMPD. Dichos anticuerpos fueron utilizados para controlar los procesos de purificación de la proteína mediante *western blot*. Una vez que la proteína fue purificada se realizó espectrometría de masas para su identificación, que resulto ser la anexina V. La colocalización del dominio citoplasmático de la β5 y de la anexina V se confirmó mediante doble tinción con inmunofluorescencia. Además, se puedo observar que el péptido bloqueaba la colocalización de las dos proteínas.

Con objetivo de conocer los mecanismos moleculares implicados en la muerte celular inducida por el péptido VVISYSMPD se determinó que los inhibidores de la proteína kinasa C (PKC) podían bloquear la muerte inducida por el péptido.

Esto sugería que la PKC esta involucrada en la cascada de señalización de la anexina y de la subunidad de la β5. La especificidad de unión entre las distintas proteínas implicadas fue demostrada mediante experimentos de interacción proteína-proteína, viéndose que la anexina V se une de manera especifica y dependiente de calcio, a la parte citoplasmática de la β5. Además, la anexina V se une a la PKC una vez activada, ejerciendo esta unión un efecto inhibidor sobre la actividad de la PKC.

Nuestros resultados sugieren que el péptido internalizado mimetiza a la anexina V impidiendo que la proteína natural se pueda unir a la parte citoplasmática de la integrina, alterando así los niveles de anexina V en el citoplasma. Esta señal parece ser suficiente para desencadenar la apoptosis celular. Con el propósito de estudiar los efectos del péptido en los procesos de angiogénesis se realizaron ensayos *in vivo* que demostraron que el péptido VVISYSMPD es capaz de interrumpir la formación de la red celular que hacen las células endoteliales en matrigel. Además el peptido es capaz de inhibir la angiogénesis en los modelos animales.

αvβ5 Integrin-Dependent Programmed Cell Death Triggered by a Peptide Mimic of Annexin V

Summary

The diverse cytoplasmic domain sequences within the various integrin subunits are critical for integrin-mediated signaling into the cell (outside-in signaling) and for activation of ligand binding affinity (inside-out signaling). Here we introduce an approach based on phage display technology to identify molecules that specifically interact with the cytoplasmic domain of the β5 integrin subunit. We show that a peptide selected for binding specifically to the β5 cytoplasmic domain (VVISYSMPD) induces apoptosis upon internalization. The cell death process induced by VVISYSMPD is sensitive to modulation by growth factors and by protein kinase C (PKC), and it cannot be triggered in β5 null cells. Finally, we show that the VVISYSMPD peptide is a mimic of annexin V. Our results suggest a functional link between the αvβ5 integrin, annexin V, and programmed cell death. We propose the term ìendothanatosî to designate this phenomenon.

Introduction

Cell surface receptors of the integrin family are important regulators of cell behavior. Integrins mediate cell adhesion, proliferation, migration, and survival (Hynes, 1992, 1999; Giancotti and Ruoslahti, 1999; Eliceiri and Cheresh, 2001).

The diverse cytoplasmic domain sequences within the various integrin subunits are critical for integrin-mediated signaling into the cell (outside-in signaling) and for activation of ligand binding affinity (inside-out signaling) (Clark and Brugge, 1995; Clark and Hynes, 1997; Howe et al., 1998; Schlaepfer and Hunter, 1998). Often, it is the association of specific molecules with integrin cytoplasmic domains that initiates signal transduction cascades (Schwartz et al., 1995; Shattil and Ginsberg, 1997; Schlaepfer and Hunter, 1998; Liu et al., 2000; Aplin and Juliano, 2001).

The β5 cytoplasmic domain has been reported to control cell migration and proliferation (Pasqualini and Hemler, 1994; Klemke et al. 1994; Clark and Hynes, 1997; Aplin et al., 1998). Certain postadhesion events are regulated through a pathway that requires both αvβ5 and PKC activity (Tang et al., 1999). However, αvβ5-dependent mechanisms for cytoplasmic domain control of cell signaling are not well understood. To date, the theta-associated protein 20 (TAP 20) is the only molecule known to interact exclusively with the β5 cytoplasmic domain (Liu et al., 2000).

Extensive data have been generated based on the use of phage libraries to identify extracellular integrin ligands (Koivunen et al., 1999). The large molecular diversity represented in phage peptide libraries facilitates the identification of motifs that map to protein interaction sites (Kolonin et al., 2001; Giordano et al., 2001). For example, RGD-containing peptides with high affinity for αv integrins have been isolated by phage display and shown to be useful tools for targeting tumor vasculature in vivo (Koivunen et al., 1995; Pasqualini et al., 1997; Zetter, 1997).

We reasoned that peptides that bind to the β5 cytoplasmic domain might mimic signal transduction properties of αvβ5-associated proteins. Here we introduce an approach based on phage display technology to identify molecules that specifically interact with the cytoplasmic domain of the β5 integrin subunit.

We show that a peptide mimicking annexin V binds to the β5 cytoplasmic domain and triggers apoptosis. Annexin V is a cytosolic signaling protein known to inhibit PKC activity (Dubois et al., 1996); we demonstrate that annexin V binds only to the active form of PKC. Induction of programmed cell death by this peptide is modulated by growth factors and by PKC antagonists. Caspase activity and the expression of the β5 integrin subunit are also required. These results establish a connection between annexin V, cell adhesion, and apoptosis.

Results and Discussion

Cell adhesion through integrins affects cell survival. We have uncovered a programmed cell death pathway triggered by internalization of VVISY SMP D, a β5 cytoplasmic domain binding peptide that mimics annexin V and affects PKC-dependent signaling.

Identification of a Specific 5 Cytoplasmic Domain Binding Peptide

We isolated β5 cytoplasmic domain binding peptides by screening a phage library displaying the motif X_4YX_4 (X, any amino acid; Y, tyrosine) on a recombinant fusion protein containing the β5 cytoplasmic domain. Immobilized gluthatione-S-transferase (GST) and BSA were used as negative controls for enrichment during multiple rounds of panning; phage were sequenced from randomly selected clones after three rounds of screening (data not shown). Phage displaying the sequences DEE GYYMMR, FQFSYRYLL, SDWYYPWSW, DWPSYYEL, and VVISYSMPD were recovered with high frequency during the screening. The most commonly displayed peptide sequence (VVISYSMPD) was characterized fur-

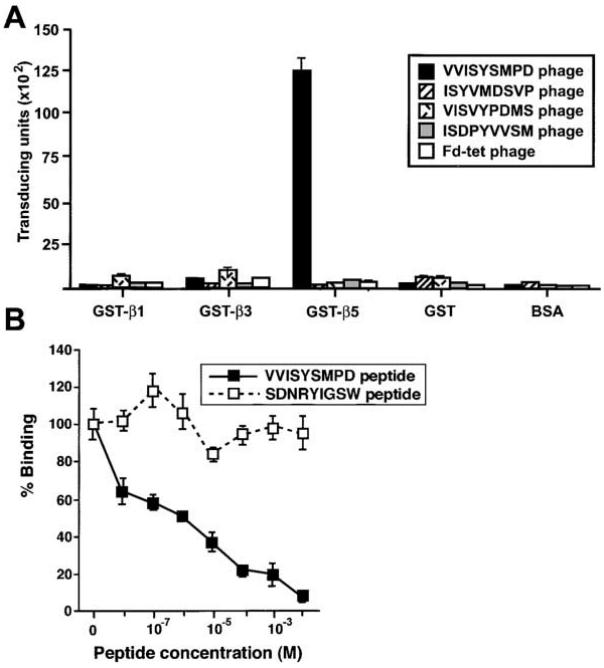

Figure 1. Phage Displaying the VVISYSMPD Peptide Binds Specifically to the β5 Integrin Cytoplasmic Domain

(A) Integrin cytoplasmic domain GST fusion proteins or GST alone were coated on microtiter wells at 10 μg/ml and incubated with β5 cytoplasmic domain binding phage (VVISYSMPD). Phage displaying scrambled versions of the VVISYSMPD peptide (ISYVMDSVP, VIS VYPDMS, and ISDPYVVSM) or fd-tet (insertless) phage were used as negative controls.

(B) Binding of VVISYSMPD phage to the β5 integrin cytoplasmic domain and inhibition with the corresponding synthetic peptide. Phage displaying VVISYSMPD were incubated on wells coated with the GST- β5 integrin cytoplasmic domain in the presence of increasing concentrations of VVISYSMPD peptide or an unrelated negative control peptide sequence (SDNRYIGSW).

ther. We first determined the specificity of the phage peptide interaction with the β5 cytoplasmic domain. Phage displaying the sequence VVISYSMPD, or scrambled versions of the peptide, were tested for binding to GST- β1, -β3, or -β5 cytoplasmic domains. The VVISYSMPD phage interacted only with GST- β5 and not with GST- β1 or GST-β 3 (Figure 1A). In contrast, control insertless phage (Fd-tet), or phage displaying the scrambled versions of the VVISYSMPD peptide, did not bind to any of the immobilized proteins. Next, we showed that the synthetic VVISYSMPD peptide specifically inhibited binding of the corresponding phage in a dose-dependent manner; a control peptide with an unrelated sequence had no effect (Figure 1B). Thus, we show that the VVISYSMPD peptide binds to the cytoplasmic domain of the β5 integrin and that the interaction is specific.

An Internalizing Version of the VVISYSMPD Peptide Triggers Apoptosis

To determine whether the VVISYSMPD peptide interferes with β5 integrin signaling, we designed and synthesized an internalizing version of this peptide by using the penetratin system for intracellular delivery. Penetratin is a peptide containing 16 amino acids that is part of the third helix of the antennapedia protein homeodomain (Derossi et al. 1998). Because penetratin (Pen) has translocating properties, it is capable of carrying hydrophilic compounds across the plasma membrane and delivering them directly to the cytoplasm without degradation (Derossi et al., 1994). We fused VVISYSMPD or a control unrelated peptide to penetratin and added a biotin moiety to visualize internalization. We used human umbilical vein endothelial cells (HUVECs) to test the effect of the internalizing peptide because these cells (1) express the αvβ5 integrin (as determined by FACS analysis with specific antibodies; Pasqualini et al., 1993), and (2) respond to growth factors such as VEGF, which activates β5-dependent signaling (Byzova et al., 2000; Eliceiri and Cheresh, 2001). Pen-VVISYSMPD and a negative control were internalized and remained in the cytoplasm of HUVECs (Figure 2A). Penetratin alone was also internalized and uniformly distributed in the cytoplasm; biotinylated peptides lacking penetratin were not internalized (data not shown).

We next evaluated cell survival and proliferation in cells exposed to Pen-VVISYSMDP. Quiescent HUVECs were stimulated with basal medium containing VEGF. After an overnight incubation, most of the VEGF-stimulated cells treated with Pen-VVISYSMPD died (Figure 2 B2). No cell death was observed when HUVECs were untreated (Figure 2B1), treated with penetratin alone, or treated with an unrelated control peptide fused to penetratin (Figures 2B3 and 2B4). Moreover, incubation of VEGF-stimulated HUVECs with Pen-VVISYSMPD induced a subdiploid peak corresponding to apoptotic cells, whereas starvation or treatment with penetratin alone had little or no effect (Figure 2C).

An early step in the induction of programmed cell death is the inversion of phosphatidylserine in the cell membrane. Such a phenomenon can be detected in a standard apoptosis assay (Fadok et al., 1992). Again, treatment of VEGF-stimulated HUVECs with Pen-VVISYSMPD induced marked cell death, whereas treatment with control peptides did not (Figure 2D). A DNA laddering assay confirmed that DNA fragmentation occurred in cells treated with Pen-VVISYSMPD but not with controls (data not shown).

To evaluate whether caspase activity was required for induction of cell death, we incubated VEGF-stimulated HUVECs with penetratin or Pen-VVISYSMPD in the presence of the caspase inhibitor z-VAD. Treatment with

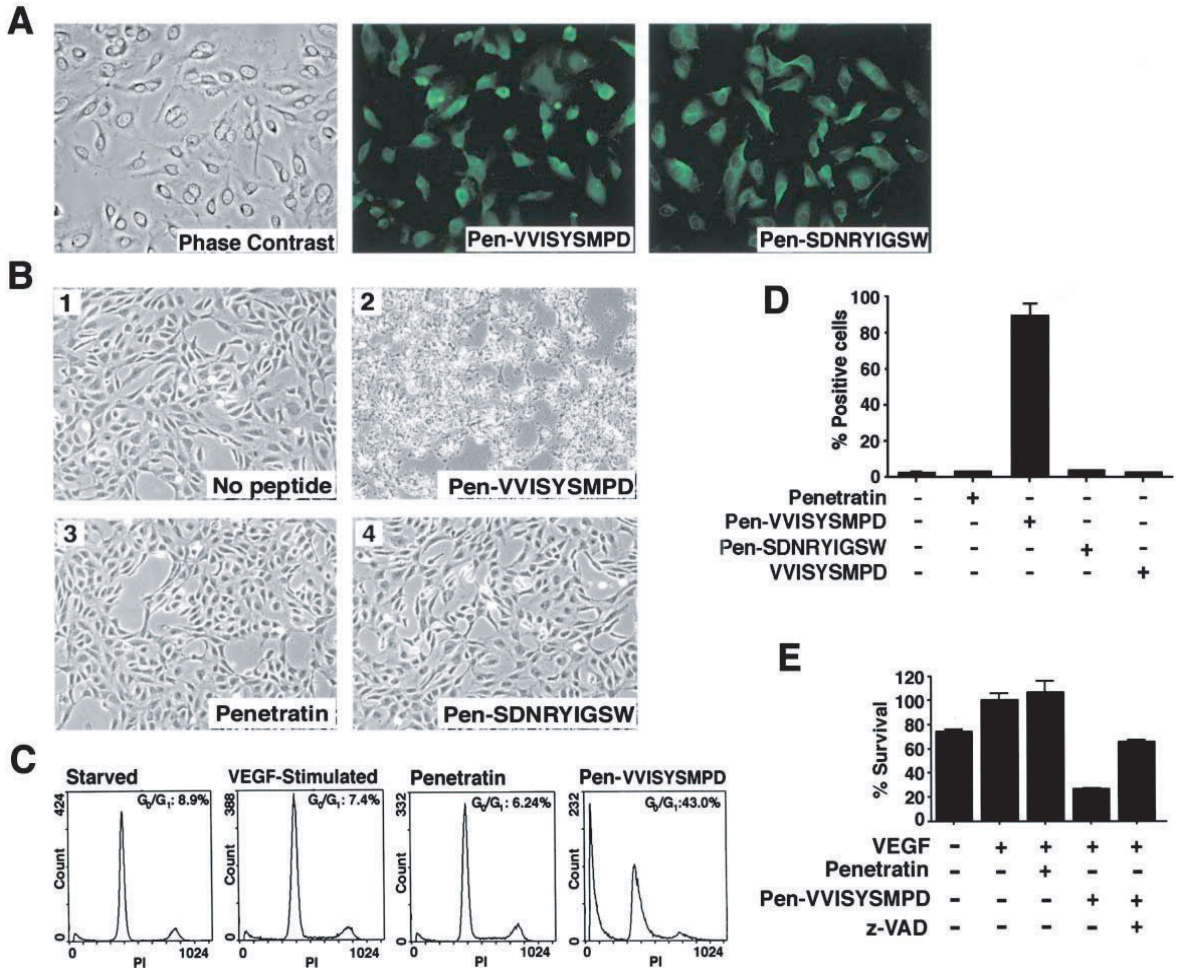

Figure 2. An Internalizing Version of the VVISYSMPD β 5 Cytoplasmic Domain Binding Peptide Triggers Cell Death

(A) Peptide internalization. Phase-contrast image of human umbilical cord endothelial cells (HUVECs) (left panel); cells incubated with the internalizing version of the VVISYSMPD peptide (Pen-VVISYSMPD) (middle panel); cells incubated with a control unrelated internalizing peptide, Pen-SDNRYIGSW (right panel).

(B) Phase-contrast images showing the effect of penetratin-VVISYSMPD (Pen-VVISYSMPD) on endothelial cells. Cells were stimulated with VEGF and were monitored after an overnight incubation without peptide (B1), with Pen-VVISYSMPD (B2), with penetratin alone (B3), or with Pen-SDNRYIGSW (B4), at equimolar concentrations.

(C) Internalization of Pen-VVISYSMPD leads to growth arrest of HUVECs at G_0/G_1 and induces programmed cell death. Cells were stained with propidium iodide (PI), and their DNA was analyzed by FACS.

(D) Apoptosis detection by annexin V staining. Cells were harvested after treatment with internalizing peptides, as indicated, and stained with ApoAlert.

(E) Effect of caspase inhibitors on cell death mediated by the internalizable VVISYSSMPD peptide was evaluated by MTT assay.

z-VAD prevented over 50% of the Pen-VVISYSMPD-induced cell death (Figure 2E). In contrast, the caspase-8 inhibitor z-IETD had no such effect (data not shown). These results show that apoptosis induced by Pen-VVI SYSMPD in HUVECs requires caspase activation, although caspase-8 is not involved in the cell death process.

As shown in Figure 2B, the internalizing form of the VVISYSMDP peptide induces apoptosis without affecting cell adhesion. To reinforce this finding, we performed two types of experiments. First, we preloaded cells (while in suspension) with the internalizing version of the VVISYSMPD peptide, and subsequently plated them on vitronectin, fibronectin, or collagen. Given that HUVECs undergo rapid cell death in the presence of the VVISYSMPD peptide, treated cells attached poorly under all the experimental conditions tested. These results support the hypothesis that VVISYSMPD does not interefere with αvβ5-mediated adhesion to vitronectin, but rather induces cell death, a process resulting in

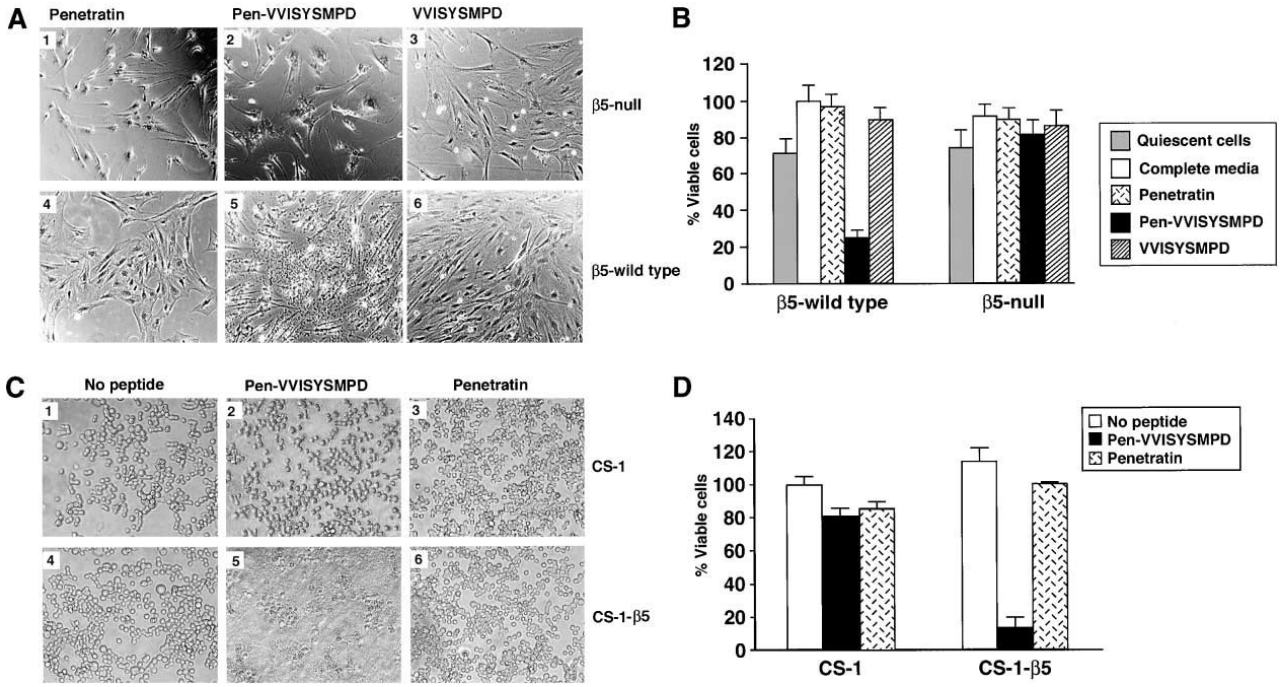

Figure 3. Cell Death Induced by Pen-VVISYSMPD Requires β 5 Expression

(A) Fibroblasts from β5 null mice (A1-A3) or from wild-type (A4-A6) were incubated with 15 μM penetratin (A1 and A4), Pen-VVISYSMPD (A2 and A5), or the VVISYSMPD peptide (A3 and A6). The cells were visualized by phase contrast (100 x magnification).

(B) Quantification of cell viability by using the MTT assay.

(C) CS-1 or CS-1- β5 cells were incubated with RPMI alone (C1 and C4), Pen-VVISYSMPD (C2 and C5), or penetratin at a concentration of 15 μM (C3 and C6) and visualized by phase contrast (100 x magnification).

(D) MTT assays were used to measure cell viability.

impaired adhesion to any substrate (data not shown). We also observed that when cells are plated on collagen or fibronectin, the internalizing version of the VVI SYSMPD peptide is still able to induce cell death. These data demonstrate that (1) αv β5 binding to vitronectin is not required to trigger this process and (2) the interaction between VVISYSMPD and the β5 cytoplasmic domain is not vitronectin dependent.

Programmed cell death is involved in many diseases as well as in wound healing and in tissue remodeling (Reed, 2002). Disruption of integrin-mediated cell-matrix interactions may lead to caspase-dependent apoptosis; two pathways, anoikis (Frisch and Francis, 1994) and integrin-mediated death (IMD) (Stupack et al., 2001), have been described. By definition, anoikis requires loss of cell adhesion (Frisch and Francis, 1994; Frisch and Ruoslahti, 1997; Frisch and Screaton, 2001; Howe et al., 2002; Meredith et al., 1998; Aoudjit and Vuori, 2001). Given that cells treated with the VVISYSMDP peptide undergo apoptosis while still attached, it is unlikely that our observations can be explained by the general phenomenon of anoikis. On the other hand, IMD occurs when 3-mediated interactions are blocked in adherent cells. However, IMD is induced by the cytoplasmic domains of β1 or β3 (but not β5), and it results from recruitment of caspase-8 to the membrane and its subsequent activation (Stupack et al., 2001). In contrast, the VVI SYSMDP peptide binds only to the β5 cytoplasmic domain (but not to 1 or 3). Finally, caspase 8 activity is not required for VVISYSMDP-induced cell death. Taken together, these observations indicate that VVISYSMDP-induced apoptosis is a programmed cell death mechanism that has not previously been described.

β5 Integrin Null Fibroblasts Are Resistant to VVISYSMPD-Induced Apoptosis, Whereas Transfection of CS-1 Cells with 5 Confers Sensitivity to VVISYSMPD

To test whether the β5 integrin subunit is required for apoptosis induction by the VVISYSMPD peptide, we compared the effects of internalizing peptides on fibroblasts isolated from β5 integrin null mice (Huang et al., 2000) and wild-type mice. Penetratin, VVISYSMPD, or Pen-VVISYSMPD was added to the culture media (Figure 3). Marked cell death was observed in wild-type fibroblasts treated with Pen-VVISYSMPD (Figure 3A5),

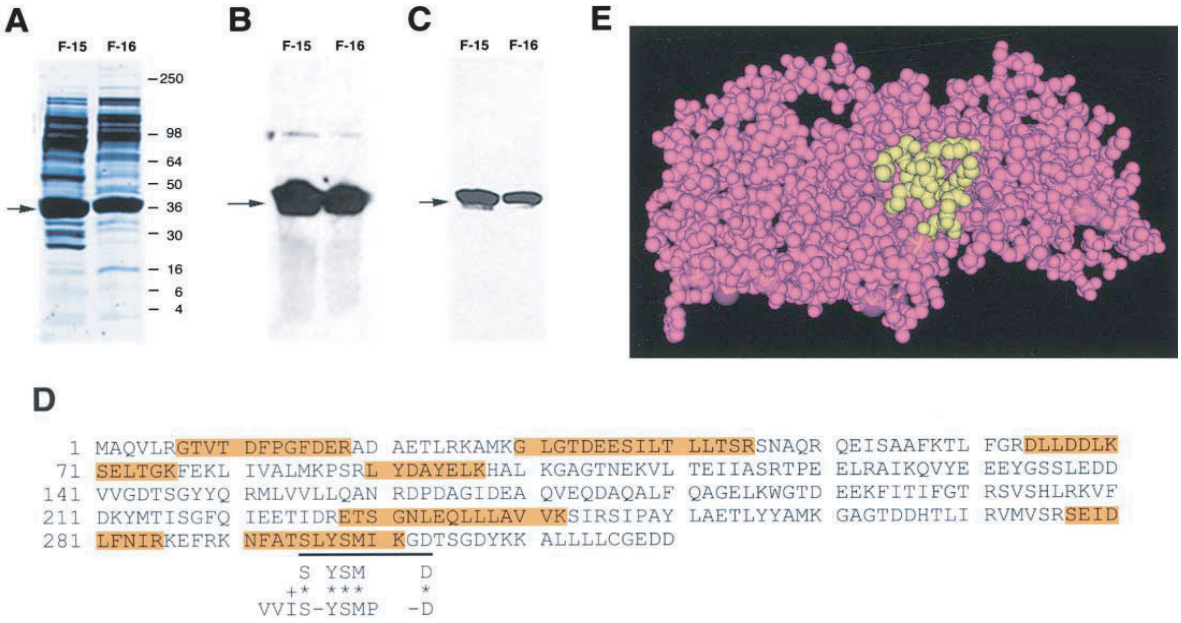

Figure 4. Identification of the Protein Mimicked by the VVISYSMPD Peptide

(A) Coomassie blue staining of proteins obtained from cell extracts after ion exchange chromatography followed by molecular weight fractionation. The arrow indicates the protein excised and processed by MALDI-TOF mass spectroscopy.

(B) Western blot analysis of fractions containing purified proteins using the anti-VVISYSPMD rabbit antiserum (generated by immunizing rabbits with VVISYSMPD-KLH).

(C) The same Western blot (Figure 4B) was stripped and reprobed with a polyclonal anti-human annexin V antibody.

(D) The amino acid sequence of the full-length h-annexin V from the NCBI database (accession number AAB60648). Boxed in orange are the seven peptides obtained by mass spectrometry from the purified protein shown in Figure 4A. The region of similarity with the VVISYSMPD peptide is underlined; identical (*) and conserved (+) amino acids are indicated.

(E) Annexin V structure showing the location of the sequence containing the β5 binding peptide (in yellow).

while fibroblasts lacking the β5 integrin were not affected (Figure 3A2). Treatment with penetratin or the noninternalizing VVISYSMPD peptide did not induce cell death (Figures 3A1, 3A3, 3A4, and 3A6). Cell viability was quantified by the 3-[4,5-dimethylthiazol-2yl]-2,5-diphenyltetrazolium bromide (MTT) assay (Figure 3B).

To reinforce that VVISYSMPD-triggered cell death requires the expression of β5, we used a different cell system in which β5 integrin-negative cells (CS-1) were transfected with β5. We showed that VVISYSMPD-triggered cell death does not occur in the absence of the β5 subunit (Figure 3C2) and does occur in 5-transfected cells (Figure 3C5). Treatment with penetratin alone did not induce cell death (Figures 3C3 and 3C6). Cell viability was quantified by the MTT assay (Figure 3D).

These results show that apoptosis induction by the membrane-permeable form of the VVISYSMPD peptide does not occur in the absence of the β5 integrin subunit.

The VVISYSMPD Peptide Is a Mimic of Annexin V

We reasoned that the VVISYSMPD peptide could mimic a β5 integrin-associated molecule. To test this hypothesis, we generated a polyclonal antibody against the peptide. The anti-VVISYSMPD serum recognized the immobilized VVISYSMPD peptide in a concentration-dependent manner. Reactivity was abrogated by preincubation with the synthetic VVISYSMPD peptide, but not with an unrelated control peptide (data not shown). When tested on Western blots of total cell extracts, the anti-VVISYSMPD polyclonal antibody reacted with a specific 36 kDa protein.

We used the anti-VVISYSMPD antibody to probe protein samples from cell extracts processed by sequential gel filtration and anion exchange column chromatography to identify the target antigen (see Experimental Procedures for details). A 36 kDa protein was enriched after the final purification step (Figure 4A) and was recognized by the anti-VVISYSSMPD antibody on Western blots (Figure 4B). Mass spectrometry analysis revealed seven unique peptides derived from the purified 36 kDa protein that matched the annexin V protein sequence (Cookson et al., 1994) in a BLAST homology search (Figure 4D). To confirm that the purified protein was annexin V, we reprobed the membrane containing the fractions enriched for the 36 kDa protein (Figure 4B) with a commercial antibody against annexin V, which readily detected the same 36 kDa antigen (Figure 4C). These results show that annexin V is the protein recognized by the anti-

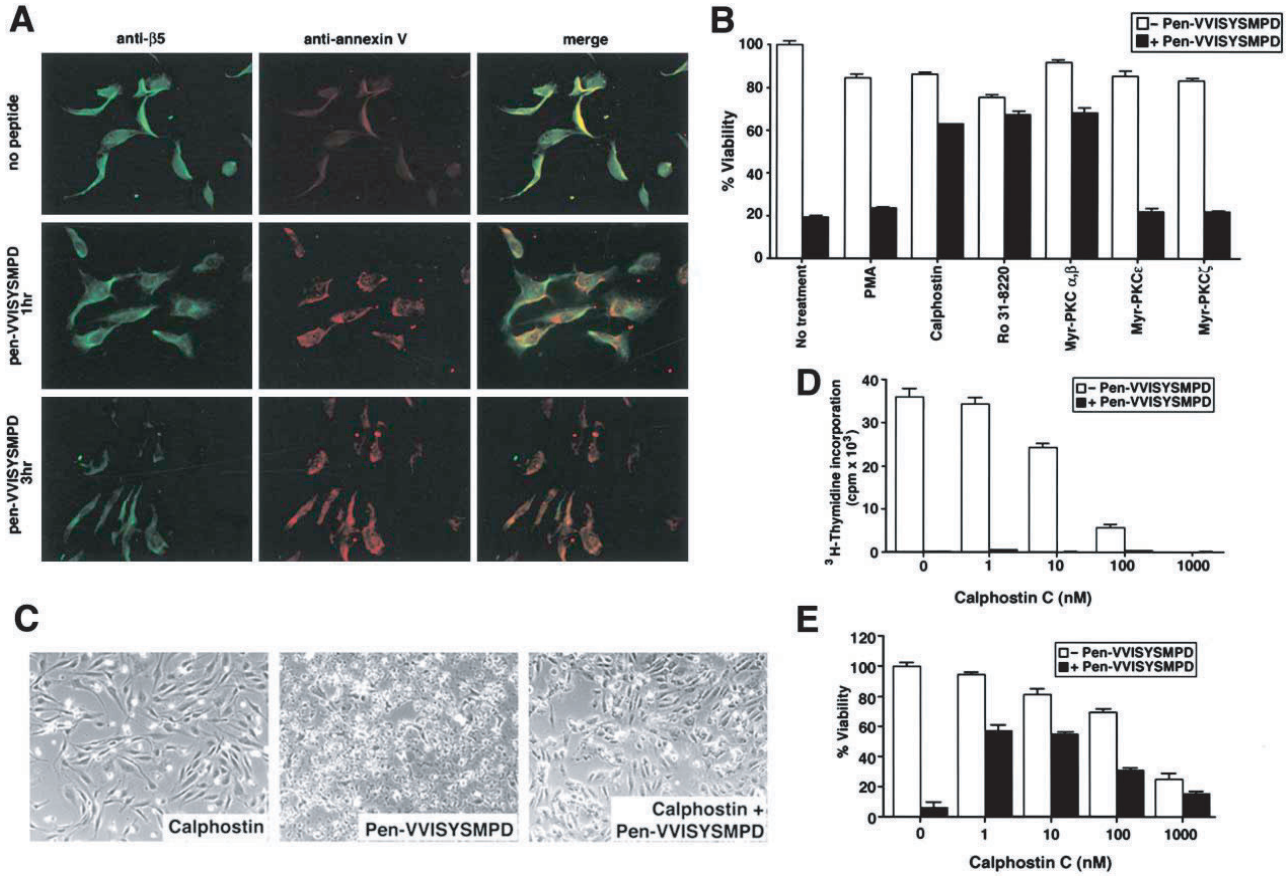

Figure 5. Localization of Annexin V with αvβ5 Integrin and a PKC Inhibitor Modulates the Apoptotic Effects in Pen-VVISYSMPD Untreated and Treated HUVECs

(A) Double immunofluorescence staining of β5 (shown in green) and annexin V (shown in red) in VEGF-stimulated cells (HUVECs). Colocalization of the β5 cytoplasmic domain and annexin V appears in yellow in the merged images (top right panel). β5 and annexin V no longer colocalize after incubation with Pen-VVISYSMPS for 1 hr (middle panels) or 3 hr (lower panels).

(B) VEGF-stimulated HUVECs were incubated with PKC inhibitors (Myr-PKC α/β, calphostin C, Ro 31-8220, Myr-PCKε , Myr-PKCζ) or PMA in the presence or absence of Pen-VVISYSMPD. Cell viability was evaluated by the MTT assay 24 hr later.

(C) The PKC inhibitor calphostin C delays apoptosis induced by Pen-VVISYSMPD in HUVECs.

(D) HUVECs were incubated with increasing concentrations of calphostin C with or without 12 μM Pen-VVISYSMPD. After an overnight incubation, proliferation was assessed by measuring [^{3}H]thymidine incorporation.

(E) Quantification of cell viability after incubation with Pen-VVISYSMPD in the presence of increasing concentrations of calphostin C.

VVISYSMPD polyclonal antibody. Analysis of a three-dimensional model of annexin V based on its structure (Sopkova et al., 1993) shows that the motif containing the β5 binding peptide is exposed on the surface of the molecule (Figure 4E).

Annexin V belongs to a family of proteins defined by their ability to bind calcium and phospholipids via a series of tandem motifs that form the core of the protein (Dubois et al., 1996). All annexins contain a putative PKC binding site, but only annexin V has been shown to function as a PKC inhibitor (Schlaepfer et al., 1992; Dubois et al., 1998). Thus, we sought to determine whether inhibition of PKC would interfere with the induction of apoptosis by the VVISYSMPS peptide.

Localization of Annexin V and the v 5 Integrin in Pen-VVISYSMPD Untreated and Treated HUVECs

Double immunofluorescence staining of β5 (shown in green) and annexin V (shown in red) in VEGF-stimulated cells (HUVECs) was used to evaluate the localization of these two proteins in proliferating and dying cells by immunofluorescence (Figure 5A). β5 (shown in green) and annexin V (shown in red) colocalize (yellow) in VEGF-stimulated cells (Figure 5A, upper panel). However, in cells treated with Pen-VVISYSMPD, annexin V is seen mainly in the cytoplasm (Figure 5A, middle panel). Loss of cytoplasmic membrane integrity (likely due to massive apoptosis induction) is seen 3 hr after treatment with

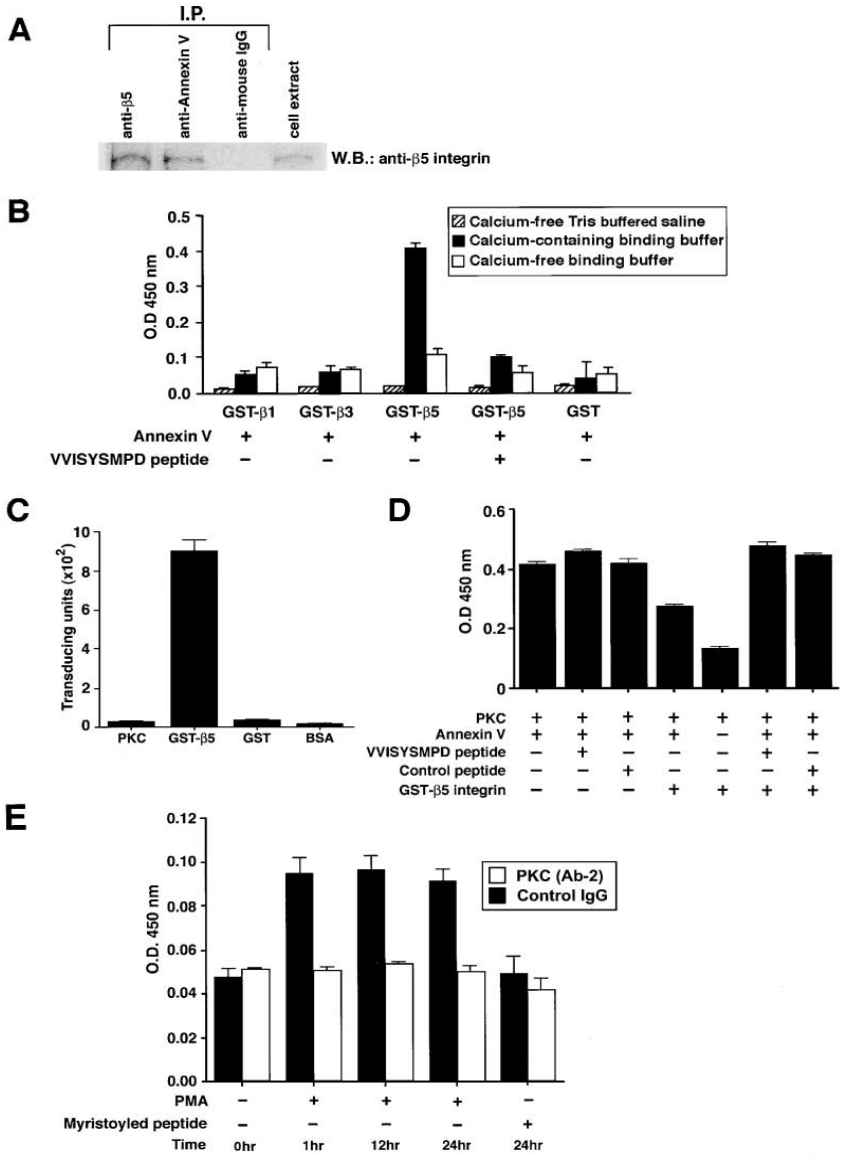

Figure 6. Annexin V Associates with the 5 Integrin Cytoplasmic Domain and Binds to Activated PKC

(A) HUVECs were lysed with RIPA buffer containing Ca^{2}, and immunoprecipitation was performed with an anti-β5 integrin antibody (lane 1), an anti-annexin V antibody (lane 2), or anti-mouse IgG as a negative control (lane 3). β5 integrin was detected by Western blot analysis by a monoclonal antibody. A crude cell extract is shown in lane 4.

(B) Annexin V binds to the β5 cytoplasmic domain. Binding of recombinant human annexin V was determined spectrophotometrically by an anti-human annexin V polyclonal antibody.

(C) The VVISYSMPD peptide does not bind to PKC. Purified PKC was coated on microtiter wells at 250 ng/ml and incubated with phage displaying the VVISYSMPD peptide. GST- β5-coated wells were used as a positive control, and wells coated with GST or BSA were used as negative controls.

(D) The β5 integrin cytoplasmic domain inhibits its binding of annexin V to PKC. Microtiter plate wells coated with PKC were incubated with annexin V with or without the GST- β5 cytoplasmic domain and VVISYSMPD peptide or with an unrelated control peptide. Binding of recombinant human annexin V to PKC was determined as described above.

(E) HUVECs incubated with PMA or with the Myr peptide for the indicated times were used as the source of immunocaptured PKC. Binding of annexin V to PKC was analyzed by incubating each sample well with 1.5 μg/ml recombinant human annexin V. Bound annexin V was detected spectrophotometrically with an anti-human annexin V polyclonal antibody. Control IgG was used as a negative control.

Pen-VVISYSMPD. However, cells remained attached (Figure 5A, lower panels).

Furthermore, in order to define the VVISYSMPD peptide interacting site within the β5 cytoplasmic domain, we engineered phage particles displaying several sequences within the β5 tail. Then, using phage binding assays with both the VVISYSMPD peptide and the native annexin V protein, we mapped the binding site within a short domain containing the sequence FQSERSRARYE MAS. This domain, as expected, is not present in other integrin cytoplasmic domains. In addition, we also demonstrated that the VVISYSMPD peptide had properties similar to the actual sequence present in annexin V by synthesizing the annexin V peptide SLYSMIKGD (Figure 4D) and showing that this peptide binds equally well to the cytoplasmic domain of β5 (data not shown).

PKC Activity Is Required for VVISYSMPD-Induced Cell Death

The role of annexin in signal transduction and the mechanism(s) by which annexin V inhibits PKC activity remain elusive. It has been proposed that the identification of a protein that regulates the relative concentrations of annexin V and PKC near the membrane may control PKC signaling events (Dubois et al., 1996). However, such a protein has not yet been identified. On the other hand, PKC signaling regulates β5 function and controls

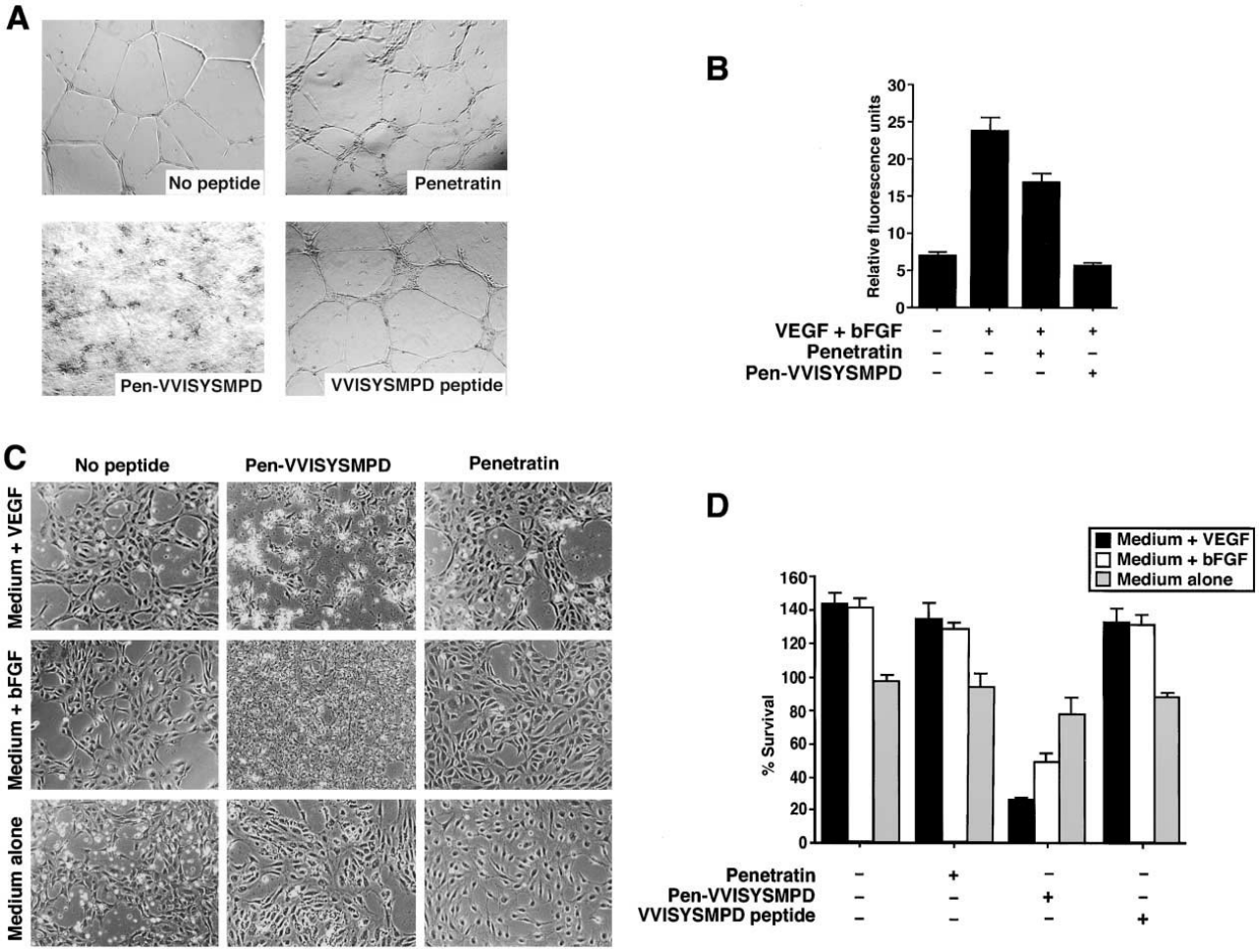

Figure 7. Pen-VVISYSMPD-Induced Cell Death Results in Angiogenesis Inhibition In Vitro and In Vivo

(A) HUVECs were plated in Matrigel-coated plates and photographed 24 hr after incubation with penetratin, Pen-VVISYSMPD, or the VISYSMPD peptide alone (magnification 4 x).

(B) Matrigel supplemented with growth factors was injected into mice in the presence or absence of penetratin or Pen-VVISYSMPD. Neovascularization within the Matrigel plugs was determined by measurement of the levels of injected FITC-labeled lectin recovered by using a fluorimeter (485 nm).

(C) Phase-contrast images showing the effect of Pen-VVISYSMPD on growth factor-stimulated HUVECs. Cells were monitored after an overnight incubation with either culture medium without growth factors, or after stimulation with VEGF or bFGF. Monolayers were treated with Pen-VVISYSMPD or penetratin alone, at equimolar concentrations.

(D) Proangiogenic factors (VEGF and bFGF) enhance Pen-VVISYSMPD-induced cell death. Endothelial cell viability was evaluated by the MTT assay.

cell survival in endothelial cells (Tang et al., 1999; Lewis et al., 1996). Serine/threonine kinases are activated upon integrin stimulation, and inhibitors of PKC block cell attachment and spreading in vitro (Vuori and Ruoslahti, 1993; Nakamura and Nishizuka, 1994; Chen et al., 1994). The C-terminal domain of annexin V associates with and inhibits PKC in the presence of Ca^{2} (Schlaepfer et al., 1992; Raynal et al., 1993; Rothhut et al., 1995; Dubois et al., 1995). These observations led us to hypothesize that PKC regulates β5-dependent apoptosis induced by Pen-VVISYSMPD. To verify this hypothesis, we tested the effects of Pen-VVISYSMPD in the presence of different agents that interfere with PKC activity, namely, PMA, Myr-PKC α/β, calphostin C, Ro31-8220, PCKε , and Myr PKCζ . We demonstrated that the PKC inhibitors Myr-PKC α/β, calphostin C, and Ro31-8220 inhibit VVISYSMPD-induced cell death (Figure 5B). These results also show that conventional PKCs play a key role in VVISYSMPD-mediated cell death.

Because calphostin C is a well-established PKC inhibitor used extensively in the literature, we have expanded our studies by the use of this reagent (Figures

6C and 6D).

High concentrations of calphostin C induced cell death (Zhu et al., 1998). However, at low concentrations (1ñ10 nM), we show that calphostin C inhibits PKC activity without significant induction of cell death (Figure 5D). Apoptosis induced by the VVISYSMPD peptide was markedly reduced in the presence of low concentrations of calphostin C (Figure 5D). A [^{3}H]thymidine incorporation assay revealed that cell proliferation was completely blocked by Pen-VVISYSMPD (Figure 5D). However, when apoptosis induction was evaluated, there were more viable cells in the wells exposed to both Pen-VVISYSMPD and calphostin C than in monolayers treated with only Pen-VVISYSMPD (Figure 5E).

These data show that VVISYSMPD-induced apoptosis is blocked by inhibition of PKC, and they indicated that PKC activity regulates the proapoptotic effects of the VVISYSMPD peptide.

Annexin V Associates with the β5 Integrin Cytoplasmic Domain

The experimental evidence described above indicated that annexin V interacts with the β5 cytoplasmic domain. To show that annexin V associates with β5 integrin in vivo, we performed reciprocal coimmunoprecipitation with antibodies against the β5 integrin or annexin V and probed the immunoprecipitates on Western blots with a well-characterized anti-β5 antibody. A specific band corresponding to the β5 integrin subunit was detected (Figure 6A). These data demonstrate that annexin V associates with β5 integrin in cells.

To show that the interaction between annexin V and the β5 integrin cytoplasmic domain is specific, we used protein binding assays (Figure 6B). Recombinant annexin V was incubated with GST-β5, or with β1 or β3 GST fusion proteins as negative controls. Because Ca^{2} is required for the association between annexin V, PKC, and phospholipids (Mira et al., 1997), we tested whether Ca^{2} would also enhance the interaction between annexin V and β5. Three different buffers were used in the binding experiments: Tris-buffered saline, and a buffer that mimics cytoplasmic conditions (termed binding buffer) with or without Ca^{2} (Figure 6B). Bound annexin V was detected with a specific antibody against annexin V. A highly specific interaction between annexin V and the GST-β5 cytoplasmic domain was observed (Figure 6B). Ca^{2} was required for the interaction, since annexin V binding was not detected when Ca^{2}-free buffers were used. The interaction between the β5 cytoplasmic domain and annexin V was specifically inhibited by the VVISYSMPD peptide (Figure 6B), but not by a control peptide (data not shown). Thus, the VVISYSMPD peptide mimics the binding site through which annexin V associates with the cytoplasmic domain of the β5 integrin subunit.

To rule out the possibility that the VVISYSMPD peptide might induce apoptosis by its direct inhibition of PKC, we tested whether the peptide binds to the enzyme. If the peptide interacted with PKC, it might also affect the interaction between annexin V and PKC. Phage binding assays eliminated both possibilities, as no binding of VVISYSMPD-displaying phage to PKC was detected; the β5-GST protein was used as a positive control (Figure 6C).

Annexin V has been shown to bind to PKC (Schlaepfer et al., 1992), and we examined whether the VVISYSMPD peptide could interfere with this interaction. Protein binding assays showed that the VVISYSMPD peptide does not affect the binding of annexin V to PKC (Figure 6D). In contrast, the GST-β5 integrin cytoplasmic domain blocked the binding of annexin V to PKC by about 40%. Importantly, the interaction between annexin V and PKC was rescued when VVISYSMPD peptide and GST-β5 were incubated jointly. Taken together, these results show that binding of annexin V to the cytoplasmic domain of β5 integrin is blocked by VVISYSMPD peptide.

Interestingly, PMA does not prevent VVISYSMPD-induced cell death, because it facilitates PKC binding to annexin V (Figure 6E). Consistent with this result, a specific inhibitor of conventional PKCs blocks binding of annexin V to PKC (Figure 6E) and inhibits VVISYSMPD-induced cell death (Figure 5). These results support a key role for PKC activity and subsequent inhibition by annexin V in the VVISYSMPD-induced cell death process.

Having established that cell death induced by VVI SYSMPD is modulated by PKC, we observed that PKC activity is required for annexin V binding; yet, it is through annexin V-dependent PKC inhibition that cell death is induced by the β5-cytoplasmic domain binding peptide. Moreover, based on experiments performed with specific PKC inhibitors, conventional PKCs mediate VVI-SYSMPD-induced cell death.

Angiogenic Growth Factors Enhance VVISYSMPD-Induced Programmed Cell Death In Vitro and In Vivo

To determine whether angiogenic factors modulate apoptosis induced by Pen-VVISYSMPD, we evaluated cell death after stimulation with factors that activate endothelial cells. HUVECs treated with Pen-VVISYSMPD in the presence of VEGF or basic fibroblast growth factor (bFGF) underwent rapid apoptosis in comparison to the controls (Figure 7C). Penetratin or the VVISYSMPD peptide alone were used as negative controls and had no effect under identical conditions. Therefore, cell death induced by Pen-VVISYSMPD is markedly enhanced by angiogenic growth factors. These observations led us to hypothesize that Pen-VVISYSMPD might function as an inhibitor of angiogenesis.

In response to specific stimuli, endothelial cells plated on Matrigel develop into networks of capillary-like structures. Using VEGF-stimulated HUVECs plated in Matrigel as a model of neovascularization, we showed that incubation with Pen-VVISYSMPD completely inhibits the formation of a vascular network, whereas penetratin or the VVISYSMPD peptide alone did not have any apparent effect (Figure 7A). To expand our findings, we also assessed the ability of the β5 integrin cytoplasmic domain binding motif to inhibit neovascularization in vivo. Subcutaneous implantation of Matrigel plugs containing a combination of bFGF plus VEGF in nude mice induces vessel growth within 5 days. When tested in this model, Pen-VVISYSMPD completely inhibited angiogenesis induced by both growth factors, while penetratin alone had no effect (Figure 7B). These results clearly show that the β5 cytoplasmic domain binding peptide inhibits neovascularization. Consistent with these observations, we found that the angiogenic factors (VEGF and bFGF) enhance Pen-VVISYSMPD-induced cell death (Figure 7C). VEGF is highly effective in accelerating VVI SYSMPD-mediated cell death (Figure 7C, upper panel). Although bFGF is also effective, it is less potent than VEGF under the experimental conditions tested (Figure 7C, middle panel). Finally, Pen-VVISYSMPD has little effect on nonproliferating endothelial cells cultured in medium without growth factors (Figure 7C, lower panel). Endothelial cell viability in this experiment was also evaluated by the MTT assay (Figure 7D).

Conclusions

We demonstrate that there is a connection between the regulation of PKC activity by annexin V and the induction of cell death in a β5-dependent manner. Also in agreement with our findings is the recent serendipitous copurification of annexin V with the integrin β5 subunit (Andersen et al., 2002).

Our data reveal a structural basis for the regulation of PKC-mediated cell survival and provide insights into the mechanism of action of annexin V. We show that a short synthetic peptide mimic of annexin V induces cell death and that the mechanisms underlying this phenomenon were completely different from those of anoikis or of IMD. We propose the term "endothanatos" (death from inside) to designate this β5-dependent cell death pathway.

Experimental Procedures

Reagents

GST fusion proteins expressing β1, β3, or β5 integrin cytoplasmic domains cloned into the vector pGEX were purified according to the manufacturerís instructions (Amersham Pharmacia Biotech). Anti-β5 integrin antibodies (IA9 and IVA4) were a kind gift from Dr. Martin Hemler), the anti-GST antibody was from Amersham Pharmacia Biotech, horseradish peroxidase (HRP)-conjugated anti-rabbit and anti-goat secondary antibodies were purchased from Sigma-Aldrich. The anti-human annexin V antibody was produced by Hyphen BioMed and is distributed by diaPharma. Recombinant human VEGF was purchased from BD Pharmingen. Annexin V was purchased from Santa Cruz Biotechnology. Synthetic peptides, the keyhole limpet hemocyanin (KLH) conjugates, and penetratin chimeras were purchased from Anaspec.

Cell Culture

Single-donor HUVECs were purchased from Clonetics and were cultured in complete endothelial media (EGM BulletKit, Clonetics) according to the manufacturerís instructions. Cells were used at passage 3 to 5. Starved HUVECs were grown in EBM-2 (endothelial basal media, serum-free, Clonetics). MDA-MB-435 cells were obtained from American Type Culture Collection (ATCC). Primary fibroblast cultures were established from mouse brain and grown in Dulbeccoís modified Eagleís media (DMEM) from GIBCO containing 10% fetal calf serum (FCS). For assays using β5 null cells, confluent fibroblasts were plated in 12 wells (5×10^4 cells per well) in complete media and were allowed to attach (fibroblasts used in our experiments were not stimulated with specific growth factors). The medium was replaced by starvation medium; 24 hr later, peptides were added in complete media, and cells were incubated for 12 hr at 37 C. CS-1 (Farishian and Whittaker, 1979; Thomas et al., 1993) and CS-1 cells stably transfected with a 5wt integrin subunit domain were described previously (Filardo et al., 1996). Cells were cultured in RPMI, 1% HEPES, 10% FCS, 2 mM L-glutamine, and 100 u/ml Penicillin/Streptomycin SO_4.

Phage Display Screenings and Phage Binding Assays

A phage display random peptide library displaying the insert X_4YX_4 (where X is any amino acid and Y is a tyrosine residue) was used in the screenings; phage input was 3×10^{10} transducing units (TU). GST fusion proteins were coated on microtiter wells as previous described (Smith and Scott, 1993; Koivunen et al., 1993). Phage binding assays on purified proteins were carried out as described (Giordano et al., 2001). GST- β1, GST- β3, GST- β5, and GST (at 1 μg in 50 μl phosphate buffered saline [PBS]) were immobilized on microtiter wells overnight at 4 C. Wells were washed twice with PBS, blocked with PBS/3% BSA for 2 hr at room temperature, and incubated with 10^9 TU of VVISYSMPD phage, scrambled versions of the VVISYSMPD peptide (ISYVMDSVP, VISVYPDMS, and ISD PYVVSM), or fd-tet phage in 50 μl PBS/1.5% BSA. After 1 hr at room temperature, wells were washed ten times with PBS, and phage were recovered by bacterial infection. VVISYSMPD or SDNRYIGSW were used as synthetic peptides to evaluate competitive inhibition of phage binding. ELISA with polyclonal anti-GST (Amersham) confirmed the presence and concentration of the GST-fusion proteins on the wells. To test binding of the VVISYSMPD phage to PKC, microtiter-wells were coated at 4 C overnight with 250 ng/ml of purified PKC (Promega), GST- β5 fusion protein (positive control), or GST or BSA (negative controls). VVISYSMPD phage (10^{10} TU) was added to each well, and the binding assay was performed as described above.

Peptide Internalization and Visualization

Uptake of biotinylated peptides into cells was monitored as described previously (Derossi et al., 1994; Theodore et al., 1995). HUVEC cultures were washed, and the media were replaced with complete media containing 10 μg/ml biotinylated peptide. After 2 hr, the cultures were washed with PBS, fixed, permeabilized with ethanol:acetic acid (9:1, v:v) for 5 min at 20 C, blocked for 30 min with 10% FCS in PBS, incubated for 1 hr with FITC-conjugated streptavidin, and washed with PBS prior to visualization with an inverted fluorescence microscope.

Double Immunofluorescence

HUVECs were fixed in methanol for 10 min and were incubated with a monoclonal anti-β5 antibody (IVA4) (diluted 1/300) and a polyclonal anti-annexin V antibody (diluted 1/200). The secondary antibodies were Cy3-anti-rabbit and FITC-anti-mouse IgG (Jackson Immuno-Research Laboratories). Cells were examined by fluorescence microscopy (Olympus).

Proliferation and Cell Viability Assays

Cell proliferation was measured as described previously (Pasqualini and Hemler, 1994). Briefly, 4 x 10^4 HUVECs growing in 24-well plates were starved for 24 hr in unsupplemented EGM-2 media. Twenty-four hours later, the media were supplemented with VEGF (final concentration of 20 nM) and with each peptide (final concentration of 15 μM). After incubation for 18 hr, 50 μl of media containing [^{3}H]thymidine (1 μCi/ml; Amersham) was added to each well. Six hours later, the media were removed, and the cells were fixed in 10% trichloroacetic acid (TCA) for 30 min at 4 C, washed with ethanol, and solubilized in 0.5 N NaOH. Incorporation of radioactivity was determined by liquid scintillation counting with an LS 6000SC Beckman scintillation counter. Cell viability was assessed by measurement of cellular metabolism of MTT (Sigma) at 37 C. Cells growing in 24-well plates were treated with penetratin chimeras for 12 hr, washed twice with PBS, incubated in complete media containing MTT (500 μg/ml per well) for 2-4 hr, and solubilized with 0.1 N HCl in isopropanol (Mosmann, 1983). Samples were subsequently read at 570 nm in a plate reader (Bio-Tek Instruments). CS-1 and CS-1-β5 cells were grown in 48-well plates and were treated with penetratin or Pen-VVISYSMPD for 12 hr.

Cell viability was performed as described above.

Apoptosis Assays

Induction of apoptosis was determined by two methods. First, DNA content was analyzed by propidium iodide (PI) staining. Approximately 1 x 10^6 cells were harvested in complete media after incubation in EBM-2 plus VEGF (25 ng/ml) and 15 μM penetratin or Pen-VVISYSMPD peptide for 4, 8, or 12 hr. The cells were washed in PBS, resuspended in 0.5 ml of PI solution (50 μg/ml PI, 0.1% Triton X-100, and 0.1% sodium citrate), incubated for 24 hr at 4 C, and counted with an XL Coulter System (Coulter Corporation) with a 488 nm laser. Twelve thousand cells were counted for each histogram, and cell cycle distributions were analyzed with the Multicycle program.

Annexin V staining was performed to monitor early stages of apoptosis as described in the ApoAlert Annexin V Technical Bulletin (Clontech). Briefly, HUVECs growing in 35 x 10 mm plates were incubated with the indicated peptides for various times, harvested, washed, and resuspended in binding buffer supplemented with anti-annexin V antibody. Samples were incubated for 10-15 min at room temperature and were analyzed by FACS. To inhibit caspase activity, 80 μM z-VAD or z-IETD (Calbiochem) was added to the cells with each peptide. In assays performed with PKC inhibitors, HUVECs were starved in EBM-2 media for 24 hr, the media were supplemented with 20 nM VEGF, 12 μM peptides as indicated in the figure legends, and calphostin C (1 μm, 100 nM, 10 nM, and 1 nM; Sigma), and the cells were incubated for an additional 14 hr.

Protein-Protein Interaction Assays

GST fusion proteins containing the β1, β3, or β5 cytoplasmic domains or GST alone were coated onto 96-well plates at 5 μg/well to test the binding of annexin V to the integrin cytoplasmic domain. Purified annexin V was added at 2 μg/ml in three different buffers: Tris-buffered saline, a binding buffer (100 mM KCl, 3 mM NaCl, 3.5 mM MgCl, 10 mM PIPES [pH 8]), and a binding buffer containing 2 mM $CaCl_2$. After 3 hr, binding of annexin V to the GST fusion proteins was detected with an anti-annexin V antibody (diluted 1/100) followed by HRP-conjugated anti-goat IgG. To confirm that equal amounts of the GST fusion proteins were bound to the plates, parallel experiments were performed by ELISA using a 1:1500 dilution of an anti-GST antibody (data not shown; Amersham Pharmacia Biotech). To evaluate the interaction of PKC and annexin V, purified PKC (Promega) was coated at 250 ng/ml onto a microtiter-well plate and incubated with annexin V alone (2 μg/ml) or in combination with GST-β5 integrin cytoplasmic domain (1 g/ml) and VVISYSMPD peptide (12 μM). For the immunocapture assays, PKC was immobilized from HUVEC extracts as described (Park et al., 1999). Specifically, 96-well plates were coated overnight at 4 C with 1 μg/ml anti-PKC (Ab-2; Oncogene). Wells were subsequently rinsed with wash buffer (PBS, 0.1% Tween), followed by blocking buffer (3% BSA in PBS) for 1 hr at room temperature. Blocking buffer was removed, and sonicated HUVEC cell extracts were added and incubated for 2 hr at room temperature. Wells were washed three times with wash buffer, and 2 μg/ml of recombinant annexin V was added to the wells, which were incubated overnight at 4 C. Unbound protein was removed by three applications of wash buffer. Binding of annexin V to PKC was detected with an anti-annexin V antibody (diluted 1/100) followed by an HRP-conjugated anti-goat IgG.

Western Blot Analysis and Immunoprecipitation

For Western blotting, total cell extracts were prepared from MDA-MB-435 breast carcinoma cells and HUVECs by solubilization in SDS sample buffer. Lysates were resolved on 4%-20% gradient SDS-polyacrylamide (SDS-PAGE) gels, and proteins were transferred to nitrocellulose membranes. The membranes were blocked and incubated with primary antibodies diluted in blocking buffer (anti-VVISYSMPD antibody diluted 1:3000; anti-annexin V antibody diluted 1:200). The membranes were washed and were incubated with secondary antibodies, a horseradish peroxidase-linked conjugate of anti-rabbit or anti-goat IgG. Reactive bands were visualized using Enhanced Chemiluminescence (ECL) (Pierce). For immunoprecipitation, cells were lysed in cytoplasmic buffer containing 1% NP-40, 2 mM $CaCl_2$, and a protease inhibitor cocktail (Sigma). After a preclearing with protein A-Sepharose (Amersham Pharmacia Biotech), 1 μg/ml annexin V or β5 integrin antibodies was added to the lysates. Two hours later, antibody complexes were isolated with 30 μl of protein A-Sepharose and washed three times with lysis buffer before addition of loading buffer. Proteins were resolved on 4%-20% gradient SDS-PAGE gels, and annexin V was detected by Western blot as described above.

Protein Biochemistry and High-Pressure Liquid Chromatography

We used standard protocols for antigen purification by affinity chromatography (Dean et al., 1985; Gilbert, 1987). MDA-MB-435 cells were lysed in water, sonicated for 1 min, clarified by centrifugation (100,000 x g for 1 hr), and treated with a protease inhibitor cocktail (Sigma). The supernate were loaded onto a 200 ml gel filtration Superdex 75 column (Pharmacia LKB Biotech) preequilibrated with 50 mM Tris (pH 7.5), 50 mM NaCl. One-milliliter fractions were collected and analyzed by Western blotting with purified IgG from serum raised against the VVISYSMPD peptide (and it was repeated for every purification stage). Fractions recognized by the anti-VVISYSMPD antibody from the gel filtration step were subjected to Mono-Q (HR 5/5) anion exchange high-pressure liquid chromatography (Pharmacia). The column was loaded with buffer A (10 mM Tris-HCl [pH 7.5]) and was eluted with a linear 0-0.5 M NaCl gradient, and 1 ml fractions were collected. Proteins in fractions positive for the anti-VVISYSMPD peptide were concentrated, separated on 4%-20% gradient SDS-PAGE gels (BioRad), and stained with colloidal Coomassie blue. The reactive bands were excised from the gel and digested with trypsin, essentially as described previously

(Shevchenko et al., 1996). The resulting tryptic peptide mixtures were analyzed by microcolumn liquid chromatography-tandem mass spectrometry. The protein was determined to be human annexin V by peptide mass fingerprinting and a BLAST search of the GenPept database (ftp://ftp.ncbi.nlm.nih.gov/genbank/genpept.fsa.gz).

In Vitro and In Vivo Neovascularization Assays

Matrigel (150 µl per well; BD Pharmingen) was added to 24-well tissue culture plates and was allowed to solidify at 37 C for 10 min (Montesano et al., 1983). HUVECs were starved in basal EBM-2 media for 18-24 hr. Ten thousand cells were added to triplicate wells and allowed to settle onto Matrigel for 30 min at 37 C. The media were replaced by fresh complete EBM-2 media with or without peptide chimeras (12 µM). The plates were photographed with an inverted microscope (Olympus) 24 hr later. In vivo neovascularization assays were carried out by injection of ice-cold Matrigel (250 l) containing VEGF (75 ng/ml) and bFGF (200 ng/ml) plus 12 µM penetratin or Pen-VVISYSMPD subcutaneously into the flanks of athymic nude mice (Prewett et al., 1999). Five days later, each mouse was injected intravenously with 20 µg FITC-lectin (Vector Laboratories). The plugs were harvested after 30 min and were homogenized in 500 µl of RIPA buffer (1 PBS, 1% nonidet-40, 0.5% sodium deoxycholate, and 0.1% sodium dodecyl sulfate). Neovascularization was quantified fluorimetrically by measurement of the uptake of FITC-lectin into plugs (HTS 7000 plus, Bioassay reader, Perkin Elmer). Mice injected with FITC-lectin alone were used as controls to determine the fluorescence background. Data are shown after background subtraction.

Acknowledgments

We thank Drs. Claudio Joazeiro, Dean Sheppard, and Kristiina Vuori for comments on the manuscript and reagents, and Drs. Carlos Caulin and Ricardo Giordano for helpful insights. This work was supported by a grant from the NCI (CA91134) to R.P. and CA90810 to W.A. and by the Gilson-Longenbaugh Foundation (to R.P. and W.A.). M.C.V. was supported by a predoctoral fellowship from the Department of Defense.

References

Andersen, M.H., Berglund, L., Petersen, T.E., and Rasmussen, J.T. (2002). Annexin-V binds to the intracellular part of the beta (5) integrin receptor subunit. Biochem. Biophys. Res. Commun. 292, 550-557.

Aoudjit, F., and Vuori, K. (2001). Matrix attachment regulates Fas-induced apoptosis in endothelial cells: a role for c-flip and implications for anoikis. J. Cell Biol. 152, 633-643.

Aplin, A.E., and Juliano, R.L. (2001). Regulation of nucleocytoplasmic trafficking by cell adhesion receptors and the cytoskeleton. J. Cell Biol. 155, 187-191.

Aplin, A.E., Howe, A., Alahari, S.K., and Juliano, R.L. (1998). Signal transduction and signal modulation by cell adhesion receptors: the role of integrins, cadherins, immunoglobulin-cell adhesion molecules, and selectins. Pharmacol. Rev. 50, 197-263.

Byzova, V.T., Goldman, K.C., Pampori, N., Thomas, A.K., Bett, A., Shattil, J.S., and Plow, F.E. (2000). A mechanism for modulation of cellular responses to VEGF: activation of the integrins. Mol. Cell 6, 6851-6860.

Chen, Q., Kinch, M.S., Lin, T.H., Burridge, K., and Juliano, R.L. (1994). Integrin-mediated cell adhesion activates mitogen-activated protein kinases. J. Biol. Chem. 269, 26602-26605.

Clark, E.A., and Brugge, J.S. (1995). Integrins and signal transduction pathways: the road taken. Science 268, 233-239.

Clark, E.A., and Hynes, R.O. (1997). Keystone symposium on signal transduction by cell adhesion receptors. Biochim. Biophys. Acta 1333, R9-R16.

Cookson, B.T., Engelhardt, S., Smith, C., Bamford, H.A., Prochazka, M., and Tait, J.F. (1994). Organization of the human annexin V (ANX5) gene. Genomics 20, 463-467.

Dean, P.D.G., Johnson, W.S., and Middle, F.A. (1985). Affinity Chromatography: A Practical Approach (Arlington, VA: IRL Press).

Derossi, D., Joliot, A.H., Chassaing, G., and Prochiantz, A. (1994). The third helix of the Antennapedia homeodomain translocates through biological membranes. J. Biol. Chem. 269, 10444-10450.

Derossi, D., Chassaing, G., and Prochiantz, A. (1998). Trojan peptides: the penetratin system for intracellular delivery. Trends Cell Biol. 8, 84ñ87.

Dubois, T., Oudinet, J.P., Russo-Marie, F., and Rothhut, B. (1995). In vivo and in vitro phosphorylation of annexin II in T cells: potential regulation by annexin V. Biochem. J. 310, 243-248.

Dubois, T., Oudinet, J.P., Mira, J.P., and Russo-Marie, F. (1996). Annexins and protein kinases C. Biochim. Biophys. Acta 1313, 290-294.

Dubois, T., Mira, J.P., Feliers, D., Solito, E., Russo-Marie, F., and Oudinet, J.P. (1998). Annexin V inhibits protein kinase C activity via a mechanism of phospholipid sequestration. Biochem. J. 330, 1277-1282.

Eliceiri, B.P., and Cheresh, D.A. (2001). Adhesion events in angiogenesis. Curr. Opin. Cell Biol. 13, 563-568.

Fadok, V.A., Voelker, D.R., Campbell, P.A., Cohen, J.J., Bratton, D.L., and Henson, P.M. (1992). Exposure of phosphatidylserine on the surface of apoptotic lymphocytes triggers specific recognition and removal by macrophages. J. Immunol. 148, 2207-2216.

Farishian, R.A., and Whittaker, J.R. (1979). Tyrosine utilization by cultured melanoma cells: analysis of melanin biosynthesis using [14C] thiouracil. Arch. Biochem. Biophys. 198, 449-461.

Filardo, E.J., Deming, S.L., and Cheresh, D.A. (1996). Regulation of cell migration by the integrin subunit ectodomain. J. Cell Sci. 109, 1615-1622.

Frisch, S.M., and Francis, H. (1994). Disruption of epithelial cell-matrix interactions induces apoptosis. J. Cell Biol. 124, 619-626.

Frisch, S.M., and Ruoslahti, E. (1997). Integrins and anoikis. Curr. Opin. Cell Biol. 9, 701-716.

Frisch, S.M., and Screaton, R.A. (2001). Anoikis mechanisms. Curr. Opin. Cell Biol. 13, 555ñ562.

Giancotti, F.G., and Ruoslahti, E. (1999). Integrin signaling. Science 285, 1028-1032.

Gilbert, M.T. (1987). High Performance Liquid Chromatography (Littleton, MA: John Wright-PSG).

Giordano, R.J., Cardo-Vila, M., Lahdenranta, J., Pasqualini, R., and Arap, W. (2001). Biopanning and rapid analysis of selective interactive ligands. Nat. Med. 7, 1249-1253.

Howe, A., Aplin, A.E., Alahari, S.K., and Juliano, R.L. (1998). Integrin signaling and cell growth control. Curr. Opin. Cell Biol. 10, 220-231.

Howe, A.K., Aplin, A.E., and Juliano, R.L. (2002). Anchorage-dependent ERK signaling-mechanisms and consequences. Curr. Opin. Genet. Dev. 12, 30-35.

Huang, X., Griffiths, M., Wu, J., Farese, R.V., Jr., and Sheppard, D. (2000). Normal development, wound healing, and adenovirus susceptibility in beta5-deficient mice. Mol. Cell. Biol. 20, 755ñ759.

Hynes, R.O. (1992). Integrins: versatility, modulation and signaling in cell adhesion. Cell 69, 11-25.

Hynes, R.O. (1999). Cell adhesion: old and new questions. Trends Cell Biol. 9, M33-M37.

Klemke, R.L., Yebra, M., Bayna, E.M., and Cheresh, D.A. (1994). Receptor tyrosine kinase signaling required for integrin alpha v beta 5-directed cell motility but not adhesion on vitronectin. J. Cell Biol. 127, 859-866.

Koivunen, E., Gay, D.A., and Ruoslahti, E. (1993). Selection of peptides binding to the alpha 5 beta 1 integrin from phage display library. J. Biol. Chem. 268, 20205-20210.

Koivunen, E., Wang, B., and Ruoslahti, E. (1995). Phage libraries displaying cyclic peptides with different ring sizes: ligand specificities of the RGD-directed integrins. Biotechnology (NY) 13, 265-270.

Koivunen, E., Restel, B.H., Rajotte, D., Lahdenranta, J., Hagedorn, M., Arap, W., and Pasqualini, R. (1999). Integrin-binding peptides derived from phage display libraries. Methods Mol. Biol. 129, 3-17.

Kolonin, M., Pasqualini, R., and Arap, W. (2001). Molecular addresses in blood vessels as targets for therapy. Curr. Opin. Chem. Biol. 5, 308-313.

Lewis, J.M., Cheresh, D.A., and Schwartz, M.A. (1996). Protein kinase C regulates alpha v beta 5-dependent cytoskeletal associations and focal adhesion kinase phosphorylation. J. Cell Biol. 134, 1323-1332.

Liu, S., Calderwood, D.A., and Ginsberg, M.H. (2000). Integrin cytoplasmic domain-binding proteins. J. Cell Sci. 113, 3563-3571.

Meredith, J., Jr., Mu, Z., Saido, T., and Du, X. (1998). Cleavage of the cytoplasmic domain of the integrin beta3 subunit during endothelial cell apoptosis. J. Biol. Chem. 273, 19525-19531.

Mira, J.P., Dubois, T., Oudinet, J.P., Lukowski, S., Russo-Marie, F., and Geny, B. (1997). Inhibition of cytosolic phospholipase A2 by annexin V in differentiated permeabilized HL-60 cells. Evidence of crucial importance of domain I type II Ca2 -binding site in the mechanism of inhibition. J. Biol. Chem. 272, 10474-10482.

Montesano, R., Orci, L., and Vassalli, P. (1983). In vitro rapid organization of endothelial cells into capillary-like networks is promoted by collagen matrices. J. Cell Biol. 97, 1648-1652.

Mosmann, T. (1983). Rapid colorimetric assay for cellular growth and survival: application to proliferation and cytotoxicity assays. J. Immunol. Methods 65, 55-63.

Nakamura, S., and Nishizuka, Y. (1994). Lipid mediators and protein kinase C activation for the intracellular signaling network. J. Biochem. (Tokyo) 115, 1029-1034.

Park, J.E., Lenter, M.C., Zimmermann, R.N., Garin-Chesa, P., Old, L.J., and Rettig, W.J. (1999). Fibroblast activation protein, a dual specificity serine protease expressed in reactive human tumor stromal fibroblasts. J. Biol. Chem. 274, 36505-36512.

Pasqualini, R., and Hemler, M.E. (1994). Contrasting roles for integrin beta 1 and beta 5 cytoplasmic domains in subcellular localization, cell proliferation, and cell migration. J. Cell Biol. 125, 447-460.

Pasqualini, R., Bodorova, J., Ye, S., and Hemler, M.E. (1993). A study of the structure, function and distribution of beta 5 integrins using novel anti-beta 5 monoclonal antibodies. J. Cell Sci. 105, 101-111.

Pasqualini, R., Koivunen, E., and Ruoslahti, E. (1997). αv integrins as receptors for tumor targeting by circulating ligands. Nat. Biotechnol. 15, 542-546.

Prewett, M., Huber, J., Li, Y., Santiago, A., OíConnor, W., King, K., Overholser, J., Hooper, A., Pytowski, B., Witte, L., et al. (1999). Antivascular endothelial growth factor receptor (fetal liver kinase 1) monoclonal antibody inhibits tumor angiogenesis and growth of several mouse and human tumors. Cancer Res. 59, 5209-5218.

Raynal, P., Hullin, F., Ragab-Thomas, J.M., Fauvel, J., and Chap, H. (1993). Annexin 5 as a potential regulator of annexin 1 phosphorylation by protein kinase C. In vitro inhibition compared with quantitative data on annexin distribution in human endothelial cells. Biochem. J. 292, 759-765.

Reed, J.C. (2002). Apoptosis-based therapies. Nat. Rev. Drug Discov. 1, 111-121.

Rothhut, B., Dubois, T., Feliers, D., Russo-Marie, F., and Oudinet, J.P. (1995). Inhibitory effect of annexin V on protein kinase C activity in mesangial cell lysates. Eur. J. Biochem. 232, 865-872.

Schlaepfer, D.D., and Hunter, T. (1998). Integrin signalling and tyrosine phosphorylation: just the FAKs? Trends Cell Biol. 8, 151-157.

Schlaepfer, D.D., Jones, J., and Haigler, H.T. (1992). Inhibition of protein kinase C by annexin V. Biochemistry 31, 1886-1891.

Schwartz, M.A., Schaller, M.D., and Ginsberg, M.H. (1995). Integrins: emerging paradigms of signal transduction. Annu. Rev. Cell Dev. Biol. 11, 549-599.

Shattil, S.J., and Ginsberg, M.H. (1997). Perspectives series: cell adhesion in vascular biology. Integrin signaling in vascular biology. J. Clin. Invest. 100, 1-5.

Shevchenko, A., Wilm, M., Vorm, O., and Mann, M. (1996). Mass spectrometric sequencing of proteins silver-stained polyacrylamide gels. Anal. Chem. 68, 850-858.

Smith, G.P., and Scott, J.K. (1993). Libraries of peptides and proteins displayed on filamentous phage. Methods Enzymol. 217, 228-257.

Sopkova, J., Renouard, M., and Lewit-Bentley, A. (1993). The crystal structure of a new high-calcium form of annexin V. J. Mol. Biol. 234, 816-825.

Stupack, D.G., Puente, X.S., Boutsaboualoy, S., Storgard, C.M., and Cheresh, D.A. (2001). Apoptosis of adherent cells by recruitment of caspase-8 to unligated integrins. J. Cell Biol. 155, 459-470.

Tang, S., Gao, Y., and Ware, J.A. (1999). Enhancement of endothelial cell migration and in vitro tube formation by TAP20, a novel beta 5 integrin-modulating, PKC theta-dependent protein. J. Cell Biol. 147, 1073-1084.

Theodore, L., Derossi, D., Chassaing, G., Llirbat, B., Kubes, M., Jordan, P., Chneiweiss, H., Godement, P., and Prochiantz, A. (1995). Intraneuronal delivery of protein kinase C pseudosubstrate leads to growth cone collapse. J. Neurosci. 15, 7158-7167.

Thomas, L., Chan, P.W., Chang, S., and Damsky, C. (1993). 5-Bromo-2-deoxyuridine regulates invasiveness and expression of integrins and matrix-degrading proteinases in a differentiated hamster melanoma cell. J. Cell Sci. 105, 191-201.

Vuori, K., and Ruoslahti, E. (1993). Activation of protein kinase C precedes alpha 5 beta 1 integrin-mediated cell spreading on fibronectin. J. Biol. Chem. 268, 21459-21462.

Zetter, B.R. (1997). On target with tumor blood vessel markers. Nat. Biotechnol. 15, 1243-1244.

Zhu, D.M., Narla, R.K., Fang, W.H., Chia, N.C., and Uckun, F.M. (1998). Calphostin C triggers calcium-dependent apoptosis in human acute lymphoblastic leukemia cells. Clin. Cancer Res. 4, 2967-2976.

5. Péptidos que se unen a inhibidores de las caspasas

Resumen

Las proteínas inhibidoras de las caspasas, IAP (*inhibitor of apoptosis proteins*) representan una familia de proteínas antiapoptóticas que se encuentran tanto en los invertebrados como en los vertebrados. Los tres miembros de esta familia que se han encontrado en humanos son: XIAP, cIAP1 y cIAP2. Estas proteínas inhiben apoptosis al unirse e inactivar la caspasa 3 o la 7. Además la proteína XIAP se une e inhibe a la caspasa 9, que es la proteasa que regula la apoptosis a través de la vía del citocromo c mitocondrial.

Los estudios previos han demostrado que el segundo dominio BIR (*baculovirus IAP repeat*), dominio común para todas las IAPs, era necesario y suficiente para inhibir el efecto proteolítico de las caspasas 3 y 7. Este dominio consta de unos 70 aminoácidos que tienen un dominio de unión al zinc. En cambio, para suprimir la acción de la caspasa 9 es necesario el tercer motivo (BIR3). Estos resultados sugieren que un dominio por si solo puede tener actividad anti-apoptótica. Con el fin de descubrir los posibles lugares de interacción de XIAP con otras moléculas diseñamos un experimento usando la técnica de *phage display*.

La proteína de fusión GST-XIAP se incubó con una genoteca peptídica que estaba incorporada en bacteriófagos. Después de tres rondas de selección, los bacteriófagos que se unían específicamente a GST-XIAP fueron secuenciados. Se encontró que un 84% expresaban un motivo común que se podía esquematizar en: C D/E/P aromático +/- X C. Todos estos bacteriófagos que compartían esta secuencia común se unían específicamente XIAP pero no a survivin (otra IAP) o a la GST utilizada para formar la proteína recombinante. Además se demostró que dos de las secuencias aisladas reconocían de manera especifica el dominio (BIR2) o la combinación de este con sus respectivos dominios adyacentes. Se sintetizaron las secuencias peptídicas expresadas por los bacteriófagos (CEFESC, CPFKQC, ARGKER), que se unían selectivamente al BIR2 manteniendo su estructura cíclica. Con este material se hicieron los estudios de inhibición de la unión del fago con la proteína mediados por el péptido. Estos estudios mostraron ser específicos, pues las versiones lineares de estos péptidos no tenían el mismo efecto, como tampoco ninguno de los péptidos usados como control negativo. Además, la inhibición por el péptido era dependiente de la dosis. El hecho de que las caspasa 3 y 7 (el ligando natural) compitieran con la unión de los bacteriófagos al BIR2 confirmó la especificidad de unión de los péptidos al dominio BIR2.

Para valorar la función biológica de los péptidos identificados se sintetizaron versiones internalizables de las tres secuencias descritas anteriormente usando la penetratina como sistema de administrador intracelular. Nuestros resultados mostraron que CPKKQC era capaz de reducir la viabilidad en células de leucemia, mientras que las formas no internalizables no tenían ningún tipo de efecto.

Estos resultados sugieren que la producción de péptidos miméticos, seguida de una estrategia de maduración de la afinidad para incrementar la especificidad de unión, podría ser utilizada como moduladores de la muerte celular programada. Esto sugiere que los péptidos derivados de los fagos podrían ser el punto de partida para la generación de moléculas pequeñas que se unen e inhiben la actividad de XIAP. Estas moléculas pudieran ser utilizadas como una nueva estrategia para el tratamiento de tumores.

Peptides Targeting Caspase Inhibitors*

Here we report on the identification of peptides targeting the X-inhibitor of apoptosis protein (XIAP). XIAP functions as a caspase inhibitor and is a member of the inhibitors of apoptosis (IAP) family of proteins. IAPs are often overexpressed in cancers and leukemias and are associated with an unfavorable clinical prognosis. We have selected peptides from a phage library by using recombinant full-length human XIAP or a fragment containing only the baculovirus IAP repeat 2 (BIR2) domain. A consensus motif, C(D/E/P)(W/F/Y)-acid/basic- X C, was recovered from two independent screenings by using different libraries. Phage-displaying variations of the consensus sequence bound specifically to the BIR2 domain of XIAP but not to other IAPs. The interaction was specific as it could be blocked by the cognate synthetic peptides in a dose-dependent manner. Phage displaying the XIAP-binding motif CEFESC bound to the BIR2 domain of XIAP with an estimated dissociation constant of 1.8 nM as determined by surface plasmon resonance. Protein-protein interaction assays revealed that caspase-3 and caspase-7 (but not caspase-8) blocked the binding of the CEFESC phage to XIAP, indicating that this peptide targets a domain within XIAP that is related to the caspase-binding site. In fact, the sequence EFES is homologous to a loop unique to the executioner caspase-3 and caspase-7 that are targeted by XIAP. Finally, we demonstrated that an internalizing version of the XIAP-binding peptide identified in our screenings (PFKQ) can induce programmed cell death in leukemia cells. Peptides interacting with XIAP could serve as prototypes for the design of low molecular weight modulators of apoptosis.

The inhibitor of apoptosis proteins (IAPs) [1] represent a family of anti-apoptotic proteins found in both vertebrates and invertebrates (reviewed in Ref. 1). All of the human IAP homologs have been shown to inhibit programmed cell death (1, 2). The human IAP family members, XIAP, c-IAP1, and c-IAP2, bind to caspase-3 and caspase-7 with inhibitory constant values (K_i) of 0.2-10 nM (3-5). XIAP also binds to and suppresses specifically caspase-9, an initiator caspase, that is at the apical protease in the cytochrome c/mitochondrial pathway for apoptosis (6-9).

All of the IAP family members have at least one and up to three copies of an 70-amino acid zinc-binding domain termed the baculovirus IAP repeat (BIR) (1). We have performed mutagenesis-based studies to show that in the context of XIAP, the second of the three BIR domains (BIR2) is necessary and sufficient to inhibit the effector proteases caspase-3 and caspase-7 (10). In contrast, for XIAP to suppress caspase-9, the third BIR domain is required (11). These data suggest that a single BIR domain can mediate anti-apoptotic activity. To map functionally relevant interacting sites within molecules associating with XIAP, we screened peptide libraries using the full-length protein and on the isolated BIR2 domain.

We identified XIAP ligands containing the motif CEFESC. This motif appears to mimic the XIAP-binding site within specific caspases because the binding of this peptide to XIAP is inhibited by preincubation with caspase-3 and caspase-7 but not by caspase 9. Binding assays using individual phage displaying this motif and a panel of purified targets confirmed that the phage interacts specifically with the BIR2 domain in a pattern consistent with caspase-type ligands. No binding was observed when BIR1, BIR3, or the RING finger domain of XIAP were tested nor when other IAP family members such as cIAP1, cIAP2, NAIP, and Survivin were evaluated under the same experimental conditions. We also show that XIAP-binding peptides can affect cell viability. Taken together, our results contribute to the understanding of the structural requirements and functional domains that are important in the regulation of programmed cell death.

EXPERIMENTAL PROCEDURES

Plasmids, Protein Expression, and Purification- Cloning and synthesis of full-length XIAP and the XIAP fragments BIR1, BIR2, BIR3, BIR1-2, BIR2-3, and RING as well as full-length cIAP1, cIAP2, NAIP, and Survivin have been described previously (4, 10, 12). Recombinant caspase proteins containing His_6 tags were prepared as described previously (8) and were a gift from Dr. G. Salvesen (The Burnham Institute, La Jolla, CA).

Identification of XIAP-binding Peptides by Phage Display- fUSE5-based phage peptide libraries displaying either cyclic or linear random peptides (C X_4C or X_6; C = cysteine and X = random amino acid) were made and screened as described previously (13, 14). Polystyrene 96-well plates were coated with 50 μl/well of 1 mg/ml GST-XIAP fusion protein or GST fusion proteins of various fragments of XIAP, cIAP1, cIAP2, NAIP, Survivin, BSA, or GST in PBS overnight at 4 C. The wells were washed with PBS, blocked with 3% BSA (first round of panning), casein (second round), or -globulins (third round) for 1 h, and incubated with 10^{10} transducing units (TU) of the primary library for 1 h at room temperature. The wells were washed nine times in PBS, 0.01% Tween 20 to remove unbound phage and once with PBS. Bound phages were eluted by adding 200 μl of a log-phase K91Kan terrific broth culture and amplified overnight in 10 ml of LB medium containing 40 g/ml tetracycline. Randomly selected phage clones from the third round of panning were sequenced as described previously (15). Individual phage clones displaying similar peptide motifs were tested for specific binding to GST fusion proteins of XIAP, fragments of XIAP, cIAP1, cIAP2, NAIP, Survivin, BSA, or GST alone. These binding assays were performed following the protocol of the initial screening. The number of bound phage was determined by plating serial dilutions of the recovered phage-bacteria mixture on LB agar plates containing 40 μ g/ml tetracycline.

Peptide Synthesis - Peptides were synthesized with an ACT-350 multiple peptide synthesizer by using Fmoc synthesis on Rink amide MBHA resin or Fmoc-Lys(-LC- D-Biotin)-Rink amide-MBHA resin for C-terminally biotinylated peptides. The peptides were cleaved with 92.5% trifluoroacetic acid, 2.5% water, 2.5% EDTA, and 2.5% TIS and precipitated with cold ethyl ether. Quantitative cyclization was achieved in 20% Me_2SO, H_2O, pH 4.0 -7.0 in 1 day as described previously (16). Crude peptides were purified by high pressure liquid chromatography on a reverse phase C-18 column with a gradient of water/

[1] The abbreviations used are: IAP, inhibitor of apoptosis; XIAP, X-inhibitor of apoptosis protein; BIR, baculovirus IAP repeat; GST, glutathione S-transferase; BSA, bovine serum albumin; PBS, phosphate-buffered saline; TU, transducing units; Fmoc, N-(9-fluorenyl) methoxycarbonyl; Pen, penetratin.

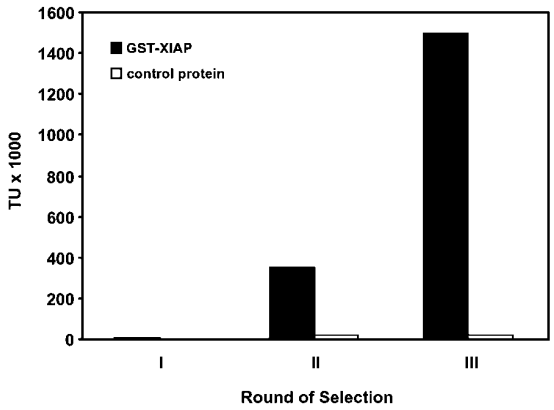

FIG. 1. **Enrichment of XIAP-binding phage on recombinant** XIAP. A CX_4C random phage-display peptide library was selected on immobilized GST-XIAP as described under "Experimental Procedures." Aliquots of the recovered phage-bacteria mixture were plated on LB plates containing tetracycline to determine the number of TU recovered. Data represent the number of TU recovered from wells coated either with GST-XIAP (black bars) or a control protein (white bars; casein for screening round II, bovine γ-globulins for screening round III).

acetonitrile containing 0.1% trifluoroacetic acid. The purified peptides showed one peak by analytical high pressure liquid chromatography, and the molecular weight was confirmed by matrix-assisted laser desorption ionization time-of-flight mass spectroscopy.

Caspase Competition Assays - Inhibition of phage binding to XIAP by recombinant caspases was assayed by coating polystyrene 96-well plates with 1 μg/well of recombinant XIAP protein (50 μl of a 1 mg/ml solution), various fragments of XIAP, or control proteins (as indicated) in PBS overnight at 4 C. The wells were washed once with PBS, blocked with 3% BSA for 1 h, washed again, and incubated with various amounts of recombinant active caspases-3, -7, or -8 for 30 min at room temperature. The wells were then washed once with PBS, and XIAP-binding or control phage was added (10^8 TU/well) and incubated for 30 min. Wells were then washed nine times with PBS, 0.01% Tween 20, and washed once more in PBS. Bound phage were eluted by adding 200 μl of a log-phase K91Kan terrific broth culture. The number of bound phage was determined as described above.

Surface Plasmon Resonance - The interaction of XIAP-binding phage and control phage with the BIR2 domain of XIAP was investigated using the BIAcore 3000 system (BIAcore, Uppsala, Sweden). GST-BIR2 was covalently attached by its primary amine residues to CM5 sensor chips (17). Binding was detected in resonance units after injecting phage in a range of concentrations in HBS buffer (10 mM HEPES, pH 7.4, with 0.15 M NaCl, 3.0 mM EDTA, and 0.05% surfactant P20). After each run, the chip surfaces were regenerated with 10 mM glycine, pH 4.5. Non-linear regression analysis was used to determine equilibrium-binding constants that fit to a single site-binding model (18 - 20).

Peptide Internalization and Cell Viability Assays - Uptake of penetratin-linked peptides into OCI/AML-4 cells (an acute myeloblastic leukemia cell line, for review see Ref. 21) was monitored as described previously (22). Cells growing in 24-well plates were incubated with increasing doses (1 - 20 M) of penetratin alone, synthetic peptides alone (CEFESC, CPFKQC, or ARGKER), or penetratin-linked versions of each peptide. Cell viability was assessed at different time points (12, 24, and 72 h).

TABLE I
Sequences of XIAP-binding peptides

Randomly selected phage clones displaying the XIAP-binding motif were grouped into three subsets based on the amino acid residue at position 2.

	C	D	W	T	H	C
	C	D	W	R	V	C
	C	D	W	L	T	C
	C	D	W	L	T	C
	C	D	W	L	T	C
	C	D	W	N	Q	C
	C	D	F	I	M	C
	C	D	W	V	F	C
	C	D	F	K	A	C
	C	D	F	V	G	C
	C	E	Y	K	E	C
	C	E	E	N	L	C
	C	E	F	L	F	C
	C	E	F	F	F	C
	C	E	K	F	P	C
	C	E	F	A	Q	C
	C	E	F	A	Q	C
	C	E	H	Y	P	C
	C	E	F	E	S	C
	C	P	F	I	R	C
	C	P	F	T	E	C
	C	P	F	D	R	C
	C	P	Y	R	H	C
	C	P	F	M	A	C
	C	P	F	K	E	C
	C	P	F	H	T	C
	C	P	Y	K	Q	C
	C	P	F	K	Q	C
	C	P	F	A	A	C
	C	P	Y	H	E	C
	C	P	Y	R	R	C
	C	P	Y	R	F	C
Motif:	C	D/E/P	Aromatic	/	X	C

RESULTS

Identification of XIAP-binding Peptides - XIAP-binding peptides were identified by selecting phage display peptide libraries on immobilized human GST-XIAP. The libraries contained six amino acid inserts in which either all six residues were randomized or the first and last positions were fixed as cysteines to promote cyclization by disulfide bonding (X_6 or CX_4C libraries, respectively). The enrichment of phage on XIAP was monitored by counting the number of TU recovered from the XIAP-coated wells *versus* the number recovered from wells coated with the control protein. We observed a pronounced enrichment for phage binding to GST-XIAP (Fig. 1). The DNA inserts of 36 randomly chosen phage clones (18 from the X_6 library and 18 from the CX_4C library) recovered from the third round of biopanning on XIAP were sequenced. A total of 32 phage clones derived from both libraries displayed the consensus motif C-(E/D/P)-(aromatic amino acid = W/Y/F)-charged amino acid-(X = random)-C (Table I). In addition, marked enrichment was observed for phage displaying the motif (8 of 18 in the second round and 16 of 18 in the third round by using the X_6 library). In contrast, biopanning experiments using the same libraries on other IAPs such as Survivin or on GST protein alone failed to select for phage with the above consensus motif, demonstrating the specificity of the selection process.

Phage Specificity and Mapping of Binding Sites on XIAP- The specificity of XIAP-binding phage was tested in individual phage-binding assays on immobilized GST-XIAP or GST fusion proteins of other members of the IAP family such as Survivin, cIAP1, cIAP2, and NAIP. Representative data are shown for

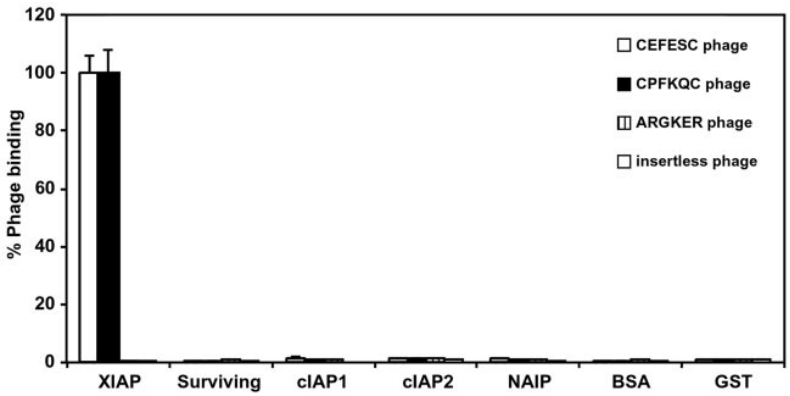

FIG. 2. **CEFESC and CPFKQC selectively bind to XIAP but not to other IAP family members.** Phage displaying no peptide insert (fd-tet), the XIAP-binding sequences CEFESC or CPFKQC, or a control sequence ARGKER were incubated in microtiter plate wells coated with 2 μg of various GST fusion proteins (XIAP, Survivin, cIAP1, cIAP2, and NAIP), GST alone, or BSA. Bound phage were recovered by bacterial infection. Transduced bacteria were grown overnight on LB plates containing tetracycline to determine the number of TU recovered. Data are expressed as the percentage relative to the number of TU recovered from wells coated with GST-XIAP (set to 100%). Data represent the means from triplicate platings ± S.D.

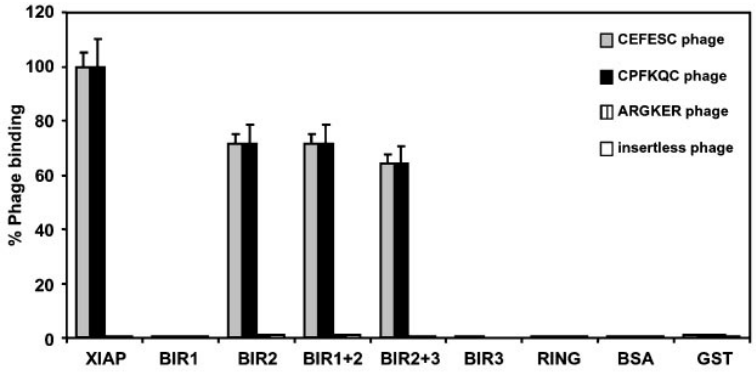

FIG. 3. **XIAP-binding phage interact with the BIR2 domain of XIAP.** Phage were incubated in microtiter plate wells coated with 2 g of immobilized GST fusion proteins representing full-length XIAP, various fragments of XIAP, or BSA (control). Bound phage were rescued and quantified by colony counting as in Fig. 2.

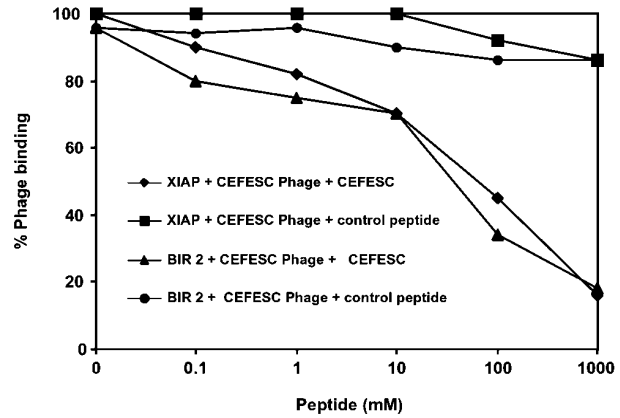

FIG. 4. **Synthetic peptides displaying phage-derived sequences bind XIAP.** Binding of CEFESC phage to XIAP is inhibited by the cognate peptide. Binding of phage displaying the XIAP-binding peptide-CEFESC or a control peptide (ARKGER) to GST-XIAP or GST-BIR2 was measured as in Fig. 2 in the presence or absence of cyclic CEFESC-synthetic peptide. Data represent the means from triplicate platings ± S.D. and are expressed as the percentage relative to the number of TU obtained in the absence of synthetic peptides.

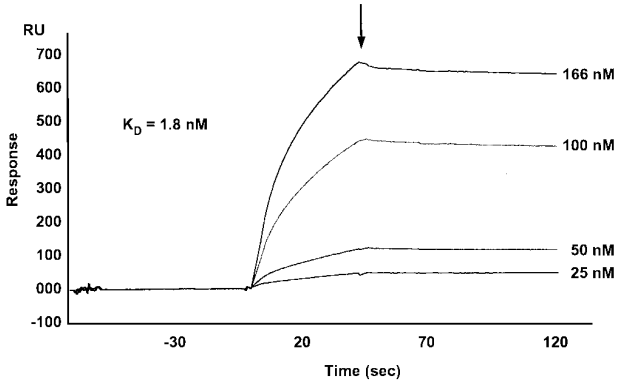

FIG. 5. Surface plasmon resonance characterizes the binding of the CEFESC-phage to the BIR2 domain of XIAP. Recombinant BIR2 of XIAP was immobilized on a sensor chip, and a range of concentrations of CEFESC phage was injected over the chip surface. Data represent resonance units plotted as a function of time. The arrow indicates the time at which the mobile phase was switched to the buffer lacking phage. The binding constant (K_D) was estimated from association and dissociation rate constants using sensograms analyzed by Bioevaluation 3.0 (BIAcore) software.

two of the XIAP-binding phage displaying the CEFESC- or the CPFKQC-peptide. Controls were insertless fd-tet phage and phage-displaying ARGKER, an unrelated control insert. In these assays, both the CEFESC and CPFKQC phage bound to XIAP but not to the other IAP family members, BSA, or GST. Control phage did not bind to GST-XIAP, indicating specificity. These data confirm the specificity of phage clones displaying the consensus motif for XIAP binding (Fig. 2).

We next mapped the domain within XIAP that mediates the binding of the isolated phage clones using a panel of XIAP

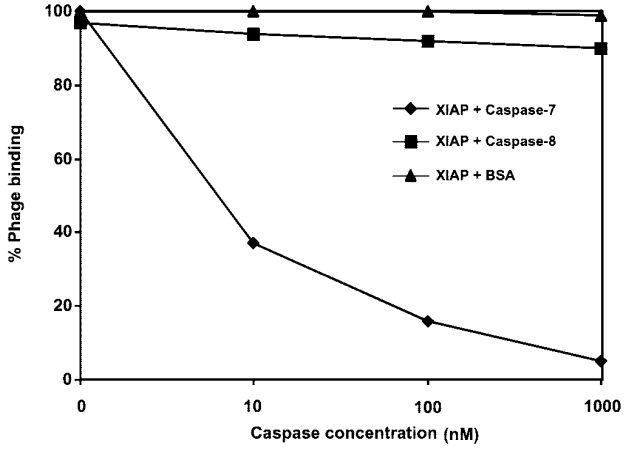

FIG. 6. Caspase-7 but not caspase-8 inhibits binding of phage to XIAP. GST-XIAP or GST alone were immobilized on microtiter plate wells (100 ng/well) and incubated with recombinant caspase-7 or caspase-8 (control) in a total volume of 50 μl at the indicated concentrations. XIAP-binding CEFESC-phage were added at 10^7 TU/well and incubated for 1 h, and bound phage were recovered after washing. Recovered phage were quantified as in Fig. 2.

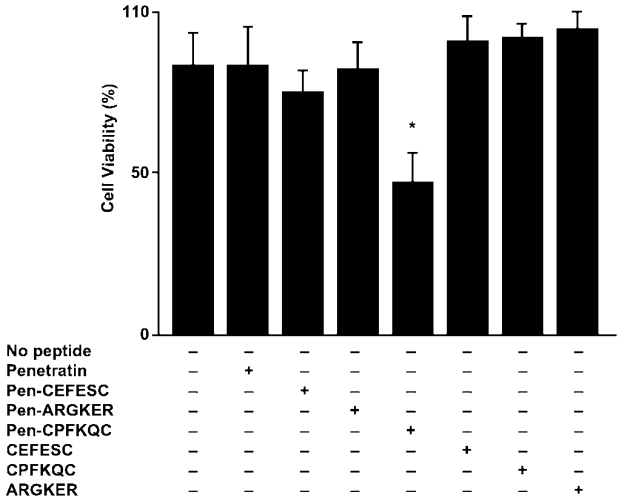

FIG. 7. An internalizing version of the XIAP-binding peptide triggers cell death. Internalization of Pen-CPFKQC leads to growth arrest and induces programmed cell death in OCI/AML-4 cells. Cell viability (%) was evaluated at 72 h after no treatment (No peptide) or incubation with multiple peptides as indicated. Pen-CPFKQC decreased cell viability. *, $p < 0.01$. Shown are mean ± S.E. obtained from triplicate wells.

deletion mutants expressed as GST fusion proteins. XIAP-binding phage bound to GST fusion proteins containing the BIR2 domain of XIAP alone or the BIR2 domain in combination with flanking domains. In contrast, fragments of XIAP containing only the BIR1, BIR3, or RING domains failed to adsorb XIAP-binding phage. The insertless fd-tet phage as well as the control ARGKER-phage did not bind to either GST-XIAP or GST-BIR2, indicating that the target proteins do not bind recombinant phage nonspecifically (Fig. 3).

Synthetic Peptides Representing Phage-derived Sequences Bind XIAP- To further confirm that the peptides displayed on XIAP-binding phage interact with XIAP independently of other phage components, experiments were performed using synthetic peptides. Cyclic peptides corresponding to the sequences displayed by XIAP-binding phage clones were synthesized and tested for their ability to specifically inhibit phage binding to GST-XIAP and GST-BIR2. The cyclic peptides but not the irrelevant control peptides inhibited phage binding of the corresponding phage clones in a concentration-dependent manner (Fig. 4). Non-cyclic versions of the same peptides failed to prevent phage binding.

Binding Properties of XIAP-binding Phage - To further characterize the interaction of XIAP-binding phage with the BIR2 domain, we used surface plasmon resonance. The BIR2 domain of XIAP was conjugated to the chip surface (solid phase) and phage displaying a XIAP-binding peptide were used as an analyte (mobile phase). A variety of concentrations of phage displaying CEFESC, CPFKQC, or CDFKAC were injected, and the CEFESC-phage clone was the strongest binder of the three phages analyzed (Fig. 5). This phage bound to BIR2 with an estimated k_a of 4.9×10^5 M^{-1} s^{-1}. Upon switching to phage-free flow solution, a very slow dissociation of phage from the chip surface was observed with an approximate k_d of 8.6×10^{-4}. A K_D of 1.8 nM was estimated for binding of the CEFESC-phage to BIR2 as compared with a K_D of >10 μM for either insertless fd-tet phage or phage displaying a control peptide-ARGKER.

XIAP-binding Phage and Caspases Compete for Binding to XIAP- Because the BIR2 domain of XIAP has been shown to be necessary and sufficient for binding caspases-3 and -7 (10), we asked whether these caspases compete with XIAP-binding phage for binding to XIAP. GST-BIR2 or various GST control proteins were immobilized on glutathione-Sepharose and incubated with XIAP-binding CEFESC-phage in the presence or absence of recombinant caspase-3 or -7. Recombinant caspase-8 was used as a control because it does not bind XIAP (3). The binding of CEFESC-phage to BIR2 was inhibited in a concentration-dependent manner upon the addition of caspase-7 or caspase-3. In contrast, neither BSA nor caspase-8 blocked the binding of CEFESC-phage to XIAP (Fig. 6). These data suggest that phage displaying the CEFESC-peptide occupy sites on the BIR2 domain that overlap with or are adjacent to sites involved in caspase binding.

To determine whether the XIAP-targeting peptides could affect cell viability, we designed and synthesized internalizing versions of the CEFESC-, CPFKQC-, or ARGKER-peptides (negative control) by using the penetratin system for intracellular delivery. Penetratin (Pen) is a peptide containing 16 amino acids that is part of the third helix of the antennapedia protein homeodomain (22). Because penetratin has translocating properties, it is capable of carrying hydrophilic compounds across the plasma membrane and delivering them directly to the cytoplasm without degradation (22). We fused the XIAP-binding peptides or a control unrelated peptide to penetratin and added a biotin moiety to visualize internalization. We used leukemia cells (OCI/AML-4) as a model system to test the effect of the internalizing peptides because these cells (i) express XIAP and caspases and (ii) respond to regulators of apoptosis (21). Pen-linked peptides were internalized and remained in

the cytoplasm (data not shown). Penetratin alone was also internalized and uniformly distributed in the cytoplasm. Peptides lacking penetratin were not internalized (data not shown). We evaluated cell survival in the cells exposed, internalizing versions of the XIAP-binding peptides. After a 72-h incubation, reduced cell viability was observed in cells treated with Pen-CPFKQC (Fig. 7). No cell death was observed when cells were untreated, treated with penetratin alone, or treated with an unrelated control peptide fused to penetratin. Moreover, incubation with non-internalizing versions of each synthetic peptide had no effect (Fig. 7).

DISCUSSION

IAPs are overexpressed in a variety of cancers and leukemias, and antagonistic small molecules could be useful for modifying the antiapoptotic activity of XIAP in vivo. In this study, we screened phage-display peptide libraries in search of short peptide motifs capable of binding this caspase-inhibitory protein. An analysis of the peptides displayed by phage binding to XIAP revealed a consensus sequence in which position 1 is invariably a cysteine, position 2 is either an acidic residue (aspartic acid or glutamic acid) or a proline, and position 3 is usually an aromatic amino acid (tryptophan, phenylalanine, or tyrosine) followed by two variable amino acids and finally a cysteine. Although position 4 was variable among the XIAP-binding phage randomly sequenced, the most highly represented types of amino acids at position 4 were charged (lysine, arginine, histidine, aspartic acid, or glutamic acid in 13 of 32 cases). The binding of these phage to XIAP was highly selective with no evidence of significant interactions with other members of the IAP family of proteins such as cIAP1, cIAP2, NAIP, or Survivin. Thus, the XIAP-binding phage recognize a binding site unique to XIAP, which may be exploitable for applications aimed either at detecting XIAP or selectively inhibiting XIAP function.

We showed that the isolated peptides bind to the BIR2 domain of XIAP. The specificity of the motif for BIR2 was confirmed independently by repeating library screenings using GST-BIR2 as a target, resulting in the selection of phage whose inserts shared the same consensus sequence, which was obtained originally using GST full-length XIAP. Interactions of these peptide motifs with BIR2 are biologically relevant, because our previous studies indicate that the BIR2 domain is necessary and sufficient for inhibiting caspases-3 and -7 (10). Functional studies using the cyclic XIAP-binding peptides show that these probes do not act as repressors of XIAP-mediated caspase inhibition. We also show that an internalizing version of the XIAP-binding peptide identified in our screenings (PFKQ) can induce programmed cell death in leukemia cells in a specific, dose-dependent, and time-dependent manner. These findings suggest that development of peptidomimetics following affinity maturation strategies to increase binding affinity may lead to tools that can be used as modulators of programmed cell death.

During programmed cell death, effector caspase zymogens are cleaved at conserved aspartic acid residues, generating large and small subunits, which together constitute the active protease. The activation of effector caspases such as caspases-3 and -7 is a nearly universal event associated with apoptosis induced by multiple stimuli. Our previous observation that XIAP and other IAP family proteins directly bind active executioner caspases-3 and -7, resulting in their potent suppression in vitro and in cultured cells (3, 4), suggests a general mechanism for IAP-mediated apoptosis inhibition. Recently, a naturally occurring IAP inhibitor termed Smac/DIABLO has been identified (23, 24). Smac performs a critical function in apoptosis by eliminating the inhibitory effect of IAPs on caspases. Smac promotes not only the proteolytic activation of procaspase-3 but also the enzymatic activity of mature caspase-3, both of which depend upon the ability of Smac to interact physically with IAPs. A seven-residue peptide derived from the N terminus of Smac promotes procaspase-3 activation in vitro (23). Although the amino acid sequence of this peptide is different from our sequences, identification of Smac and Omi provides further evidence that inhibition of IAPs by peptides represents a viable approach to induction of apoptosis in mammalian cells.

Interestingly, the sequence EFES, which is embedded in one of the XIAP-binding phage in a cyclic context (CEFESC), occurs in caspase-3, a protease that binds to BIR2 of XIAP with a $K_D \leq 5$ nM (10). This sequence is located in the 381-loop of caspase-3 in a region only found in caspases-3 and -7. Because this loop is important in the binding of BIR2 to caspases-3 and -7 (5, 25, 26) (for review see Ref. 27), one might speculate that the EFES-containing peptide corresponds to an important region within the caspase-3-XIAP interacting site. In fact, the recently reported x-ray crystallographic structure of the XIAP-BIR2 domain/caspases-3 and -7 complex shows that the substrate-binding pocket within these caspases is formed by four surface loops, L1, L2, L3, and L4 (5, 25, 26). The sequence EFES is exposed for binding within the 381-loop, and the second Glu residue in the sequence corresponds to an interaction site between caspase-3 and BIR2 (5). This observation underscores the power of phage display technology for the mapping for biologically relevant protein-interacting sites.

Although XIAP is widely expressed, abnormally high levels of XIAP have been observed in certain types of leukemias and solid tumors (28). Overexpression of XIAP has also been shown to render tumor cells more resistant to apoptosis induction by anti-cancer drugs in vitro (2). Thus, agents that interfere with XIAP activity may be useful to treat cancers. The phage-derived peptides described here could provide a starting point for the generation of small molecule compounds that bind to and inhibit XIAP, thereby providing a new approach to the treatment of malignancies. Alternatively, cell membrane-penetrating versions of XIAP-binding peptides or tumor-targeted delivery of genes expressing XIAP-binding peptides fused to ubiquitin ligases could potentially be exploited as mechanism-based strategies for improved cancer treatment.

Acknowledgments - We thank Drs. Guy S. Salvesen, Frank C. Marini III, and Luiz V. Rizzo for critical reading of this paper and helpful insights.

REFERENCES

1. Salvesen G. S., and Duckett C. S. (2002) Nat. Rev. Mol. Cell. Biol. 3, 401 - 410
2. LaCasse, E. C., Baird, S., Korneluk, R. G., and MacKenzie, A. E. (1998) Oncogene 17, 3247 - 3259
3. Deveraux, Q., Takahashi, R., Salvesen, G. S., and Reed, J. C. (1997) Nature 388, 300 - 303

4. Roy, N., Deveraux, Q. L., Takashashi, R., Salvesen, G. S., and Reed, J. C. (1997) EMBO J. 16, 6914 - 6925
5. Riedl, S. J., Renatus, M., Schwarzenbacher , R., Zhou, Q., Sun, C., Fesik, S. W., Liddington, R. C., and Salvesen, G. S. (2001) Cell 104, 791 - 800
6. Nicholson, D. W., and Thornberry, N. A. (1997) Trends Biol. Sci. 22, 299 - 306
7. Salvesen, G. S., and Dixit, V. M. (1997) Cell 91, 443 - 446
8. Thornberry, N., and Lazebnik, Y. (1998) Science 281, 1312 - 1316
9. Stennicke H. R., and Salvesen G. S. (2000) Methods Enzymol. 322, 91 - 100
10. Takahashi, R., Deveraux, Q., Tamm, I., Welsh, K., Assa-Munt, N., Salvesen, G. S., and Reed, J. C. (1998) J. Biol. Chem. 273, 7787 - 7790
11. Deveraux, Q. L., Leo, E., Stennicke, H., Welsh, K., Salvesen, G., and Reed, J. C. (1999) EMBO J. 18, 5242 - 5251
12. Tamm, I., Wang, Y., Sausville, E., Scudiero, D. A., Vigna, N., Oltersdorf, T., and Reed, J. C. (1998) Cancer Res. 58, 5315 - 5320
13. Scott, J. K., and Smith, G. P. (1990) Science 249, 386 ñ389
14. Koivunen, E., Wang, B., Dickinson, C. D., and Ruoslahti, E. (1994) Methods Enzymol. 245, 346 - 369
15. Koivunen, E., Wang, B., and Ruoslahti, E. (1995) Biotechnology 13, 265 - 270
16. Tam, J. P. (1988) Proc. Natl. Acad. Sci. U. S. A. 85, 5409 - 5413
17. Xie, Z., Schendel, S., Matsuyama, S., and Reed, J. C. (1998) Biochemistry 37, 6410 - 6418
18. Kalinin, N., Ward, L., and Winzor, D. (1995) Anal. Biochem. 228, 238 - 244
19. Morelock, M. M., Ingraham, R. H., Betageri, R., and Jakes, S. (1995) J. Med. Chem. 38, 1309 - 1318
20. Myszka, D., Arulananthm, P., Sana, T., Wu, Z., Morton, T., and Ciardelli, T. (1996) Protein Sci. 5, 2468 - 2478
21. Koinstinen P., Wang C., Yang G. S., Wang Y. F., Williams D. E., Lyman S. D., Minden M. D., and McCulloch E. A. (1991) Leukemia 5, 704 - 711
22. Derossi D., Joliot, A. H., Chassaing, G., and Prochiantz, A. (1994) J. Biol. Chem. 269, 10444 - 10450
23. Chai, J., Du, C., Wu, J.-W., Kyin, S., Wang, X., and Shi, Y. (2000) Nature 406, 855 - 862
24. Hegde, R., Srinivasula, S., Zhang, Z., Wassell, R., Mukattash, R., Cilenti, L., DuBois, G., Lazebnik, Y., Zervos, A., Fernandes-Alnemri, T., and Alnemri, E. (2002) J. Biol. Chem. 277, 432 - 435
25. Huang, Y., Park, Y. C., Rich, R. L., Segal, D., Myszka, D. G., and Wu, H. (2001) Cell 104, 781 - 790
26. Chai , J., Shiozaki, E., Srinivasula, S. M., Wu, Q., Dataa, P., Alnemri, E. S., and Shi, Y. (2001) Cell 104, 769 - 780
27. Stennicke H. R., Ryan C. A., and Salvesen, G. S. (2002) Trends Biochem. Sci. 27, 94 - 101
28. Tamm, I., Kornblau, S. M., Segall, H., Krajewski, S., Welsh, K., Scudiero, D. A., Tudor, G., Myers, T., Qui, Y. H., Monks, A., Sausville, E., Andreeff, M., and Reed, J. C. (2000) Clin. Cancer Res. 6, 1796 - 1803

6. Rápido análisis de ligandos que interaccionan selectivamente

Resumen

Muchas de las terapias dirigidas se basan en la diversidad molecular de la superficie celular. La caracterización de las moléculas de superficie de los distintos tipos celulares es de gran ayuda para el diseño de terapias dirigidas. Los intentos previos para estudiar esta diversidad usando genotecas fágicas han resultado dificultosos, debido principalmente a que los fagos se han incubado en células en suspensión o en cultivos monocapa. En estas condiciones los lavados de los bacteriófagos unidos inespecíficamente producen la pérdida de la mayor parte de los ligandos específicos.

Con el propósito de mejorar las técnicas actuales de caracterización de moléculas de superficie basadas en la selección de ligandos celulares específicos hemos desarrollado una nueva metodología que nos permite aislar ligandos de una manera más eficiente tanto evitando la pérdida de potenciales ligandos como incrementando la selección de aquellos que tienen baja afinidad. Esta nueva técnica se basa en la distinta solubilidad que presenta el fago unido a las células respecto al fago libre. Para ello, se resuspenden las células de interés en medio con BSA (albúmina sérica bovina) y se incuban con la genoteca bacteriofágica. Este proceso se desarrolla a cuatro grados para minimizar las uniones posteriores o la internalización de los receptores. El conjunto se transfiere a una solución orgánica no-micelable, se somete a centrifugación e inmediatamente se introduce al nitrógeno líquido para que las fases orgánicas queden separadas. La parte inferior del tubo que contiene el precipitado celular y el fago unido a la superficie de las células, se corta y se transfiere a un nuevo tubo. El fago que no se ha unido a las células permanece soluble en la fase acuosa superior, debido a que la fase orgánica es hidrofóbica, y excluye los materiales solubles en agua. De esta forma con una simple centrifugación se evita una serie de múltiple lavados para descartar el fago que no se ha unido a la superficie celular.

Esta nueva tecnología se aplicó con el fin de aislar péptidos que se unieran a receptores de la superficie de las células endoteliales. Nuestro interés se centró en aislar de manera específica ligandos que reconocieran receptores de la célula endotelial una vez estimulada con el factor de crecimiento VEGF (*vascular endothelial growth factor*). Para ello en primer lugar se incubó una genoteca bacteriofágica con las células endoteliales no estimuladas y se recuperó la fase acuosa con el fago no unido a las células. De esta manera se descartan todos los fagos que se unen a receptores que se expresan de manera constitutiva. El fago recuperado en el paso anterior se añadió a un cultivo de células endoteliales estimuladas con el VEGF y se siguió el proceso de selección de bacteriófagos descrito anteriormente. Después de dos rondas adicionales de selección siguiendo el mismo proceso, se secuenciaron al azar los insertos de 34 clones de los cuales se escogieron 21 para comprobar que la unión era específica de las células endoteliales estimuladas con VEGF. Se encontró que estos clones tuvieron mayor especificidad de unión a las células endoteliales previamente estimuladas con VEGF que a aquellas que no lo habían sido.

El alineamiento de las secuencias peptídicas de los 34 clones seleccionados al azar mostraron que el 70% de ellos tenían motivos peptídicos presentes en la secuencia proteica de la familia del VEGF. Seleccionamos el péptido CPQPRPLC para su estudio y posterior caracterización ya que compartía una secuencia común con tres fagos aislados en el mismo *panning*. Se observó que este péptido se unía a dos miembros de la familia del VEGF receptor, el VEGFR1 (*VEGF receptor 1*) y el NRP-1 (*neuropilin-1*), siguiendo un patrón de reconocimiento similar al usado por VEGF-B. Así mismo $VEGF_{165}$ inhibía la unión del fago al receptor, confirmando los estudios previos que mostraban competición por la unión al receptor del $VEGF_{165}$ y el VEGF-B. La especificidad de la unión del fago al receptor se confirmó debido a que dicha unión era inhibida por el péptido sintético expresado en la secuencia bacteriofágica.

Nuestros resultados sugieren que el péptido CPQPRPLC mimetiza a la familia del VEGF-B e interacciona específicamente con el VEGFR-1 y NRP-1. Estos resultados muestran que esta nueva metodología puede ser de gran valor para aislar pares de ligandos-receptores en poblaciones

celulares. La diversidad de aplicaciones de este nuevo método para el uso en las células provenientes de pacientes abre las puertas a muchas aplicaciones clínicas, como podría ser la investigación de marcadores en células leucémicas o combinaciones con aspirados de tumores sólidos.

Biopanning and rapid analysis of selective interactive ligands

Here we introduce a new approach for the screening, selection and sorting of cell-surface–binding peptides from phage libraries. Biopanning and rapid analysis of selective interactive ligands (termed BRASIL) is based on differential centrifugation in which a cell suspension incubated with phage in an aqueous upper phase is centrifuged through a non-miscible organic lower phase. This single-step organic phase separation is faster, more sensitive and more specific than current methods that rely on washing steps or limiting dilution. As a proof-of-principle, we screened human endothelial cells stimulated with vascular endothelial growth factor (VEGF) and constructed a peptide-based ligand-receptor map of the VEGF family. Next, we validated the motif PQPRPL as a novel chimeric ligand mimic that binds specifically to VEGF receptor-1 and to neuropilin-1. BRASIL may prove itself a superior method for probing target cell surfaces with a broad range of potential applications.

Probing the molecular diversity of cell surfaces is required for the development of targeted therapies[1]. However, selections of phage libraries on cell surfaces are often challenging experiments. First, non-specific clones are recovered when phage libraries are incubated with cell suspensions or monolayers. Second, removal of background by repeated washes is both labor-intensive and inefficient. Third, cells and potential ligands are lost during the washing steps required.

To address these obstacles, we devised a method termed biopanning and rapid analysis of selective interactive ligands (BRASIL) from an assay described to measure receptor binding of specific yet low-affinity ligands[2–5]. BRASIL allows separation of phage-cell complexes from the remaining unbound phage; this is accomplished by a differential centrifugation that drives the cells from a hydrophilic environment into a non-miscible organic phase. Because the organic phase is hydrophobic, it excludes water-soluble materials surrounding cell surfaces. Bound phage are recovered from the cell pellet whereas the unbound phage remain soluble in the upper aqueous phase, eliminating the need for repeated washes. As a single centrifugation step is required, BRASIL is simpler and more convenient than current cell-panning techniques. Mapping ligand-receptors by BRASIL may allow an understanding of binding requirements for receptor families and enable peptide isolation for cell-targeting applications.

Cell binding to a defined test phage ligand

We set out to study cell binding by using BRASIL to test an established ligand-receptor pair. Experiments were designed using RGD-4C phage (displaying the motif ACDCRGDCFCG, termed RGD-4C peptide), which is a specific ligand for α_v integrins [6–8]. We reasoned that cell-surface–bound phage could be specifically carried through an organic phase and recovered by infection of the host bacteria. α_v integrin-expressing Kaposi's sarcoma cells (KS1767) were detached, incubated on ice with RGD-4C phage or control insertless phage (termed fd-tet), and the mixture was separated by differential centrifugation through the organic phase. The number of phage transducing units (TU) recovered from the cell pellets is shown in Fig. 1 a. Phage recovery correlated directly with increasing phage input and the recovery ratio (phage output from organic lower layer/phage input from aqueous upper layer) decreased with host bacteria saturation (Fig. 1 a). Under non-saturating conditions, the ratio of specific (RGD-4C) phage to control (fd-tet) phage (termed 'enrichment') ranged from 100 to 500. We show that the binding of RGD-4C phage to KS1767 cells is specific because such cell-phage binding is inhibited by the corresponding synthetic RGD-4C peptide in a dose-dependent manner; negative control peptides GRGESP (Fig. 1 b) or CARAC (data not shown) at the same molar concentrations had no inhibitory effect. No phage were present at the bottom of the tube or in the organic phase in the absence of KS1767 cells (data not shown). Next, we compared BRASIL with conventional cell-panning strategies that require washing steps. The number of RGD-4C phage recovered by BRASIL was significantly higher (t-test, $P < 0.01$) than the number of the same phage recovered when a conventional phage-cell binding strategy involving washing was used (Fig. 1c). Conversely, significantly lower background (t-test, $P < 0.01$) with the negative control phage was observed (Fig. 1 c). Given the significant increase in recovery of specific phage and the substantial decrease in background, the overall accuracy (cell-specific phage recovery) improved consistently by more than one order of magnitude when BRASIL was used relative to conventional cell-panning methods.

Screening VEGF-stimulated ECs

Once the method was optimized with a well-defined ligand-receptor pair, we tested whether BRASIL could also be used to screen phage display random peptide libraries on cells; endothelial cells (ECs) stimulated with vascular endothelial growth factor (VEGF) were used. We designed a two-step panning strategy to isolate phage that bind to angiogenic ECs. First, to decrease non-specific binding, we pre-cleared the phage library on starved ECs (before panning on the same cell line stimulated with recombinant $VEGF_{165}$); starved human umbilical vein ECs (HUVECs) were incubated with the phage library and centrifuged through the organic phase (Fig. 2 a). Second, the unbound phage pool left in the aqueous phase was transferred to a fresh tube and incubated with $VEGF_{165}$ -stimulated HUVECs. After centrifugation through the organic phase, phage bound to the $VEGF_{165}$-stimulated HUVEC pellet were recovered by bacterial infection, amplified and subjected to two more rounds of selection (Fig. 2 a).

Analysis of phage-displayed peptides

To test the selection method, we compared 21 phage clones randomly chosen for binding to starved HUVECs and to VEGF-stimulated HUVECs. Fourteen out of 21 clones (67%) had a greater than 150% enhancement (range, 1.5–8.7-fold; median, 2.2-fold)

in the ratio of cell binding upon VEGF stimulation normalized to control insertless phage (data not shown). Sequence alignment analysis of 34 clones randomly chosen from the selected phage revealed that 24 clones (70%) of the phage recovered by BRASIL had peptide motifs that could be mapped to sequences present in VEGF family members (Table 1).

Next, we chose the CPQPRPLC phage and CNIRRQGC phage (a representative phage out of three different clones displaying the motif IRR$^{E}/_{Q}$) for in vitro phage binding assay on VEGF receptor-1 (VEGFR-1). The receptor was immobilized on a microtiter well-plate and incubated with CPQPRPLC phage, CNIRRQGC phage or fd-tet as a negative control. Both CPQPRPLC and CNIRRQGC phage bound to VEGFR-1 (Fig. 2 b). The CPQPRPLC phage bound best with an average of over 1,000-fold enrichment observed over each of the controls used: CPQPRPLC phage binding to VEGFR-1 over bovine serum albumin (BSA) and CPQPRPLC phage over fd-tet phage binding to VEGFR-1 (Fig. 2 b).

The CPQPRPLC sequence matched motifs found within the VEGF-B isoforms (Fig. 2 c). VEGF-B has two mRNA splice variants generated by the use of different, but overlapping, reading frames of exon 6 (isoforms 167 and 186), which diverge in sequence in their C termini[9]. The pentapeptide motif PRPLC is found in the recombinant human VEGF B 167 (VEGF-B$_{167}$) C terminus region encoded by exon 6B, starting at the second residue after the boundary between exons 5 and 6B. PRPLC is a neuropilin-1 (NRP-1) binding domain [10]. On the other hand, the tetrapeptide motif PQPR—which overlaps with PRPLC and also with the phage-displayed CPQPRPLC peptide—is found in the C terminal of recombinant human VEGF B 186 (VEGF-B$_{186}$), and encoded by exon 6A. PQPR is embedded within a 12-residue known NRP-1 binding site[10]. The motif IRR $^{E}/_{Q}$ also showed ho-

Table 1

Alignment of peptide sequences isolated by BRASIL and VEGF family members

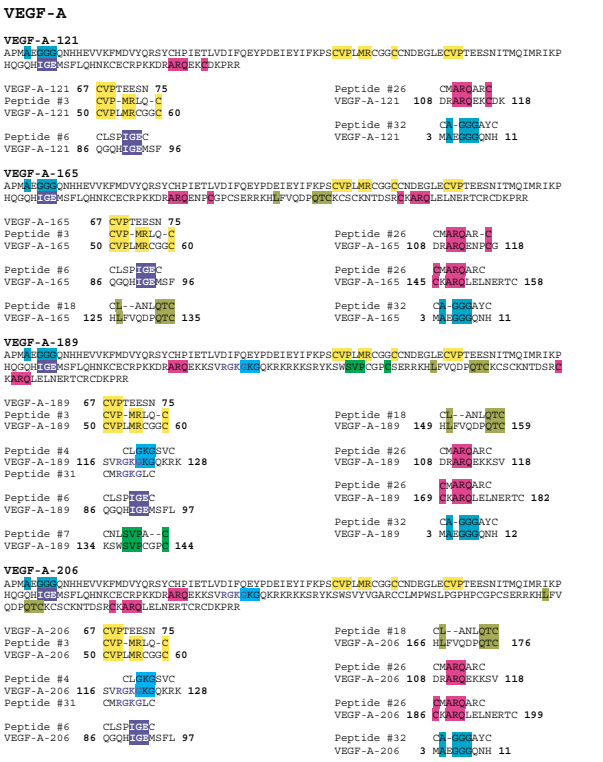

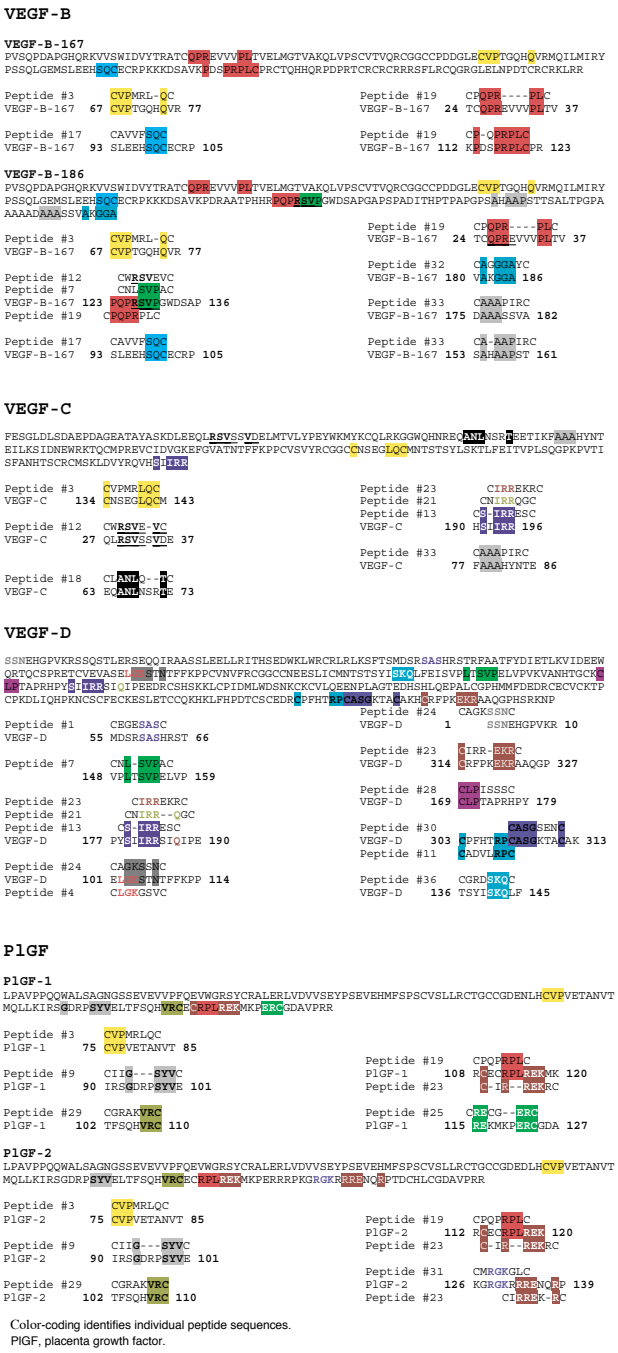

Color-coding identifies individual peptide sequences.
PlGF, placenta growth factor.

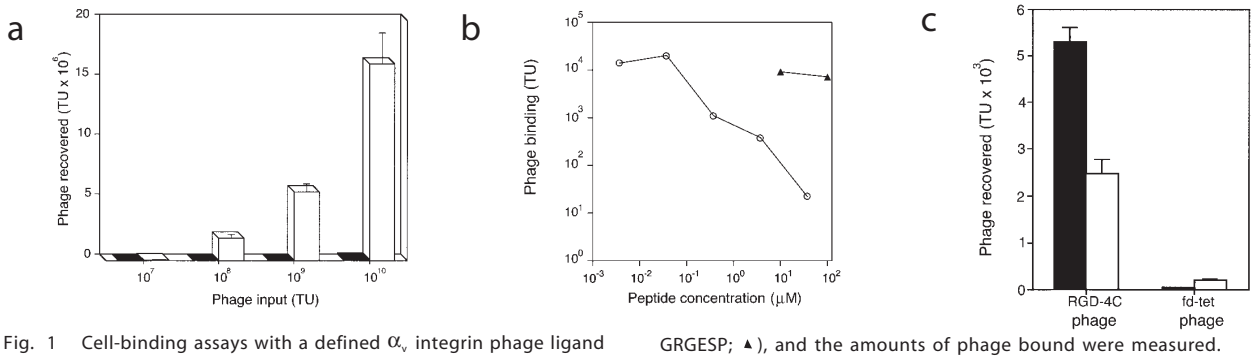

Fig. 1 Cell-binding assays with a defined α_v integrin phage ligand and phage-cell –binding optimization with BRASIL. a, Amounts of RGD-4C phage (□) and insertless control phage (fd-tet; ■) bound to KS1767cells at increasing phage inputs were compared. b, Specific inhibition of phage binding by the cognate synthetic peptide. RGD-4C phage were incubated with KS1767 cells in the presence of increasing concentrations of RGD-4C peptide (○) or a control peptide (sequence GRGESP; ▲), and the amounts of phage bound were measured. Comparison between conventional panning methods and BRASIL (■) RGD-4C or control phage were incubated with KS1767 cells. Bound phage were assayed by passing through the organic phase or by washing the cells 3 times with PBS/0.1% BSA (□). The experiments were performed 3 times with similar results. Bars represent mean ± s.e.m. from triplicates.

mology to VEGF family members (Table 1) but it was not studied further here.

CPQPRPLC is a chimeric VEGF mimic

We evaluated the binding of phage displaying the peptide CPQPRPLC to a panel of VEGF receptors (Fig. 3 a). CPQPRPLC bound to VEGFR-1 and to NRP-1, but not to VEGF receptor-2 (VEGFR-2) or to neuropilin-2 (NRP-2); this pattern is the receptor recognition profile of VEGF-B (ref. 9). CPQPRPLC phage binding to VEGFR-1 and to NRP-1 was inhibited by pre-incubation with $VEGF_{165}$ (Fig. 3 b) but not with platelet-derived growth factor-(PDGF-BB; data not shown). These results are consistent with the fact that $VEGF_{165}$ and VEGF-B isoforms compete for binding to VEGFR-1 (ref. 9) and suggest that CPQPRPLC and $VEGF_{165}$ might recognize closely related or overlapping binding sites. Finally, binding of CPQPRPLC phage to the immobilized VEGFR-1 and NRP-1 was specific because it could be inhibited by the corresponding synthetic peptides in a concentration-dependent manner (Fig. 3 c and d). These data show that 1) CPQPRPLC is a chimeric VEGF-B-family mimic, and 2) this peptide interacts specifically with VEGFR-1 and NRP-1.

Discussion

Our results show that organic phase separation is an efficient and convenient method for phage selection. On side-by-side comparison to current protocols, BRASIL was more sensitive and more

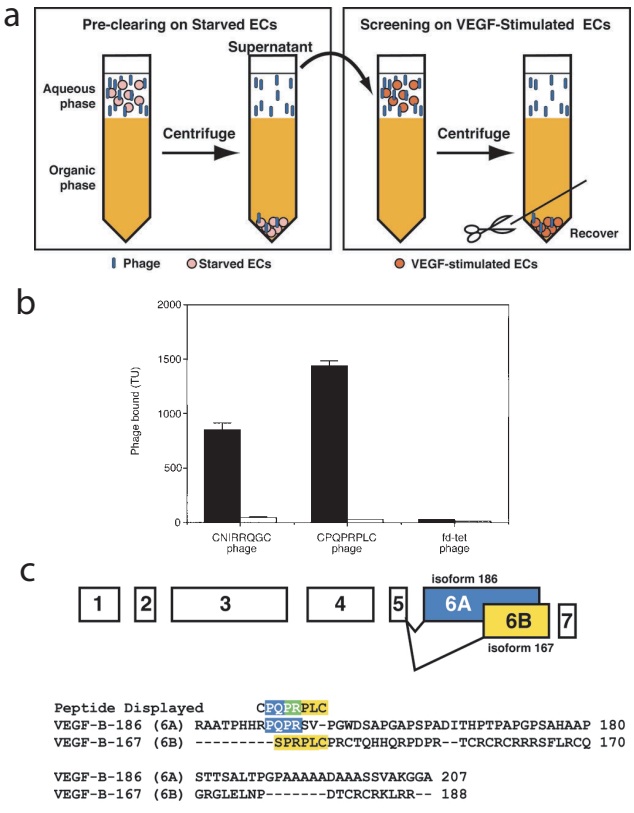

Fig. 2 Screening $VEGF_{165}$-stimulated HUVECs by BRASIL. a, Panning strategy to isolate phage that bind to activated ECs. Starved HUVECs were incubated with the peptide phage library, and the cells were separated by centrifugation through the organic phase. The supernatant containing the unbound phage was transferred to $VEGF_{165}$-stimulated HUVECs and after incubation, cells and bound phage were separated by centrifugation through the organic phase. The cell-bound phage in the pellet were rescued by infection, amplified and used for another round of biopanning. b, Binding of the selected phage clones (CPQPRPLC, CNIRRQGC, and control) to the immobilized VEGFR-1 (■) compared with binding to BSA (□). VEGFR-1 was used to coat the microtiter plate. The individual wells were then incubated with equal amounts of each individual phage. Bars represent mean ± s.e.m. from duplicate wells. c, Homology analysis of the CPQPRPLC sequence. Exon organization of the two VEGF-B isoforms (modified from ref. 9) is shown. Sequences of exon 6A of $VEGF\text{-}B_{186}$ and of exon 6B of $VEGF\text{-}B_{167}$ are compared with the sequence of the phage display-selected peptide. Overlapping motif sequences are shown in colors corresponding to the respective exons of origin (exon 6A, blue; exon 6B, yellow): CPQPRPLC is a chimera between the motifs PQPR ($VEGF\text{-}B_{186}$, residues 145–148) and PRPLC ($VEGF\text{-}B_{167}$, residues 138 –142).

Methods

Reagents. A phage display random peptide library based on the vector fUSE5 (ref. 15) displaying the insert CX_6C (C, cysteine; X, any amino-acid residue) was constructed with a size between 1×10^6 and 1×10^7, as described[16]. Human $VEGF_{165}$ (Pharmingen, San Jose, California), human VEGFR-1 (Oncogene Research Products, Boston, Massachusetts), rat NRP-1/Fc, rat NRP-2/Fc, VEGFR-2/Fc (all 3 receptor domains fused to the Fc region of human IgG_1), PDGF-BB, anti-VEGFR-1 (polyclonal anti-Flt1), and anti-human VEGF polyclonal antibody (R&D Systems, Minneapolis, Minnesota), dibutyl phthalate, cyclohexane (Sigma-Aldrich) and synthetic peptides (AnaSpec, San Diego, California) were obtained commercially. HUVECs and KS1767 cells were described [6–8,12].

BRASIL optimization. Cells were collected with PBS and 5 mM EDTA, washed with MEM, and re-suspended in MEM containing 1% BSA at 1×10^6 cells per ml and incubated with phage within 1.5-ml Eppendorf tubes. To minimize post-binding events such as receptor-mediated internalization, cells and media were kept on ice unless otherwise stated. After 4 h, 100 µl of the cell-phage suspension was gently transferred to the top of a non-miscible organic lower phase (200 µl in a 400 µl-Eppendorf tube) and centrifuged at 10,000 g for 10 min. The most suitable organic phase combination was dibutyl phthalate:cyclohexane (9:1 [v:v]; d = 1.03 g ml $^{-1}$) but other phthalate combinations with the appropriate density (dibutyl phthalate:diisooctyl phthalate; 4:6 [v:v]) were used with similar results. The tube was snap frozen in liquid nitrogen, the bottom of the tube sliced off, and the cell-phage pellet transferred to a new tube; this optional freeze-cut technique prevents cross-contamination with the phage remaining in the aqueous phase. As part of the method optimization, we have tested the effects of the organic phase and of the optional freeze-thaw phase on phage infectivity. Increasing amounts of phage (ranging from $1 \times 10^3 - 1 \times 10^9$) were incubated in 100 µl of bacterial culture phase plus organic phase admixture (varying from 0% to up to 20% v:v bacterial culture). After 15 min, bound phage were amplified by the addition of 100 µl of Eschericia coli K91kan at log-phase. The genes inducing tetracycline resistance in the host bacteria were induced by adding low tetracycline concentrations[12,15,16], infection and proceeded for 1 h. The triplicates were plated at multiple dilutions, and the number of colonies counted after an overnight incubation of the plates at 37 °C. No significant differences in the phage infection ratios were observed under the conditions tested. We also compared phage recovery with or without the snap-freeze step under each of the conditions. No substantial decrease was noted in the amounts of test phage recovered (data not shown). These data suggest that limited exposure to the organic mixture and a brief freeze-thaw had no measurable adverse affects on the infection of bacteria and recovery of phage. However, because decreases in phage infectivity with other phage-peptide libraries might occur under these conditions, we advise that these results should not be extrapolated without testing. Bound phage were rescued by infection with 200µl of E. coli K91kan host bacteria in log phase [12,15,16]. To evaluate binding specificity, phage and cells were incubated with the cognate or control synthetic peptides for competition assays.

Binding assays with phage clones. KS1767 cells were detached with cold EDTA and re-suspended in MEM containing 1% BSA. αv integrin-binding RGD-4C phage were used as defined ligands. The cell suspension was incubated with RGD-4C phage or a control phage with no peptide insert (fd-tet phage). Increasing amounts of either phage were added to the cells in suspension and the cell –phage admixture was then incubated for 4 h on ice. Cells were then separated by centrifugation through the organic phase. Bound phage were recovered and colonies were counted. To compare BRASIL to conventional methods that require an additional washing step, 200 µl of the cell suspension were incubated with phage for 4 h on ice. Then, unbound phage from 100- µl aliquots were removed either by centrifuging over the organic phase or by washing the cells 3 times with 1 ml PBS containing 0.3% BSA. Competitive inhibition was evaluated by comparing synthetic RGD-4C and control peptides (CARAC or GRGESP) at the same molar ratios.

Screening assays with phage libraries. HUVECs at 80% confluence cultured in endothelial basal medium (EBM-2; Clonetics, San Diego, California) without supplements for 24 h were defined as 'starved HUVECs'. The medium was then replaced by EBM-2 supplemented with 20 ng ml $^{-1}$ $VEGF_{165}$, and the cells, cultured under these conditions for another 18 h, were defined as "VEGF-stimulated HUVECs". Cells were collected with ice-cold PBS and 5 mM EDTA, washed once with EBM-2 plus 1% BSA, and re-suspended in the same medium at 1×10^7 cells per ml. In the pre-clearing step, 1×10^6 starved HUVECs were incubated with 1×10^9 transducing units (TU) of unselected library for 2 h on ice; the mixture was then centrifuged through the organic phase. In a screening step, the unbound phage remaining in the aqueous upper phase (supernatant) was transferred to a fresh tube and incubated with 1×10^6 VEGF-stimulated HUVECs. After 4 h on ice, the cell-phage complexes were separated by centrifugation through the organic lower phase. Phage were recovered from the pellet by infection of log phase E. coli K91kan [12,15,16].

Binding assays on purified receptors. VEGFR-1, VEGFR-2, NRP-1 and NRP-2 (at 1 µg in 50 µl PBS) were immobilized on microtiter wells overnight at 4 °C. Wells were washed twice with PBS, blocked with PBS/3% BSA for 2 h at room temperature, and incubated with 1×10^9 TU of CPQPRPLC phage, CNIRRQGC phage or fd-tet phage in 50 µl of PBS/1.5% BSA. After 1 h at room temperature, wells were washed 9 times with PBS and phage were recovered by bacterial infection. Serial dilutions were plated onto Luria –Bertani (LB) medium supplemented with tetracycline [12,15,16]. $VEGF_{165}$, PDGF-BB or synthetic peptides were used to evaluate competitive inhibition of phage binding. ELISA with polyclonal anti –VEGFR-1 serum or anti-human IgG (VEGFR-2, NRP-1 and NRP-2) confirmed the presence and concentration of the receptors on the wells. To show that the VEGF receptors were functionally active, $VEGF_{165}$ (50 ng ml $^{-1}$) was incubated with the immobilized receptors for 2 h at room temperature; following three washes, $VEGF_{165}$ binding was evaluated by ELISA by using VEGF-specific antibodies (data not shown).

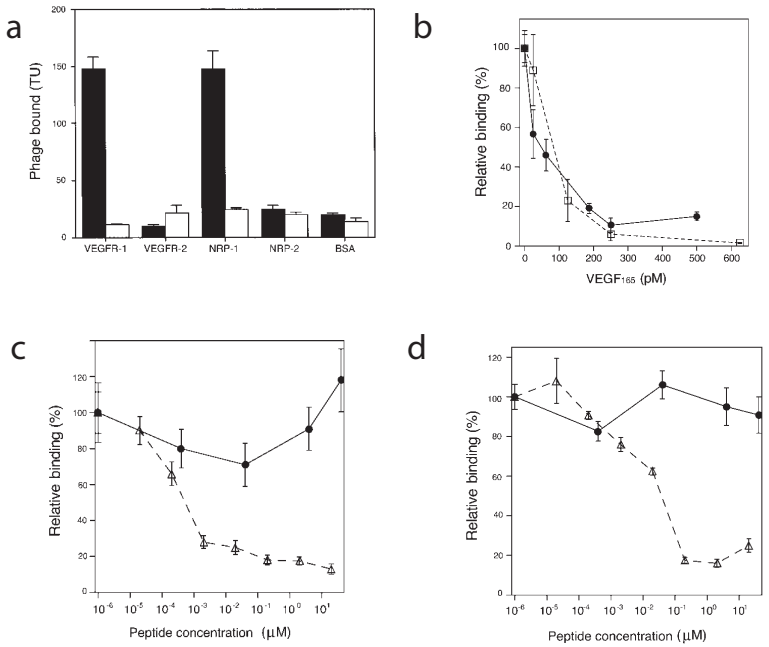

Fig. 3 Binding of the CPQPRPLC peptide to immobilized VEGF receptors. Recombinant VEGFR-1 and -2 and NRP-1 and -2 were used to coat microtiter plates. CPQPRPLC or control phage were added to the wells. a, Binding of CPQPRPLC phage (■) and control phage (□) to the immobilized receptors. b, Inhibitory effect of VEGF $_{165}$ on the binding of CPQPRPLC phage to VEGF receptors. CPQPRPLC phage were incubated with the immobilized VEGFR-1 (●) or NRP-1 (□) in the absence or presence of VEGF $_{165}$ (0–600 pM). No binding inhibition was observed by using PDGF-BB (up to 8 nM) as a negative control (data not shown). c and d, The binding of CPQPRPLC phage to VEGFR-1 (□ c) and NRP-1 (d) is specific. The cognate peptide CPQPRPLC (△), but not a control peptide (●) inhibits phage binding to the immobilized receptor. Phage were incubated in the presence of increasing amounts of the synthetic CPQPRPLC peptide or of the negative control peptide CARAC. A specific, dose-dependent inhibition is noted. The experiments were performed 3 times with similar results. Shown are mean ± s.e.m. from triplicate wells.

specific than techniques that rely on washing or limiting dilution steps to eliminate background during successive rounds of selection. BRASIL may represent an improvement over conventional cell-panning methods.

Because of our interest in targeting vascular endothelium [6–8,11,12], we screened a phage-display random peptide library on VEGF $_{165}$-stimulated ECs. We identified a VEGF-receptor ligand with the sequence CPQPRPLC that resembles the motif PRPLC (an NRP-1 binding site found in VEGF-B $_{167}$) and the overlapping motif PQPR (found embedded within a 12-residue NRP-1-binding epitope of VEGF-B $_{186}$; ref. 10). Thus, the motif PQPRPL appears to be a chimera between overlapping binding sites on different VEGF-B isoforms. Binding assays using individual phage on a panel of purified targets confirmed that the CPQPRPLC phage interacts specifically with VEGF receptors in a pattern consistent with VEGF-B-type ligands [9]. These results suggest that the C terminal regions of both VEGF-B isoforms bind to VEGFR-1 and NRP-1 and are in agreement with recent results of deletion and site-directed mutagenesis studies of VEGF-B isoforms [10]. Further mutational experiments are needed to confirm the VEGF-B receptors that are recognized by the motifs PRPLC and PQPR individually. Also of importance is the observed difference in the ability of the synthetic peptide CPQPRPLC to block phage binding to VEGF receptors. Our results suggest that the CPQPRPLC peptide is approximately 100-fold more efficient in blocking phage binding to VEGFR-1 than to NRP-1. It is tempting to speculate that our chimeric motif interacts with VEGF receptors differentially; if so, this may be due to differences in the number of peptide-binding sites on each receptor, or in the affinity of the interaction at each binding site. Alternatively, such ligand-receptor interactions may be dependent on the conditions used for the binding assay. Full understanding of binding mechanisms awaits elucidation of the X-ray crystal structures of VEGFR-1– or NRP-1–CPQPRPLC peptide complexes. Although one can not as yet assert that BRASIL will be well suited for any cell-selection application, our data show that vascular targets[13] can clearly be found in EC membranes.

We also compared BRASIL and conventional cell-panning methods side-by-side to test the specific binding of the recently identified β_2 integrin-antagonist peptide CPCFLLGCC containing the motif Leu-Leu-Gly (ref. 14). BRASIL was again consistently and reproducibly superior when selection was performed on β_2 integrin-expressing cells (unpublished observations). We are adapting the method for use with phage displaying larger polypeptides or folded proteins such as enzymes or antibodies (J.L., W.A. and R.P., unpublished data).

Importantly, BRASIL is also of value for targeting and isolating ligand–receptor pairs in cell populations derived from clinical samples. The method may be used in tandem with fine-needle aspirates of solid tumors or fluorescence-activated cell sorting of leukemic cells obtained from patients. Moreover, because multiple samples and several rounds of pre-clearing and selection can be performed in a few hours with minimal loss, automation for high-throughput screening, and clinical applications are likely to follow.

Acknowledgments

This work was supported by the NIH (CA90270 and CA8297601 to RP; CA90270 and CA9081001 to W.A.) and by a Gillson-Longenbaugh Foundation Award (to R.P. and W.A.). R.J.G. was supported by FAPESP (Brazil), M.C.V. by the Department of Defense and J.L. by the Susan G. Komen Breast Cancer Foundation.

1. Brown, K.C. New approaches for cell-specific targeting: Identification of cell-selective peptides from combinatorial libraries. Curr. Opin. Chem. Biol. 4, 16 –21 (2000).
2. Hatzfeld, J.A., Hatzfeld, A. & Maigne, J. Fibrinogen and its fragment D stimulate proliferation of human hemopoietic cells in vitro. Proc. Natl. Acad. Sci. USA 79, 6280 –6284 (1982).
3. Ouaissi, M.A., Afchain, D., Capron, A. & Grimaud, J.A. Fibronectin receptors on Trypanosoma cruzi trypomastigotes and their biological function. Nature 308, 380 –382 (1984).
4. Levesque, J.P., Hatzfeld, A. & Hatzfeld, J. A method to measure receptor binding of ligands with low affinity. Application to plasma proteins binding assay with hemopoietic cells. Exp. Cell Res. 156, 558 –562 (1985).
5. Giordano, R., Chammas, R., Veiga, S.S., Colli, W. & Alves, M.J. An acidic component of the heterogeneous Tc-85 protein family from the surface of Trypanosoma cruzi is a laminin binding glycoprotein. Mol. Biochem. Parasitol. 65, 85 –94 (1994).
6. Pasqualini, R., Koivunen, E. & Ruoslahti, E. αv integrins as receptors for tumor targeting by circulating ligands. Nature Biotechnol. 15, 542 –546 (1997).
7. Arap, W., Pasqualini, R. & Ruoslahti, E. Cancer treatment by targeted drug delivery to tumor vasculature in a mouse model. Science 279, 377 –380 (1998).
8. Ellerby, H.M. et al. Anti-cancer activity of targeted pro-apoptotic peptides. Nature Med. 5, 1032 –1038 (1999).
9. Olofsson, B., Jeltsch, M., Eriksson, U. & Alitalo, K. Current biology of VEGF-B and VEGF-C. Curr. Opin. Biotechnol. 10, 528 –535 (1999).
10. Makinen, T. et al. Differential binding of vascular endothelial growth factor B splice and proteolytic isoforms to neuropilin-1. J. Biol. Chem. 274, 21217 –21222 (1999).
11. Kolonin, M., Pasqualini, R. & Arap, W. Molecular addresses in blood vessels as targets for therapy. Curr. Opin. Chem. Biol. 5, 308 –313 (2001).
12. Pasqualini, R., Arap, W., Rajotte, D. & Ruoslahti, E. In vivo selection of phage-display libraries. in Phage Display: A Laboratory Manual (eds. Barbas, C.F., III, Burton, D.R., Scott, J.K. & Silverman, G.J.) 1 –24 (Cold Spring Harbor Laboratory Press, New York, 2000).
13. Soker, S., Takashima, S., Miao, H.Q., Neufeld, G. & Klagsbrun, M. Neuropilin-1 is expressed by endothelial and tumor cells as an isoform-specific receptor for vascular endothelial growth factor. Cell 92, 735 –745 (1998).
14. Koivunen, E. et al. Inhibition of β_2 integrin-mediated leukocyte cell adhesion by leucine-leucine-glycine motif-containing peptides. J. Cell Biol. 153, 1 –13 (2001).
15. Smith, G.P. & Scott, J.K. Libraries of peptides and proteins displayed on filamentous phage. Methods Enzymol. 217, 228 –257 (1993).
16. Koivunen, E. et al. Integrin-binding peptides from phage display peptide libraries. Integrin Protocols. Methods Mol. Biol. 129, 3 –17 (1999).

7. Mapeo de la vasculatura humana mediante phage display

Resumen

La diversidad molecular de los vasos sanguíneos aún esta casi totalmente por descubrir. Anteriormente la técnica del *phage display in vivo* se ha aplicado para seleccionar péptidos que reconocen específicamente los vasos sanguíneos de los ratones. Estos péptidos se han usado como portadores para dirigir drogas citotóxicas, péptidos proapoptóticos, inhibidores de metaloproteasas, genes, citocinas, etc. Ciertos ligandos y receptores aislados en los ratones se han utilizado para identificar los posibles homólogos humanos. Sin embargo, debido a la mayor heterogeneidad y complejidad de los genes humanos es muy poco probable que se puedan administrar drogas de manera dirigida mediante péptidos aislados en los ratones.

Con el objetivo de analizar la diversidad de la vasculatura humana hemos desarrollado un método de selección de péptidos *in vivo* utilizando el método del *phage display*. Para ello se administró una genoteca séptica por via intravenosa a un paciente terminal. Al dejar circular libremente dicha genoteca peptídica durante 15 minutos se facilitó la llegada de los bacteriófagos a la vasculatura de todos los tejidos. Inmediatamente se efectuaron biopsias en los distintos órganos, por un lado para los estudios histopatológicos y por el otro para recuperar los bacteriófagos.

Los insertos de DNA de los fagos seleccionados se secuenciaron y se tradujeron a las correspondientes secuencias peptidicas. Para estudiar la distribución de los insertos de la genoteca peptídica desarrollamos un programa informático que facilitara el análisis de las secuencias cortas de amino ácidos. Este programa analiza la frecuencia relativa con la que todas las posibles combinaciones de tripéptidos se recuperan de cada órgano analizado. Para determinar la distribución de los insertos peptídicos que se habían unido a un tipo específico de vasculatura de cada tejido comparamos la frecuencia relativa con la que cada motivo tripeptídico aparecía en cada órgano estudiado con las frecuencias correspondientes de una genoteca no seleccionada. Los resultados obtenidos mostraron que la distribución de las secuencias peptídicas en los tejidos no es al azar sino que algunos grupos de péptidos aparecían con mayor frecuencia en distintos órganos.

Los motivos peptídicos más repetidos para cada órgano fueron introducidos en una base de datos Blast para comprobar su homología con las proteínas conocidas. Una de las secuencias peptídicas encontradas en la próstata tenía homología con a la interlecina 11 (IL-11), una citocina cuya interacción con el endotelio y el epitelio de la próstata se había descrito previamente. Para demostrar la especificidad de la unión a la próstata de dicho péptido, hicimos experimentos de bacteriófago-*overlay* en secciones tisulares. Los resultados obtenidos demostraron que el fago que portaba la secuencia aminoacídica RRAGGS, que mimetiza la IL-11, se unía específicamente al endotelio y al epitelio de la próstata humana, pero no al órgano control. Además, cuando se utilizó un fago que expresaba una secuencia peptídica al azar no hubo ningún tipo de unión a las secciones tisulares de la próstata.

Para confirmar la unión ligando-receptor usamos ensayos de unión *in vitro* con los que demostramos la interacción del bacteriófago que expresa la secuencia CGRRAGGSC con el receptor de la IL-11 (IL-11Rα). La especificidad se vio también confirmada cuando esta unión entre el péptido y la IL-11Rα fue inhibida por el ligando (IL-11) proporcionalmente a la concentración utilizada.

Nuestros resultados para validar el método mostraron que al menos algunos de los conjuntos ligando-receptor son detectables en múltiples sujetos no relacionados entre si. Además, podemos destacar que este método permite la selección de péptidos específicos que se unen a los receptores que son expresados *in vivo*. Esta selección de péptidos *in vivo* podría ser de gran utilidad para aplicaciones clínicas.

Steps toward mapping the human vasculature by phage display

The molecular diversity of receptors in human blood vessels remains largely unexplored. We developed a selection method in which peptides that home to specific vascular beds are identified after administration of a peptide library. Here we report the first in vivo screening of a peptide library in a patient. We surveyed 47,160 motifs that localized to different organs. This large-scale screening indicates that the tissue distribution of circulating peptides is nonrandom. High-throughput analysis of the motifs revealed similarities to ligands for differentially expressed cell-surface proteins, and a candidate ligand–receptor pair was validated. These data represent a step toward the construction of a molecular map of human vasculature and may have broad implications for the development of targeted therapies.

Despite major progress brought about by the Human Genome Project [1,2], the molecular diversity of blood vessels has just begun to be uncovered. Many therapeutic targets may be expressed in very restricted but highly specific and accessible locations in the vascular endothelium. Thus potential targets for intervention may be overlooked in high-throughput DNA sequencing or in gene arrays because these approaches do not generally take into account cellular location and anatomical and functional context.

We developed an in vivo selection method in which peptides that home to specific vascular beds are selected after intravenous administration of a phage-display random peptide library [3]. This strategy revealed a vascular address system that allows tissue-specific targeting of normal blood vessels [4,5] and angiogenesis-related targeting of tumor blood vessels [6–10]. Although the biological basis for such vascular heterogeneity remains unknown, several peptides selected by homing to blood vessels in mouse models have been used by several groups as carriers to guide the delivery of cytotoxic drugs [9], pro-apoptotic peptides [6], metalloprotease inhibitors [7], cytokines [11], fluorophores [12] and genes [13]. Generally, coupling to homing peptides yields targeted compounds that are more effective and less toxic than the parental compound [6,9,11]. Moreover, vascular receptors corresponding to the selected peptides have been identified in blood vessels of normal organs [14] and in tumor blood vessels [15,16]. Together, these results show that it is possible to develop therapeutic strategies based on selective expression of vascular receptors [17].

Although certain ligands and receptors isolated in mouse models have been useful to identify putative human homologs [10,15], it is unlikely that targeted delivery will always be achieved in humans using mouse-derived probes. Data from the Human Genome Project indicate that the higher complexity of the human species relative to other mammalian species derives from expression patterns of proteins at different tissue sites, levels or times rather from a greater number of genes [1,2]. In fact, several examples of species-specific differences in gene expression within the human vascular network have recently surfaced. The divergence in the expression patterns of the prostate-specific membrane antigen (PSMA) between human and mouse illustrates such species specificity. Selective expression of PSMA occurs in the human prostate, but not in the mouse prostate; instead, the mouse homolog of PSMA is expressed in the brain and kidney [18]. Additionally, PSMA is a marker of endothelial cells of tumor blood vessels in humans [19], whereas the mouse homolog of PSMA is undetectable in tumor-associated neovasculature in the mouse (W.D. Heston, pers. comm.). Another example of such divergence is the TEM7 gene, which is highly expressed in a selective manner in the endothelium of human colorectal adenomas [20]. By contrast, mouse Tem7 is expressed not in tumor blood vessels but in Purkinje cells instead [21]. Thus, striking species-specific differences in protein expression and ligand–receptor accessibility dictates that vascular targeting data obtained in animal models must be carefully evaluated before extrapolating to human studies.

Screening phage-display libraries in humans

We reasoned that in vivo selection of phage-display random peptide libraries in humans would advance the identification of human vascular targeting probes and facilitate development of targeted delivery of therapeutic and imaging agents to the vasculature. This study reports the initial step toward developing an in vivo phage display–based, ligand–receptor map of human blood vessels.

A large-scale preparation of a phage random peptide library containing the insert CX_7C (C, cysteine; X, any amino-acid residue) and designed to display a constrained cyclic loop within the pIII capsid protein was optimized to create the highest possible insert diversity [3]. The diversity of the library was approximately 2×10^8 and its final titer was approximately 1×10^{12} transducing units (TU) per ml.

A patient (see Methods) received an intravenous infusion of the unselected random phage library, and 15 min after infusion tissue biopsies were obtained to provide histopathological diagnosis and to recover phage from various organs (Fig. 1 a).

Here we demonstrate the feasibility of producing phage-display random peptide libraries on a very large scale and of selecting phage clones that home to different human organs in vivo through the systemic circulation (Fig. 1 b).

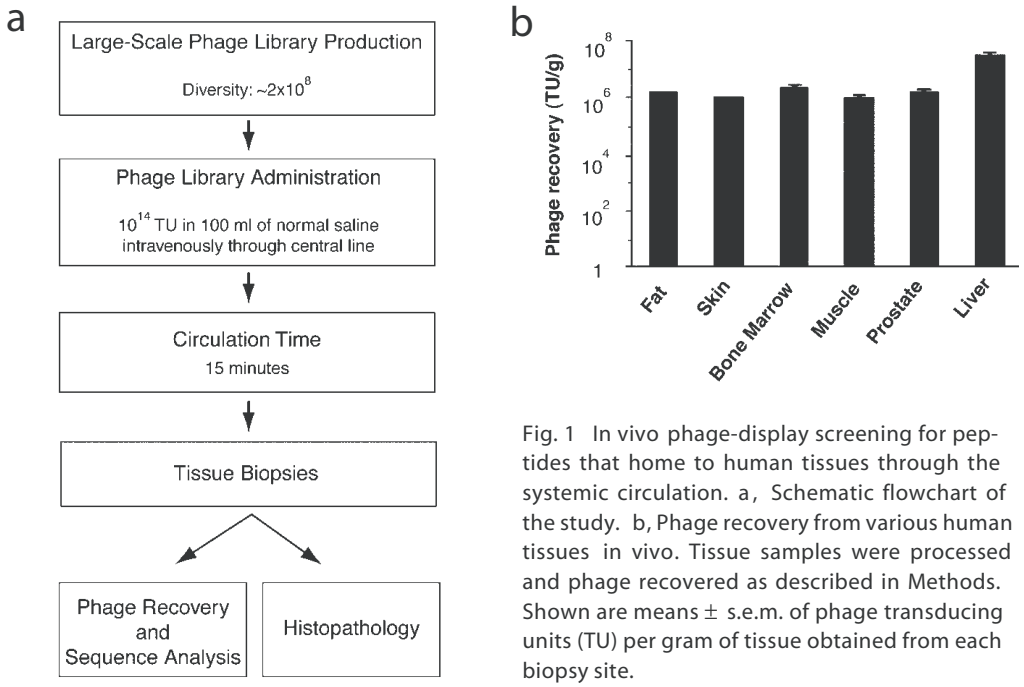

Fig. 1 In vivo phage-display screening for peptides that home to human tissues through the systemic circulation. a, Schematic flowchart of the study. b, Phage recovery from various human tissues in vivo. Tissue samples were processed and phage recovered as described in Methods. Shown are means ± s.e.m. of phage transducing units (TU) per gram of tissue obtained from each biopsy site.

High-throughput analysis of selected peptides

To analyze the distribution of inserts from the random peptide library, we designed a high-throughput pattern recognition software to analyze short amino-acid residue sequences. This automated program allowed surveillance of peptide inserts recovered from the phage library screening.

Based on SAS (version 8; SAS Institute) and Perl (version 5.0), the program conducts an exhaustive amino-acid residue sequence count and keeps track of the relative frequencies of n distinct tripeptide motifs representing all possible n_3 overlapping tripeptide motifs in both directions ($n << n_3$). This analysis was applied for phage recovered from each target tissue and for the unselected CX_7C random phage-display peptide library. Counts were recorded for all overlapping interior tripeptide motifs, subject only to reflection and single-voting restrictions. No peptide was allowed to contribute more than once for a single tripeptide motif (or a reversed tripeptide motif). Tripeptide motifs in both directions are chemically nonsymmetrical and not nessarily equivalent. However, because we often recovered forward and reverse tripeptides recognizing the same receptor by in vivo phage display, we chose to take reflection into account, with the understanding that this is not a general feature that is applicable to every ligand-receptor pair interaction. Each peptide contributed five tripeptide motifs being held fixed within a tissue. The significance of association of a given allocation of counts was assessed by the Fisher's exact test (one-tailed). Results were considered statistically significant at $P < 0.05$. In summary, to test for randomness of distribution, we compared the relative frequencies of a particular tripeptide motif from each target to those of the motifs from the unselected library; such an approach is intrinsically a large-scale contingency table association test.

Distribution of tripeptide motifs in vivo

To determine the distribution of the peptide inserts homing to specific sites after intravenous administration, we compared the relative frequencies of every tripeptide motif from each target tissue to those from the unselected library. We analyzed 4,716 phage inserts recovered from representative samples of five tissues (bone marrow, fat, skeletal muscle, prostate and skin) and from the unselected library. Tripeptide motifs were chosen for the phage insert analysis because three amino-acid residues seem to provide the minimal framework for structural formation and protein–protein interaction [22]. Examples of such biochemical recognition units and binding of ligand motifs to their receptors include RGD, LDV and LLG to integrins[23,24], NGR to aminopeptidase N/CD13 (refs 11,15) and GFE to membrane dipeptidase [4,14]. Each phage insert analyzed contained seven amino-acid residues and contributed five potential tripeptide motifs; thus, counting both peptide orientations, a total of 47,160 tripeptide motifs were surveyed.

Comparisons of the motif frequencies in a given organ relative to those frequencies in the unselected library demonstrate the nonrandom nature of the peptide distribution (Table 1); such a bias is particularly noteworthy given that only a single round of in vivo screening was performed. Of the tripeptide motifs selected from tissues, some were preferentially recovered in a single site whereas others were recovered from multiple sites. These data are consistent with some peptides homing in a tissue-specific manner and others targeting several tissues. We next adapted the ClustalW software from the European Molecular Biology Laboratory [25] to analyze the original cyclic phage peptide inserts of seven amino-acid residues containing the tripeptide motifs. This analysis revealed four to six amino-acid residue motifs that were shared among multiple peptides isolated from a given organ (Fig. 2). We searched for each of these motifs in online databases (through the National Center for Biotechnology Information

(NCBI; http://www.ncbi.nlm.nih.gov/BLAST/) and found that some appeared within known human proteins. Phage-display technology is suitable for targeting several classes of molecules (adhesion receptors, proteases, proteoglycans or growth factor receptors). Based on extensive work performed in murine models, the in vivo selection system seems to favor the isolation of peptides that recognize receptors that are selectively expressed in specific organs or tissues [17]. As our motifs are likely to represent sequences present in circulating ligands (either secreted proteins or surface receptors expressed on circulating cells) that home to vascular receptors, we compiled a panel of candidate human proteins potentially mimicked by selected peptide motifs (Table 2).

Validation of candidate ligands

It is tempting to speculate on a few biologically relevant homology hits. For example, a peptide contained within bone morphogenetic protein 3B (BMP-3B) was recovered from bone marrow. BMP-3B is a growth factor known to regulate bone development [26]. Thus, this protein may be mimicked by the isolated ligand homing to that tissue. We also isolated from the prostate a potential mimetope of interleukin 11 (IL-11), which has been previously shown to interact with receptors within endothelium and prostate epithelium [27,28]. In addition to secreted ligands, motifs were also found in several extracellular or transmembrane proteins that may operate selectively in the target tissue, such as sortilin in fat [29]. We have also recovered motifs from multiple organs; one such peptide is a candidate mimic peptide of perlecan, a protein known to maintain vascular homeostasis [30].

To test the tissue specificity of the peptides selected, we developed a phage-overlay assay for tissue sections Because of the availability and well-characterized interaction between the candidate ligand (IL-11) and its receptor (IL-11Rα), we chose the motif RRAGGS, a peptide mimic of IL-11 (Table 2), for validation. We show by phage overlay on human tissue sections (see Methods) that a prostate-homing phage displaying an IL-11 peptide mimic specifically bound to the endothelium and to the epithelium of normal prostate (Fig. 3 a), but not to control organs, such as skin (Fig. 3b). In contrast, a phage selected from the skin (displaying the motif HGGVG; Table 2), did not bind to prostate tissue (Fig. 3c); however, this phage specifically recognized blood vessels in the skin (Fig. 3 d). Moreover, the immunostaining pattern obtained with an antibody against human IL-11Rα on normal prostate tissue (Fig. 3 e) is undistinguishable from that of the CGRRAGGSC-displaying phage overlay (Fig. 3 a); a control antibody showed no staining in prostate tissue (Fig. 3 f). These findings were recapitulated in multiple tissue sections obtained from several different patients.

Finally, using a ligand–receptor binding assayin vitro, we demonstrate the interaction of the CGRRAGGSC-displaying phage with immobilized IL-11Rα at the protein–protein level (Fig. 4 a). Such binding is specific because it was inhibited by the native IL-11 ligand in a concentration-dependent manner (Fig. 4 b). Preliminary results indicate that serum IL-11 is elevated in a subset of prostate cancer patients (C.J.L., unpublished observations) and that the expression of IL-11Rα in tumors is upregulated in some cases of human prostate cancer (M.G.K., unpublished observations); these data may have clinical relevance.

Table 1 Peptide motifs isolated by in vivo phage display screening

Target organ and motif	Motif frequency (%)	P value
Unselected library		
None	NA	NA
Bone marrow		
GGG*	2.3	0.0350
GFS*	1.0	0.0350
LWS*	1.0	0.0453
ARL	1.0	0.0453
FGG	1.1	0.0453
GVL	2.3	0.0137
SGT	1.1	0.0244
Fat		
EGG*	1.3	0.0400
LLV*	1.0	0.0269
LSP*	0.9	0.0402
EGR	1.1	0.0180
FGV	0.9	0.0402
Muscle		
LVS*	2.1	0.0036
GER	0.9	0.0036
Prostate		
AGG*	2.5	0.0340
EGR	1.0	0.0340
GER	0.9	0.0382
GVL	2.3	0.0079
Skin		
GRR*	2.9	0.0047
GGH*	0.9	0.0341
GTV*	0.8	0.0497
ARL	0.8	0.0497
FGG	1.3	0.0076
FGV	1.0	0.0234
SGT	1.0	0.0234

Peptide motifs isolated by in vivo phage display screening. Motifs occurring in peptides isolated from target organs but not from the unselected phage library (Fisher's exact test, one-tailed; $P < 0.05$). Number of peptide sequences analyzed per organ: unselected library, 446; bone marrow, 521; fat, 901; muscle, 850; prostate, 1,018; skin, 980.
*, Motifs enriched only in a single tissue. Motif frequencies represent the prevalence of each tripeptide divided by the total number of tripeptides analyzed in the organ.

Discussion

Aside from in vivo phage display, use of methods such as serial analysis of gene expression (SAGE) clearly shows that the genetic progression of malignant cells is paralleled by epigenetic changes in nonmalignant endothelial cells induced by angiogenesis of the tumor vasculature[20]. Because SAGE is based on differential expression levels of transcripts, it fails to address functional interactions (for example, binding) at the protein–protein level. The complexity of the human endothelium is also apparent from recent studies showing that the profile of certain endothelial cell receptors can vary depending on ethnic background [31]. In fact, in vivo phage-display in humans might reveal diversity of receptors expressed in the blood vessels even at the level of individual patients.

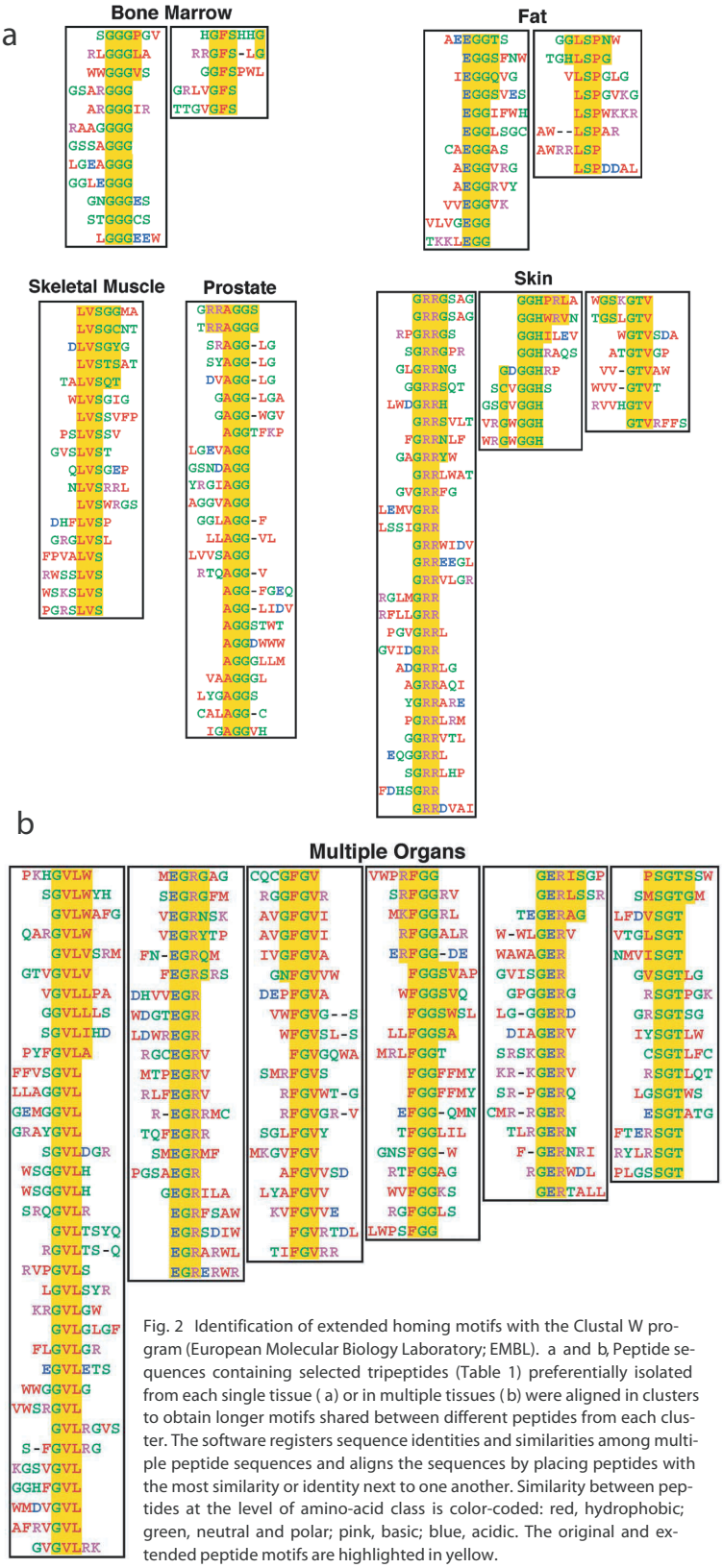

Fig. 2 Identification of extended homing motifs with the Clustal W program (European Molecular Biology Laboratory; EMBL). a and b, Peptide sequences containing selected tripeptides (Table 1) preferentially isolated from each single tissue (a) or in multiple tissues (b) were aligned in clusters to obtain longer motifs shared between different peptides from each cluster. The software registers sequence identities and similarities among multiple peptide sequences and aligns the sequences by placing peptides with the most similarity or identity next to one another. Similarity between peptides at the level of amino-acid class is color-coded: red, hydrophobic; green, neutral and polar; pink, basic; blue, acidic. The original and extended peptide motifs are highlighted in yellow.

However, our validation studies show that at least some ligand–receptor pairs are detectable in multiple unrelated subjects. Another advantage of the method described here is that selected targeting peptides bind to native receptors as they are expressed in vivo. Even if a ligand–receptor interaction is mediated through a conformational rather than a linear epitope, it is possible to select binders in the screening. Furthermore, it is often difficult to ensure that proteins expressed in array systems maintain the correct structure and folding. Thus, peptides selected in vivo may be more suitable to clinical applications.

Precedent exists to suggest that phage can be safely administered to patients, as bacteriophage were used in humans during the pre-antibiotic era [32]. Ultimately, it may become possible to determine molecular profiles of blood vessels in specific conditions; infusing phage libraries systemically before resections of lung, prostate, breast and colorectal carcinomas, or even regionally before resection of limb sarcomas may yield useful vascular targets. Exploiting this experimental paradigm systematically with the analytical tools developed here may permit the construction of a molecular map outlining vascular diversity in each human organ, tissue or disease. Translation of high-throughput in vivo phage-display technology may provide a contextual and functional link between genomics and proteomics. Based on the therapeutic promise of peptide- or peptidomimetic-targeting probes [33], clinical applications are likely to follow.

Methods

Patient selection and clinical course . A 48-y-old male Caucasian patient was diagnosed with Waldenström macroglobulinemia (a B-cell malignancy) and previously treated by splenectomy, systemic chemotherapy (fludarabine, mitoxantrone and dexamethasone) and immunotherapy (anti-CD20 monoclonal antibody). In the few months preceding his admission, the disease became refractory to treatment and clinical progression with retroperitoneal lymphadenopathy, pancytopenia and marked bone marrow infiltration by tumor cells occurred. The patient was admitted with massive intracranial bleeding secondary to thrombocytopenia. Despite prompt craniotomy and surgical evacuation of a cerebral hematoma, the patient remained comatose with progressive and irreversible loss of brainstem function until the patient met the formal criteria for brain-based determination of death [34]; such determination was carried out by an independent clinical neurologist not involved in the project. Because of his advanced cancer, the patient was considered and rejected as transplant organ donor. After surrogate written informed consent was obtained from the legal next of kin, the patient was enrolled in the clinical study. Disconnection of the patient from life-support systems followed the pro-

Table 2 Examples of candidate human proteins mimicked by selected peptide motifs

Extended motif *	Human protein containing the motif	Protein description	Accession number
Bone marrow			
PGGG	Bone morphogenetic protein 3B	Growth factor, TGF-β family member	NP_004953
PGGG	Fibulin 3	Fibrillin- and EGF-like	Q12805
GHHSFG	Microsialin	Macrophage antigen, glycoprotein	NP_001242
Fat			
EGG T	LTBP-2	Fibrillin- and EGF-like, TGF-β Interactor	CAA86030
TGGE	Sortilin	Adipocyte differentiation-induced receptor	CAA66904
GPSL H	Protocadherin gamma C3	Cell adhesion	AAD43784
Muscle			
GG SVL	ICAM-1	Intercellular adhesion molecule	P05362
LVS GY	Flt4	Endothelial growth factor receptor	CAA48290
Prostate			
RRAGG S	Interleukin 11	Cytokine	NP_000632
RRAGG	Smad6	Smad family member	AAB94137
Skin			
GRR G	TGF- β1	Growth factor, TGF-β family member	XP_008912
HGG +G	Neuropilin-1	Endothelial growth factor receptor	AAF44344
+PHGG	Pentaxin	Infection/trauma-induced glycoprotein	CAA45158
PHGG	Macrophage-inhibitory cytokine-1	Growth factor, TGF-β family member	AAB88673
+PHGG	Desmoglein 2	Epithelial cell junction protein	S38673
VTG +SG	Desmoglein 1	Epidermal cell junction protein	AAC83817
Multiple organs			
EGR G	MMP-9	Gelatinase	AAH06093
GRGE	ESM-1	Endothelial cell-specific molecule	XP_003781
NFGV V	CDO	Surface glycoprotein, Ig- and fibronectin-like	NP_058648
GER IS	BPA1	Basement membrane protein	NP_001714
SIREG	Wnt-16	Glycoprotein	Q9UBV4
+GVL W	Sialoadhesin	Ig-like lectin	AAK00757
WLVG +	IL-5 receptor	Soluble interleukin 5 receptor	CAA44081
GGF R	Plectin 1	Endothelial focal junction-localized protein	CAA91196
GGF F	TRANCE	Cytokine, TNF family member	AAC51762
+SGGF	MEGF8	EGF-like protein	T00209
PSGT S	ICAM-4	Intercellular adhesion glycoprotein	Q14773
+TGS P	Perlecan	Vascular repair heparan sulfate proteoglycan	XP_001825

For similarity searches, tripeptide motif-containing peptides (in either orientation) selected by in vivo phage display screening were used. *Extended motifs containing at least 4–6 amino acid residues (Fig. 2) were analyzed using BLAST (NCBI) to search for similarity to known human proteins. Examples of can didate proteins potentially mimicked by the peptides selected in the in vivo screening are listed. Sequences correspond to the regions of 100% identity between the peptide selected and the candidate protein. Conserved amino acid substitutions are indicated as (+). Tripeptides shown in Table 1 are highlighted. TGF, transforming growth factor; TNF, tumor necrosis factor.

cedure. This study strictly adheres to current medical ethics recommendations and guidelines regarding human research [35], and it has been reviewed and approved by the Clinical Ethics Service, the Institutional Biohazard Committee, Clinical Research Committee and the Institutional Review Board of the University of Texas M.D. Anderson Cancer Center.

The University of Texas and researchers (W.A. and R.P.) have equity in NTTX Biotechnology, which is subjected to certain restrictions under university policy; the university manages the terms of these arrangements in accordance to its conflict-of-interest policies.

In vivo phage display. Short-term intravenous infusion of the phage library (a total dose of 1 x 10^{14} phage TU suspended in 100 ml of saline) into the patient was followed by multiple representative tissue biopsies. Prostate and liver samples were obtained by needle biopsy under ultrasonographic guidance; skin, fat-tissue and skeletal-muscle samples were obtained by a surgical excision. Bone-marrow needle aspirates and core biopsy samples were also obtained. Histopathological diagnosis was determined by examination of frozen sections processed from tissues obtained at the bedside. Triplicate samples were processed for host bacterial infection, phage recovery and histopathological analysis. In brief, tissues were weighed, ground with a glass Dounce homogenizer, suspended in 1 ml of DMEM containing proteinase inhibitors (DMEM-prin; 1 mM phenylmethylsulfonyl fluoride (PMSF), 20μg/ml aprotinin, and 1μg/ml leupeptin), vortexed, and washed three times with DMEM-prin. Next, human tissue homogenates were incubated with 1 ml of host bacteria (log phase Escherichia coli K91kan; OD_{600} ~ 2). Aliquots of the bacterial culture were plated onto Luria–Bertani agar plates containing 40 μg/ml tetracycline and 100μg/ml of kanamycin. Plates were incubated overnight at 37 °C. Bacterial colonies were processed for sequencing of phage inserts recovered from each tissue and from unselected phage library. Human samples were handled with universal blood and body fluid precautions.

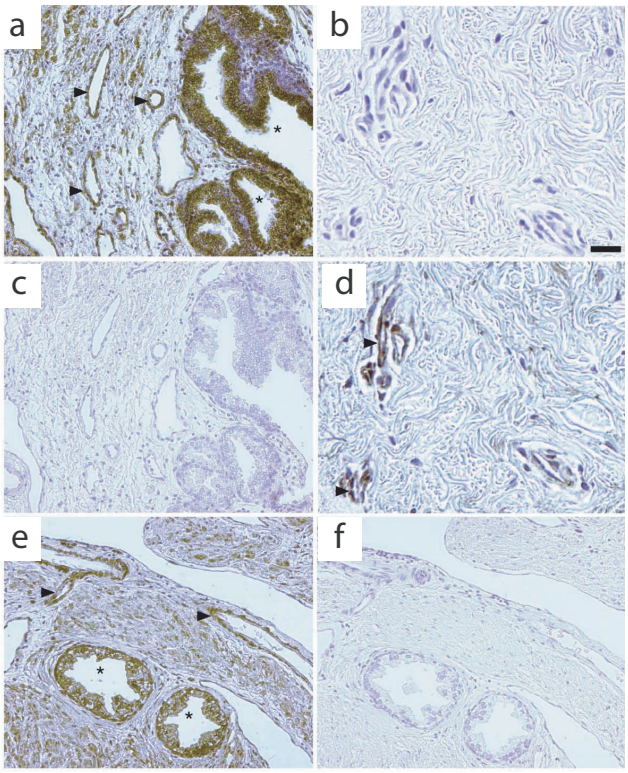

Fig. 3 Validation of the candidate receptor–ligand pairs resulting from the in vivo selection. a–f, Phage clones isolated from prostate and from skin were evaluated for binding to human tissues in an overlay assay. Shown are paraffin-embedded tissue sections of human prostate (a, c, e and f) and of human skin (b and d) overlaid with prostate-homing CGRRAGGSC-displaying phage (a and b) or skin-homing CHGGVGSGC-displaying phage (c and d). Phage were detected by using an anti-M13 phage antibody. In e, IL-11Rα expression was determined by conventional immunostaining with an anti-IL-11Rα antibody; a and e show similar immunostaining patterns (brown staining). f, Negative control antibody on prostate tissue sections. Arrowheads, positive endothelium; asterisks, positive epithelium. Scale bar, 160 μm (a, c, e and f); 40 μm (b and d).

Statistical analysis. Let p be the probability of observing a particular tripeptide motif under total randomness, and $q = 1 - p$. Under such parameters, the probability of observing K sequences characterized as a particular tripeptide motif out of n_3 total tripeptide motif sequences is binomial (n_3, p) and may be approximated by the equation $p_K = \Phi[(k + 1)/\text{sqrt}(n_3\ pq)] - \Phi[k/\text{sqrt}(n_3\ pq)]$, where Φ is the usual cumulative Gaussian probability. The value p_K may be treated as a P value in testing for total randomness of observing exactly K sequences of a particular tripeptide motif. However, this test requires exact knowledge of the true value of p, which it is difficult to obtain in practice with certainty. Therefore, to identify the motifs that were isolated in the screening, the count for each tripeptide motif within each tissue was compared with the count for that tripeptide motif within the unselected library.

Immunocytochemistry and phage overlays. Immunohistochemistry on sections of fixed human paraffin-embedded tissues was done using the LSAB+ peroxidase kit (DAKO, Carpinteria, California) as described [3]. For overlay experiments, phage was used at the concentration of 5 x 10^{10} TU/ml. For phage immunolocalization, a rabbit anti-fd bacteriophage antibody (B-7786; Sigma) was used at 1:500 dilution. For IL-11Rα immunolocalization, a goat antibody (sc-1947; Santa Cruz Biotechnology, Santa Cruz, California) was used at 1:10 dilution. Phage binding to tissue sections was evaluated by the intensity of immunostaining relative to controls.

In vitro protein binding assays. Recombinant (R&D Systems, Minneapolis, Minnesota) interleukin-11 receptor α (IL-11R α), vascular endothelial growth factor receptor-1 (VEGFR1), and leptin receptor (OB-R) were immobilized on microtiter wells (at 1 μg in 50 μl PBS) overnight at 4°C, washed twice with PBS, blocked with 3% BSA in PBS for 2 h at room temperature, and incubated with 1x 10^9 TU of CGRRAGGSC-displaying phage in 50 μl of 1.5% BSA in PBS. An unrelated phage clone (displaying the peptide CRVDFSKGC) and insertless phage (fd-tet) were used as controls. After 1 h at room temperature, wells were washed nine times with PBS, after which bound phage were recovered by bacterial infection and plated as described [3]. Either IL-11 or IL-1 (negative control) was used to inhibit phage binding to IL-11R α. Phage were incubated with the immobilized IL-11Rα in the presence of increasing concentrations of either IL-11 or IL-1. Binding of CGRRAGGSC-displaying phage on immobilized IL-11R α in the absence of interleukins was set to 100%.

Fig. 4 Characterization of CGRRAGGSC-displaying phage binding properties by using purified receptors in vitro. a, Recombinant interleukin-11 receptor (IL-11R α), vascular endothelial growth factor receptor-1 (VEGFR1), or leptin receptor (OB-R) were incubated with the CGRRAGGSC-displaying phage (■). VEGFR1 was used as a representative vascular receptor; OB-R was used because it is homologous to a coreceptor of IL-11Rα. An unrelated phage clone (displaying the peptide CRVDFSKGC, ▨) and insertless phage (fd-tet, □) were used as controls. Phage binding was evaluated and quantified as described (see Methods). b, Specificity of phage binding to the IL-11 receptor. Phage were incubated with the immobilized IL-11Rα in the presence of increasing concentrations of either IL-11 (native ligand, ●) or IL-1 (negative control, ○). The experiments were performed three times with similar results. Shown are mean ± s.e.m. from triplicate wells.

Acknowledgements

We thank R.C. Bast, Jr., R.R. Brentani, W.K. Cavenee, A.C. von Eschenbach, I.J. Fidler, W.K. Hong, D.M. McDonald, J. Mendelsohn and L.A. Zwelling for comments on the manuscript; W.D. Heston for sharing unpublished data; C.L. Cavazos, P.Y. Dieringer, R.G. Nikolova, C.A. Perez, B.H. Restel, C.P. Soto and X. Wang for technical assistance. This work was funded in part by grants from NIH (CA90270 and CA8297601 to R.P., CA90270 and CA9081001 to W.A.) and awards from the Gilson–Longenbaugh Foundation and CaP CURE (to R.P. and W.A.). M.G.K., J.L. and P.J.M. received support from the Susan G. Komen Breast Cancer Foundation, R.J.G. from FAPESP (Brazil), M.C.V. from the Department of Defense, L.C. from the NCCRA and E.K. from the Academy of Finland.

Competing interests statement

The authors declare competing financial interests; see the Nature Medicine web site (http://medicine.nature.com) for details.

RECEIVED 19 NOVEMBER 2001 ; ACCEPTED 2 JANUARY 2002

1. Lander, E.S. et al. Initial sequencing and analysis of the human genome. Nature 409 , 860–921 (2001).
2. Venter, J.C. et al. The sequence of the human genome. Science 291 , 1304–1351 (2001).
3. Pasqualini, R., Arap, W., Rajotte, D. & Ruoslahti, E. In vivo phage display. In Phage display: a laboratory manual. (eds. Barbas, C. F., Burton, D.R., Scott, J.K. & Silverman, G.J.) 1–24 (Cold Spring Harbor Laboratory Press, Cold Spring Harbor, New York, 2000).
4. Rajotte, D. et al. Molecular heterogeneity of the vascular endothelium revealed by in vivo phage display. J. Clin. Invest. 102 , 430–437 (1998).
5. Pasqualini, R. & Ruoslahti, E. Organ targeting in vivo using phage display peptide libraries. Nature 380 , 364–366 (1996).
6. Ellerby, H.M. et al. Anti-cancer activity of targeted pro-apoptotic peptides. Nature Med. 5, 1032–1038 (1999).
7. Koivunen, E. et al. Tumor targeting with a selective gelatinase inhibitor. Nature Biotechnol. 17 , 768–774 (1999).
8. Burg, M.A., Pasqualini, R., Arap, W., Ruoslahti, E. & Stallcup, W.B. NG2 proteoglycan-binding peptides target tumor neovasculature. Cancer Res. 59 , 2869–2874 (1999).
9. Arap, W., Pasqualini, R. & Ruoslahti, E. Cancer treatment by targeted drug delivery to tumor vasculature in a mouse model. Science 279 , 377–380 (1998).
10. Pasqualini, R., Koivunen, E. & Ruoslahti, E. $\alpha_v$integrins as receptors for tumor targeting by circulating ligands. Nature Biotechnol. 15 , 542–546 (1997).
11. Curnis, F. et al. Enhancement of tumor necrosis factor antitumor immunotherapeutic properties by targeted delivery to aminopeptidase N (CD13).Nature Biotechnol. 18 , 1185–1190 (2000).
12. Hong, F. D. & Clayman, G. L. Isolation of a peptide for targeted drug delivery into human head and neck solid tumors. Cancer Res. 60 , 6551–6556 (2000).
13. Trepel, M., Grifman, M., Weitzman, M.D. & Pasqualini, R. Molecular adaptors for vascular-targeted adenoviral gene delivery. Hum. Gene Ther. 11 , 1971–1981 (2000).
14. Rajotte, D. & Ruoslahti, E. Membrane dipeptidase is the receptor for a lung-targeting peptide identified by in vivo phage display. J. Biol. Chem. 274 , 11593–11598 (1999).
15. Pasqualini, R. et al. Aminopeptidase N is a receptor for tumor-homing peptides and a target for inhibiting angiogenesis. Cancer Res. 60 , 722–727 (2000).
16. Bhagwat, S.V. et al. CD13/APN is activated by angiogenic signals and is essential for capillary tube formation. Blood 97 , 652–659 (2001).
17. Kolonin, M.G., Pasqualini, R. & Arap, W. Molecular addresses in blood vessels as targets for therapy. Curr. Opinion. Chem. Biol. 5, 308–313 (2001).
18. Bacich, D.J., Pinto, J.T., Tong, W.P. & Heston, W.D. Cloning, expression, genomic localization, and enzymatic activities of the mouse homolog of prostate-specific membrane antigen/NAALADase/folate hydrolase. Mamm. Genome 12 , 117–123 (2001).
19. Chang, S.S. et al. Five different anti-prostate-specific membrane antigen (PSMA) antibodies confirm PSMA expression in tumor-associated neovasculature. Cancer Res. 59 , 3192–3198 (1999).
20. St Croix, B. et al. Genes expressed in human tumor endothelium. Science 289 , 1197–1202 (2000).
21. Carson-Walter, E.B. et al. Cell surface tumor endothelial markers are conserved in mice and humans. Cancer Res. 61 , 6649–6655 (2001).
22. Vendruscolo, M., Paci, E., Dobson, C.M. & Karplus, M. Three key residues form a critical contact network in a protein folding transition state. Nature 409 , 641–645 (2001).
23. Ruoslahti, E. RGD and other recognition sequences for integrins. Annu. Rev. Cell Dev. Biol. 12 , 697–715 (1996).
24. Koivunen, E. et al. Inhibition of β_2 integrin-mediated leukocyte cell adhesion by leucine-leucine-glycine motif-containing peptides. J. Cell Biol. 153 , 905–916 (2001).
25. Thompson, J.D., Higgins, D.G. & Gibson, T.J. CLUSTAL W: improving the sensitivity of progressive multiple sequence alignment through sequence weighting, position-specific gap penalties and weight matrix choice. Nucleic Acids Res. 22 , 4673–4680 (1994).
26. Daluiski, A. et al. Bone morphogenetic protein-3 is a negative regulator of bone density. Nature Genet. 27 , 84–88 (2001).
27. Mahboubi, K., Biedermann, B.C., Carroll, J.M. & Pober, J.S. IL-11 activates human endothelial cells to resist immune-mediated injury. J. Immunol. 164 , 3837–3846 (2000).
28. Campbell, C.L., Jiang, Z., Savarese, D.M. & Savarese, T.M. Increased expression of the interleukin-11 receptor and evidence of STAT3 activation in prostate carcinoma. Am. J. Pathol. 158 , 25–32 (2001).
29. Lin, B.Z., Pilch, P.F. & Kandror, K.V. Sortilin is a major protein component of Glut4-containing vesicles. J. Biol. Chem. 272 , 24145–24147 (1997).
30. Nugent, M.A., Nugent, H.M., Iozzo, R.V., Sanchack, K. & Edelman, E.R. Perlecan is required to inhibit thrombosis after deep vascular injury and contributes to endothelial cell-mediated inhibition of intimal hyperplasia. Proc. Natl Acad. Sci. USA 97 , 6722–6727 (2000).
31. Wu, K.K. et al. Thrombomodulin Ala455Val polymorphism and risk of coronary heart disease. Circulation 103 , 1386–1389 (2001).
32. Barrow, P.A. & Soothill, J. S. Bacteriophage therapy and prophylaxis: rediscovery and renewed assessment of potential. Trends Microbiol. 5, 268–271 (1997).
33. Latham, P.W. Therapeutic peptides revisited. Nature Biotechnol. 17, 755–757 (1999).
34. Wijdicks, E.F. The diagnosis of brain death. N. Engl. J. Med. 344 , 1215–1221 (2001).
35. Implementing Human Research Regulations; in President's Commission for the Study of Ethical Problems in Medicine and Biomedical and Behavioral Research. (The United States of America Government's Printing Office, Washington, DC; 1983).